UNIVERSITY OF CALIFORNIA

Los Angeles

Tumor-promoting Inflammation in Non-small Cell Lung Cancer

A dissertation submitted in partial satisfaction of the requirements for the degree

Doctor of Philosophy in Molecular and Medical Pharmacology

by

Rui Li

2016

ABSTRACT OF THE DISSERTATION

Tumor-promoting Inflammation in Non-small Cell Lung Cancer

by

Rui Li

Doctor of Philosophy in Molecular and Medical Pharmacology

University of California, Los Angeles, 2016

Professor Steven M. Dubinett, Chair

Lung cancer is the second most common cancer and the leading cause of cancer-associated mortality in the U.S.. The overall 5-year survival of lung cancer patients is less than 20%. The majority of patients are diagnosed with advanced stage disease. While progress has been made with targeted therapies, 5-year survival has so far improved in an incremental manner. Lung cancer is characterized by a prominent inflammatory tumor microenvironment, which in turn represents an important prognostic factor in patients. Unresolved inflammatory conditions

promoted by smoking, chronic obstructive pulmonary disease (COPD) and interstitial lung diseases increase the risk of developing lung cancer. Therefore, tumor-promoting inflammation may play a significant role in cancer initiation and progression.

The first part of this dissertation focuses on the effect of the tumor suppressor *LKB1* on promoting an inflammatory microenvironment in non-small cell lung cancers (NSCLC). Loss of function of *LKB1/STK11* is evident in approximately 30% of primary NSCLC. In murine lung cancer models, *Kras* and *Lkb1* double mutation generates highly metastatic lung tumors with different histological types. Although a variety of different mechanisms have been proposed to explain the tumor-promoting effects underlying *LKB1* deficiency, no effective therapy has been applied clinically; loss of function mutations presents a therapeutic challenge. Most recently, studies have indicated that *LKB1* loss favors an immune-suppressive microenvironment characterized by prominent inflammation, suggesting a new perspective for therapies. Utilizing normal human bronchial epithelial cells (HBECs) which were immortalized in the absence of viral onco-proteins, we find that knockdown of LKB1 elevates the production of multiple inflammatory proteins, among which CXCR2 ligands are the most abundantly secreted. Our data indicate that knockdown of LKB1 in HBECs leads to transcriptional and translational upregulation of CXCR2 ligands and conversely, forced expression of wild-type LKB1 in LKB1-null NSCLC tumor cells decreases CXCR2 ligand production. Non-supervised clustering analysis further reveals *KRAS* and *LKB1* double mutation in human NSCLC cell lines predicts higher levels of CXCR2 ligands. In addition, gene expression analysis shows that CXCR2 ligands are also significantly elevated

in murine *Kras*^{G12D}; *Lkb1*$^{-/-}$ lung tumors compared to *Kras*^{G12D} and *Kras*^{G12D}; *Tp53*$^{-/-}$ tumors. Dissection of the underlying mechanisms reveals that the NF-κB and WNT pathways regulate CXCR2 ligands downstream of LKB1. Surprisingly, regulation of the NF-κB pathway by LKB1 is independent of AMPK, but requires the MARK family proteins. Knockdown of MARKs or inhibition of MARK function by a small chemical inhibitor in HBECs recapitulates LKB1 loss-induced NF-κB activation and subsequent CXCR2 ligand upregulation. CXCR2 ligands have been reported to play an important role in tumor initiation and progression via recruitment of immune cells and endothelial cells in a variety of cancer types including NSCLC. Therefore, our findings suggest that elevation of CXCR2 ligands by LKB1 deficiency facilitates tumor development by creating a tumor-favored microenvironment. Investigating the contribution of CXCR2 ligands to LKB1-dependent malignancy may aid in the development of novel prevention as well as therapeutic strategies against LKB1-null NSCLC.

The second part of this dissertation examines the impact of dysregulated inflammation on cancer progression. The plasticity of epithelial to mesenchymal transition (EMT) program has been considered to be an essential element regulating cancer metastasis. Cancer cells undergoing EMT need to maintain the mesenchymal phenotype during metastasis but revert back to epithelial phenotypes for successful outgrowth of clones at metastatic sites. However, the determinants of EMT plasticity are not yet clear and the underlying mechanisms have not been fully explored. Recently, we have found that a subset of NSCLC cells undergo EMT in the presence of cytokines including IL-1β, TNF-α and TGF-β (within 7 days), and this occurs

concomitantly with increased cell migration and invasion. In addition, chronic exposure to these inflammatory cytokines leads to EMT memory, which refers to the phenomenon in which cells are able to maintain EMT despite withdrawal of the original stimulus. Intriguingly, in contrast to the acute EMT process, EMT memory uniquely depends on chronic cytokine exposure, and not on the signaling pathways (JNK/ERK) and transcription factors (fra-1/slug) mediating the acute EMT. Further studies demonstrate that E-cadherin is repressed via a dynamic alteration of histone modifications and subsequent DNA methylation during chronic IL-1β exposure. Furthermore, a pathway analysis of the RNA profile of these cells indicates that a large portion of the altered genes can be methylated. Phenotypically, EMT memory allows cancer cells to maintain highly migratory and invasive features during metastasis. These findings, for the first time, demonstrate that EMT memory is uniquely induced by chronic inflammation and identifies epigenetic modifications as its underlying mechanism. Better understanding of EMT will ultimately assist in the identification of targets for preventing and treating metastatic behaviors in lung cancer.

The dissertation of Rui Li is approved

Harvey R. Herschman

Jonathan Braun

Michael Alan Teitell

Steven M. Dubinett, Committee Chair

University of California, Los Angeles

2016

DEDICATION

For my parents, who have loved and supported me unconditionally

TABLE OF CONTENTS

List of Figures

Chapter Two Figures

Chapter Three Figures

ACKNOWLEDGEMENT

Foremost, I would like to express my sincerest gratitude to my mentor Dr. Dubinett for his incredible support throughout the past 5 years. The freedom he provided allows me to explore every possible path in the development of my thesis work. Although, many of them went into dead ends, he always encouraged me and guided me with his optimistic altitude, unwavering patience, strong motivation and immense knowledge. This experience really prepared me for an independent investigator with great enthusiasm, curiosity and persistence. I would also like to thank my committee members Dr. Herschman, Dr. Baun and Dr. Teitell for their encouragement, insightful suggestions and scientific challenges.

To the members from Dubinett lab, our shared time will never be forgotten. To Tonya, thank you for setting up the animal research platform and teaching me the basic techniques. Without these, I could never precede the *in vivo* studies. Thank Zhe for helping me with mouse breeding and molecular cloning, and Linh for your input in the bioinformatic analysis. Stacy and Ramin, I can't say how much I appreciate your help and advice in our daily interaction which really accelerated my growth towards an efficient communicator, better writer and critical thinker. Many thanks to Elvira, Kostyantyn, Yari, Gina, Brian and Brandon for providing your expertise and intellectual inputs. I also would like to give special thanks to my undergraduate student, Stephanie. I'm very lucky to have you working with me. Thank you for your commitment and dedication. You have more potential than you know.

Lastly, I would like to thank my friends and my families. I’m lucky to have many great friends at UCLA and the laughs and tears we shared made part of who I am today. I become more mature, responsible and ready than ever for the next stage in my life. Thank you to my parents, Jinhua Li and Shengjun Meng. I’m so blessed to have you always loving me unconditionally and supporting me in every facet of my life. You have been awesome parents and I could not ask more.

VITA

Education

2009 Bachelor of Medicine, Zhejiang University

Positions and Employment

02/2010-06/2010 Research Assistant, Department of Molecular and Medical Pharmacology, David Geffen School of Medicine at UCLA, Los Angeles CA

06/2009-09/2010 Residency, 2nd Affiliated Hospital of School of Medicine, Zhejiang University, Hangzhou, PRC

Additional Training

06/17/13-06/21/13 Next Generation Sequencing Workshop; UCLA Clinical Microarray Core

10/24/10 Flow Cytometry Workshop; UCLA Flow Cytometry Core

Honors and Awards

2014 2nd Place in Poster Competition, UCLA Department of Medicine Research Day

2014 Molecular and Medical Pharmacology Travel Award

2010-2013 Research Fellowship, China Scholarship Council

2008 Chu Kochen Scholarship for Best Student, Zhejiang University

Peer-Reviewed Publications

1. Babic I, Anderson ES, Tanaka K, Guo D, Masui K, Li B, Zhu S, Gu Y, Villa GR, Akhavan D, Nathanson D, Gini B, Mareninov S, **Li R**, Camacho CE, Kurdistani SK, Eskin A, Nelson SF, Yong WH, Cavenee WK, Cloughesy TF, Christofk HR, Black DL, Mischel PS. EGFR Mutation-induced alternative splicing of max contributes to growth of glycolytic tumors in brain cancer. *Cell Metab2013*; 17(6):1000-8
2. Wu D, Zhou Y, Zhu J, Zhao W, Zhong W, Wang Z, QIAN H, **Li R**, Fu S, Sun J. Study on matrine alleviating retinoic acid resistance in acute promyelocytic leukemia. *Chinese Journal of Hematology 2011*; (32)5.
3. Zhang SZ, Qian H, Wang Z, Fan JL, Zhou Q, Chen GM, **Li R**, Fu S, Sun J. Preliminary study on the freeze-drying of human bone marrow-derived mesenchymal stem cells. *J Zhejiang UnivSci B 2010*; 11(11):889-94.
4. Zhang J, Dai X, **Li R,** Chen J. A review on patella baja*. Chinese Journal of Orthopedic Trauma* 2010;(12)10.
5. Zhu FB, Cai XZ, Yan SG, Zhu HX, **Li R**. The effects of local and systemic alendronate delivery on wear debris-induced osteolysis *in vivo*. *Orthop Res 2010*; 28(7):893-9.
6. **Li R**, Qian H, Wang Z, Sun J, Huang H. Methods of preservation of human mesenchymal stem cell. *International Journal of Transplantation and Hemopurification 2008*;(2)29-32.

7. Wang Z, Qian H, **Li R,** Sun, Huang H. Methods of freezing dry preservation of karyocytes. International *Journal of Blood Transfusion and Hematology 2008*;(3)271-274.

Selected Conference Abstracts and Poster Presentations

1. **Li R,** S Ong, L Tran, K Krysan, S Park, TC Walser, Z Jing, SM. Dubinett. An epigenetic switch leads to EMT memory in chronic inflammation in non-small cell lung cancer. January 6-9,2016*. Fourth AACR-IASLC International Joint Conference on Lung Cancer Translational Science from the Bench to the Clinic.*
2. **Li R**, Heinrich E, Pagano PC, Walser TC, Jing Z, Krysan K, Dubinett SM. Exposure to IL-1β leads to EMT via distinct mechanisms in acute and chronic inflammation in non-small cell lung cancer. 2015. *16th World Conference on Lung Cancer*.
3. **Li R**, Walser TC, Ong S, Krysan K, Larsen JE, Minna JD, Teitell M, Shackelford D, Dubinett SM. An AMPK-independent pathway downstream of LKB1 regulates CXCR2 ligands and contributes to tumor development in non-small cell lung cancer. 2015. *15th Annual Targeted Therapies of the Treatment of Lung Cancer Meeting.*
4. **Li R**, Walser TC, Krysan K, Shackelford D, Larsen JE, Minna JD, Dubinett SM. Loss of LKB1 promotes CXCL8 production via NF-κB and WNT signaling in human bronchial epithelial cells. 2014*. IASLC-Molecular Origin of Lung Cancer*.
5. **Li R**, Walser TC, Krysan K, Shackelford D, Larsen JE, Minna JD, Dubinett SM. The contribution ofLKB1/STK11-mediated CXCL8 dysregulation to lung carcinogenesis.2013.*AACR-NCI-EORTC International Conference on Molecular Targets and Cancer Therapeutics.*
6. Cai XZ, Zhu FB, Yan SG, Zhu HX, **Li R**, LV RK. The effects of local and systemic alendronate delivery on wear debris-induced osteolysis *in vivo*. 2009. *The 2nd Annual Forum of Sino-Orthopedic Journal*

Invited Oral Presentations

1. **Li R**. Chronic inflammation leads to epigenetic switches and EMT memory in non-small cell lung cancer. March. 2016. *UCLA IIIT Seminar Research in Progress.*
2. **Li R**, T Walser, K Krysan, S Park, J Larsen, J Minna, M Teitell, D Shackelford, S Dubinett. LKB1 regulates CXCR2 ligands in non-small cell lung cancer. July 2015. *NCI Lung Cancer SPORE Workshop.*
3. **Li R**, E Heinrich, TC Walser, K Krysan, Z Jing, SM Dubinett. Exposure to IL-1β leads to EMT via distinct mechanisms in acute and chronic inflammation in non-small cell lung cancer. Nov. 2014. *UCLA Pharmacology annual retreat.*
4. **Li R**, TC Walser, K Krysan, S. Park, Y Lin, D Shackelford, JE Larsen, JD Minna, SM Dubinett. LKB1 regulates angiogenesis by CYLD-mediated inflammatory signaling in human bronchial epithelial cells. July 2014. *NCI Lung Cancer Spore Workshop.*

CHAPTER ONE: A review of the literature

Introduction of Lung Cancer

Lung cancer is the second most common type of cancer and the leading cause of cancer-related mortality in the world. In United States, there have been more than 1 million new diagnosed cases and 8 hundred thousand deaths in the past 5 years (1, 2). One out of 16 people will be diagnosed with lung cancer in their lifetime. While the incidence in men has steadily decreased due to promotion of smoking cessation, it is increasing in non-smoking women. Most lung cancer patients succumb due to metastatic disease and the overall five-year survival rate is less than 20% in the U.S. (1, 2). This is partially due to the fact that early disease is frequently asymptomatic and implementation of screening for early detection has not yet been fully implemented (3, 4).

There are two major types of lung cancer: non-small cell lung cancer (NSCLC) and small cell lung cancer. NSCLC accounts for about 85% of the cases and is further divided into three histological subtypes: adenocarcinoma, squamous cell and large cell carcinoma, the first two of which comprise the majority of NSCLC cases (5). Adenocarcinoma is the predominant type of NSCLC and the most common form among non-smokers. It is also associated with pulmonary scars and typically arises from peripheral lung tissue. Squamous cell carcinoma, however, often occurs in central airways and is strongly associated with smoking. Previous exposure to mineral or metal dust, asbestos or radon also gives rise to higher risk. The molecular pathogenesis in these two types of NSCLC involves driver mutations and definition of aberrant pathways has been utilized in tailoring therapy (2, 5).

Remarkable success has been achieved in characterizing the driver genetic abnormalities in lung cancer. For instance, in lung adenocarcinoma, approximately 25% of tumors demonstrate *KRAS* mutation and 23% bear epidermal growth factor receptor (*EGFR*) mutation (6). Other driver mutations such as *ALK*, *ERBB2* and *MET* exist in a relatively small portion of lung cancer patients. The discovery of these driver mutations has led to targeted therapies that improve

patient survival (2). For example, erlotinib and gefitinib are representative agents targeting primary *EGFR* mutation and crizotinib targets EML4-*ALK* fusion. Although drug resistance is frequently seen within one year of initiation of these therapies, newer generation agents are being developed to overcome the acquired resistance (7-9). Yet, more than 30% of tumors either do not have common driver mutations or harbor mutations in genes that so far have not been clinically targetable such as *KRAS* mutation (6, 10). In addition, loss of tumor suppressor genes, including *TP53*, *STK11* and *CDKN2*, often exaggerates the malignant behaviors of tumors and remains a therapeutic challenge (11, 12).

The Tumor Suppressor STK11/LKB1

STK11/*LKB1,* located on chromosome 19p13, was originally identified as the gene responsible for the autosomal-dominant inherited disorder Peutz-Jeghers Syndrome (PJS) (13-15). Patients with PJS develop an overgrowth of differentiated tissues in the gastrointestinal (GI) tract and demonstrate an increased predisposition toward the development of additional malignancies, including breast, ovarian, pancreatic, and lung cancers (16). Loss of *LKB1*, either by homozygous deletion or by loss of heterozygosity, has been found in up to 30% of NSCLC patients with a variety of histopathologies, including adeno, squamous, and large cell carcinoma (17-21).

LKB1 is frequently co-mutated with *KRAS* in NSCLC (18, 22). In a murine model of *LKB1*-deficient lung cancer, *Lkb1* loss combined with *Kras* mutation ($Kras^{G12D};Lkb1^{-/-}$) yields a higher frequency of NSCLC tumors and metastasis compared to *Kras* mutation alone (23). Subsequent clinical studies showed that loss of *LKB1* is a biomarker for more aggressive biology in *KRAS* mutant lung adenocarcinoma and patients in stage IV NSCLC with *KRAS* and *LKB1* mutations develop higher number of metastatic sites together with the higher frequency of extrathoracic metastasis (24, 25). These patients have a tendency towards a shorter overall

survival. In addition, *KRAS*/*LKB1* mutant tumors are refractory to a number of therapeutic strategies, including targeted therapy, standard chemotherapy and combined treatment. In a murine lung cancer co-clinical trial, *Kras*/*Lkb1* mutations greatly impaired the anti-tumor response of docetaxel compared to *Kras* mutation alone and addition of a MEK inhibitor selumetinib could not restore the sensitivity (11). Therefore, in an effort to combat this aggressive type of tumor, studies have begun to reveal the molecular abnormalities underlying *LKB1* loss.

LKB1 acts as a master upstream kinase, directly phosphorylating and activating AMP-activated protein kinase (AMPK) and 12 AMPK-related kinases (26). AMPK is known to regulate lipid and glucose metabolism and later proven to negatively regulate mTOR, a central integrator of energy inputs that controls cell growth (27-29). As such, loss of LKB1 in cancerous cells leads to over-activation of the mTOR pathway and subsequent expression of genes including cyclin D1, hypoxia inducible factor 1a (*HIF-1α*), and *MYC*, which in turn promote cell proliferation (30). Moreover, inactivation of AMPK also releases the glucose and lipid metabolism by activating enzymes such as acetyl-CoA carboxylase 1 and phosphofructo-2-kinase (31-33).

Other AMPK independent pathways are also revealed as the mechanisms of enhanced invasion and metastasis in LKB1-deficient tumors. The serine-threonine kinase SIK1 (salt-inducible kinase 1), was identified as a regulator of p53-dependent anoikis (34). Loss of SIK1 facilitated anchorage-independent growth and Matrigel invasion in breast cancers. This is correlated with development of distal metastases and poor survival in patients. The MARK (microtubule affinity-regulating kinase) family, another direct target of LKB1, controls two transcription factors Snail and YAP. Snail induced epithelial-to-mesenchymal transition (EMT) and increased lung colonization via the Src/FAK pathway in LKB1 deficient lung tumors (35). YAP has been shown to be functionally important for the tumor suppressive effects of LKB1 by promoting cell polarity and contact inhibition (36).

Although these efforts have greatly enhanced our understanding of LKB1-dependent tumor suppression and provide possible solutions to address the therapeutic difficulties associated with *LKB1* loss, treatments have not been successfully translated into the clinic. Studies have shown that tumors with both *KRAS* and *LKB1* mutations have defects in nucleotide metabolism, lysosomal maturation and autophagy, all of which are essential for cell growth and survival from energy crisis (37-39). Although laboratory investigations have shown that disturbance of these pathways can specifically shrink LKB1-deficient tumors, clinical translation has not yet occurred. As such, there is a clinical need for better delineation of the molecular profiles underlying LKB1-dependent carcinogenesis. In addition, a more thorough understanding of the early stages of tumorigenesis is the requisite initial step toward future development and application of risk assessment as well as definition of chemoprevention targets and biomarkers for patient selection. Recently, the impact of LKB1 on the inflammatory tumor microenvironment has begun to be revealed, providing a new direction for investigation (12, 40).

Tumor-promoting Inflammation and Cancer

Inflammation has been strongly associated with malignancies including lung cancer and a wide range of evidence has suggested a bi-directional interaction between malignant cells and the tumor microenvironment (TME) (41). In the intrinsic pathway, the inflammatory microenvironment is generated by genetic mutations from tumors that secrete altered inflammatory mediators. In the extrinsic pathway, the inflammatory environment is capable of promoting cancer initiation and progression. Therefore, this interaction can preferably form a vicious cycle that will not only accelerate malignant transformation from pre-neoplasm lesions but also facilitate invasive and metastatic behaviors of established cancer cells.

The intrinsic pathway

In the development of NSCLC, aberrant cell signaling as well as gene mutations have been shown to have an elevated level of inflammation. The transcription factor, NF-κB, is a master regulator of inflammatory proteins. Increased expression of NF-κB was reported in squamous dysplasia from smokers compared to normal epithelial cells from non-smokers (42). In adenocarcinoma, the NF-κB activity is significantly higher in advanced stage cancer than in early stage cancer (43). Oncogene activation or tumor suppressor silencing has been shown to induce abnormal inflammation. In human normal human bronchial epithelial cells (HBECs), introduction of *KRAS* mutation leads to enhanced secretion of VEGF and CXCL1 (44). In a murine model of lung cancer, *Kras* mutation induces higher expression of a variety of chemokines (45).

The inflammatory niche is capable of fostering the development of pre-neoplasia into full-blown cancers (46, 47). In the premalignant lesions, we showed that the increased CXCL1 production by *KRAS* mutation in HBECs was responsible for anchorage-independent cell growth, indicating of tumor initiation capacity (44). Overexpression of the transcription factor Snail, was able to induce TGF-β expression as well as Secreted Protein, Acidic and Rich in Cysteine (SPARC), both of which are known to promote tumor metastasis (48). In addition, many major cytokines in inflammation are shown to significantly contribute to tumor progression. IL-6 is shown to promote cell proliferation and apoptotic resistance by activation of stat3 pathway (49-52). IL-1β is known to induce COX-2 expression and subsequent PGE2 production (53). High level of PGE2 plays multifaceted roles in lung cancer development including angiogenesis, immune suppression, therapy resistance and metastasis (53-59). As such, inhibition of PGE2 biogenesis has been assessed as a chemoprevention for lung cancer in early phase clinical trials (60-62). Antagonists against angiogenic mediators such as VEGF have been approved for therapy while others such as those against CXCR2 ligands are undergoing evaluation (63, 64).

Another important aspect of cancer-associated inflammatory proteins is modulation of the immune response in the TME. Immune cells, including macrophages, neutrophils and

lymphocytes, are frequently present in cancerous tissues (65). For example, it has been well documented that NSCLC cells secreted a Th2 pattern of cytokine such as IL-4 and IL-10 that drives a M2 macrophage phenotype (47, 53). The M2 macrophages increase level of immunosuppressive cytokines such as IL-10 while decrease mediators that promote specific cell-mediated antitumor immune response such as IL-12. This altered balance between pro- and anti- tumor immune response eventually leads to enhanced tumor growth (66). Another example is the recruitment of myeloid-derived suppressive cells (MDSC) by PGE2, TGF-β, IL-10 and CXCR2 ligands. MDSCs assist immune escape and support angiogenesis and vasculogenesis. They also facilitate tumor invasion by secreting MMPs, uPA and other enzymes and protect from host immunity and physical injury during circulation (67-69). As a result of these findings, studies are evaluating the mechanisms of MDSC inhibition for possible clinical translation (70-72).

The anti-tumor activity of CD8+ lymphocytes can also be suppressed by upregulation of immune checkpoint proteins including such as CTLA-4 and PD-L1 (73, 74). Research from Kwok Wong's group identified EGFR pathway activation and a signature of immunosuppression by upregulation of PD-1, PD-L1 and CTL antigen-4 (CTLA-4) in NSCLC (75). In a model of lung squamous carcinoma, PD-L1 is also elevated in *Lkb1* and *Pten* loss tumors, suggesting a mechanism of immune escape (76). Studies from our group indicate that *KRAS* mutation in HBECs increases PD-L1 expression via ERK-mediated signaling.

The extrinsic pathway

Numerous epidemiological studies have shown that inflammation is tightly associated with the development of a variety of cancers. Patients with HPV or HCV infection are predisposed to cervical and hepatic cancer respectively (77, 78). Persistent inflammatory conditions such as family adenomatous polyposis and inflammatory bowel disease dramatically increase the incidence of colon cancer (79). Although the exact mechanisms of chronic obstructive pulmonary

disease (COPD)-associated lung cancer are still obscure, the epidemiological link between them is indisputable (80, 81). Perhaps the strongest evidence is the finding that patients with chronic H. Pylori infection in gastric predispose to mucosa-associated lymphoma (MALT) and eradiation of H. Pylori infection also cures MALT (82, 83).

Tobacco smoking is the strongest risk factor for the development of lung cancer (84, 85). In addition to direct mutagenic effects, smoking-induced chronic inflammation is thought to be another driver. Several studies have reported that cigarette smoking can cause elevated levels of TNF-alpha, IL-1, IL-6, CXCL8 and granulocyte-macrophage colony-stimulating factor (86-88). These acute inflammatory cytokines and chemokines may be secreted by pulmonary macrophages in reaction to foreign substrates and toxic chemicals inhaled during smoking. The inflammation cascade is thereby extended after further recruitment of more macrophages and neutrophils by the inflammatory proteins. Reactive oxygen species (ROS) mediate pro-tumor effects by the exaggeration of inflammation which places genotoxic and apoptotic stress on pulmonary epithelial cells (89). It directly induces DNA damage, lipid peroxidation, and protein carbonylation of airway alveolar epithelium and endothelial cells (90). ROS also contributes to the dysregulation of endogenous proteases/anti-proteases, accelerating lung damage due to increased elastolysis (91). Moreover, ROS in turn also activates multiple inflammatory pathways such as the NF-KB and MAPK signaling (92, 93).

Conversely, augmented activity of a negative regulator of ROS, nuclear factor erythroid 2-related factor (NFR2), has been suggested to be a promising alternative to prevent tumor initiation. *Nrf2*$^{-/-}$ mice display increased lung damage when exposed to cigarette smoking (94). One NFR2 activator sulphoraphane, a natural product, has been evaluated in models to inhibit carcinogenesis in skin, lung, colon and stomach cancers (95-98). In the case of murine colon cancer model, the benefit of sulphoraphane is clearly attributed to altered consequences of the

expression of an aberrant genetic lesion (98). However, there are controversial findings regarding the roles of *NFR2* (99-101). In the context of established cancer, NFR2 have predominate oncogenic functions (102).

Epithelial-to-Mesenchymal Transition in Tumor Progression

Another pro-tumor consequence of inflammation is induction of the epithelial-to-mesenchymal transition (EMT). EMT is characterized with loss of cell-cell and cell-basement contact and acquisition of increased cell motility and invasiveness (103-105). Epithelial markers such as E-cadherin and cytokeratin are downregulated while mesenchymal markers such as N-cadherin, Vimentin and FSP1 are upregulated. EMT occurs in both physiological and pathological processes. Following early embryogenesis, EMT is associated with both embryo implantation and formation of placenta, in particular, the trophoblast cells. Enhanced migration as well as invasion of these cells is required for the placental anchoring and creation of chorionic villi for nutrition and gas exchange between the fetus and mother. Further gastrulation including epiblast-mesoderm transition is another form of EMT (103). EMT is also actively involved in organ differentiation. For example, migration of neural crest cells is indispensable for proper development of cardiac septums, adrenal gland, and peripheral nerve system (106). In the process of wound healing, keratinocytes at the border undergo EMT to migrate and close the wound (103, 104). In the pathogenesis of organ fibrosis, epithelial cells undergoing EMT contribute to the interstitial fibroblast and myofibroblast pools (62, 107-109).

The most deadly consequence of EMT is cancer metastasis. Upon activation of the EMT program, the malignant epithelial cells shed from the primary tumor and invade the surroundings until they reach blood vessels. The mesenchymal phenotype assists these cells to survive in the circulation and migrate through the blood vessels when they arrive at distant organs (103, 104). EMT takes place as result of EMT-inducing stimuli, which can be divided into cell extrinsic and

cell intrinsic stimuli. Inflammatory mediators comprise an important source of extrinsic stimuli. For example, TGF-β has been investigated in detail for its capacity to induce EMT. This includes studies documenting the importance of the canonical Smad complex and non-Smad proteins including RHO-like GTPases, PI3K and MAPK pathways (110, 111). In the canonical pathway, different Smad proteins form a trimeric Smad complex and translocate into nucleus after activation of TβRI and TβRII. By interacting with transcription activators or repressors, the Smad complex regulates genes involved in the EMT program. For example, Smad3-Smad4 complex is shown to cooperate with Snail to repress epithelial genes including E-cadherin and Occludin (103, 110). Other inflammatory mediators such as TNF-alpha and PGE2 have also been found to be extrinsic mediators of EMT (112, 113).

On the other hand, oncogene activation or loss of a tumor suppressor is among the cell intrinsic mechanisms leading to EMT. A wide variety of oncogenic signals are associated with EMT: pathways downstream of tyrosine kinase receptors (PI3K-AKT, ERK-MAPK, EGFR/IGF/PDGF/HGF), pathways involved in differentiation (WNT/Hedgehog/Notch) and pathways in tumor microenvironment (integrin signaling, hypoxia-HIF, JAK-stat, NF-κB) (111, 114). Loss of function of tumor suppressor LKB1 is found to induce EMT via activation of SRC kinase and subsequent induction of the EMT-transcription factor (EMT-TF) Snail (35, 115).

Although numerous studies have shown that EMT plays important roles in cancer progression and metastasis *in vitro* and *in vivo*, there is an apparent paradox arising from the observation that most of the metastatic tumor clones no longer display mesenchymal phenotypes. Instead, they express high levels of E-cadherin and cytokeratin, indicating an epithelial to mesenchymal transition (MET) in distant organs (116, 117). It is still not well understood how such EMT plasticity occurs, although absence of the original heterotypic signals in the primary tumor site and presence of additional MET signals in the metastatic tumor site are among the hypotheses. At least one MET phenotype is obviously beneficial to metastasis: these epithelial cells regain

the proliferation advantage compared to their mesenchymal counterparts, which contributes the outgrowth of the macrometastasis and eventual death of patients (117).

Emerging evidence has indicated that EMT is more than facilitation of tumor dissemination but associated with resistance to cell death and senescence, failure of chemotherapy, stem cell properties and immune suppression and inflammation (104, 117). In the early stage of tumorigenesis, it is reported that Twist expression prevents cell senescence induced by inhibition of cell cycle repressor proteins such as p16/INK4a (118). Another study has demonstrated that TGF-β-treated mammary epithelial cells survived better following activation of Ras (119). The correlation of EMT with stem cell is observed in the experiments in which CD44high/CD24low human mammary epithelial cells transformed after Ras or Her2 activation displayed stem-like features with concomitant induction of EMT (120, 121). Importantly, recent studies have shown that reversion of EMT via PKA activation dramatically reduced the capacity of tumor initiation (122).

Regulation of EMT is largely attributed to its core transcription factors namely Snail1, Snail2 (Slug), Zeb1, Zeb2, Twist1 and Twist 2 (103, 104, 111). Snail1/2 belongs to the Zinc-finger protein family binding to E-boxes of E-cadherin promoter. Zeb1/2 is within the distantly related zinc finger E-box-binding homeobox family and is also able to repress E-cadherin. The Snail and Zeb families of transcription factors also repress other cellular junction proteins such as Claudins and ZO1 (123, 124). Twist1/2, however, is from the basic helix-loop-helix family of transcription factors. All of these core EMT-TFs induce EMT alone or cooperatively. Not surprisingly, the existence of multiple EMT-TFs regulates EMT in a redundant manner and balances their overall effect. Data from our group have shown that exposure to IL-1β in NSCLC induced EMT through upregulation of Slug and Zeb2 while Snail is, on the contrary, downregulated (data not shown). Forced overexpression of Snail in HBECs decreased Slug level and vice versa (data not shown). Interestingly, expression of EMT-TFs, frequently induced by inflammatory proteins, can also

trigger an inflammatory response (48). We and others have shown that overexpression of Snail or Slug increased production of cytokines or chemokines such as TGF-β and CXCL8, indicating a feed-forward loop that subsequently enhances EMT (125, 126).

Although EMT involves a genome-wide gene reprogramming, loss of E-cadherin represents a keystone of the mesenchymal phenotype. It has been shown that E-cadherin downregulation is sufficient to induce EMT and metastasis. Onder et.al found that disruption of E-cadherin expression enabled tumor metastasis through induction of EMT and anoikis resistance. Further microarray analysis demonstrated that multiple transcription factors were altered and Twist was at least partially responsible for E-cadherin loss-induced metastasis (127). Another study in NSCLC showed E-cadherin depletion facilitated invasion in a MMP-2 dependent manner with aberrant EGFR signaling (128). Although a number of studies have shown that EMT-TFs directly bind the E-cadherin promoter, epigenetic alterations such as histone modifications and DNA methylation are revealed as the repressive machinery that interrupts the otherwise active transcription of E-cadherin (111).

The Epigenetic Regulation of EMT

The epigenetics refers to the regulation of gene expression via covalent modifications without any alterations of DNA sequencing. At least three systems including histone modifications, DNA methylation and non-coding RNA-associated gene silencing are considered as the executors of the epigenetic machinery. They are actively involved in many physiological and pathological process such embryogenesis, aging, Alzheimer disease as well as cancer.

Histone is the protein unit of nucleosome that is comprised of approximately 150 base pairs of DNA and an octamer of four core histones (H2A, H2B, H3 and H4). The core histones are tightly packed in the nucleosome with amino-terminal tails extending outwards, making them assessable to different covalent modifications (129). In non-dividing cells, nucleosomes are organized into

two functional states of chromatin, euchromatin and heterochromatin (130, 131). The genome regions of euchromatin are more flexible and therefore are easily accessed by transcription factors, leading to active gene transcription. On the other hand, heterochromatins are areas where DNA is highly condensed and inaccessible to transcription factors. These areas are associated with profound gene silencing (genetic imprinting or X chromosome inactivation) and control of chromosomal stability (131, 132).

The amino-terminal tails of histone are subjected to different multivalent modifications among which, acetylation and methylation are the most intensively studied in regulation of gene expression. Acetylation of lysine residues in histones removes their positive charge and subsequently loosens histone binding with negative-charged DNA, thereby opening the condensed chromatin structure to permit access of transcriptional machinery to gene promoter (131, 133). Histone hyperacetylation such as enrichment of H3K4Ac is thus a reliable marker for transcription activation and gene expression. The alteration of acetylation is mediated either by histone acetyltransferase enzymes (HATs) or histone deacetylases (HDACs) (131). As would be anticipated, histone acetylation is lost in the promoter regions of epithelial genes in EMT. The capability of Snail-mediated gene suppression is at least partially attributed to its N-terminal SNAG domain, which helps recruit transcription repressors such as HDACs and Sin3A (134, 135). It has been reported that HDAC1 and HDAC2 can be recruited by Snail to the *Cdh1* promoter and contribute to its silencing. Treatment with trichastatin A, a HDAC inhibitor, disinhibits the repressive functions of Snail and prevents metastasis (134). Another study from the Datta group also showed that cigarette smoke condensate-induced EMT could be reversed by HDAC inhibition in NSCLC (136).

Histone methylation occurs in multiple lysine residues with the potential of one, two or three methyl groups. Compared to the correlation of histone acetylation with gene activation, histone methylation is more complicated and is associated with transcription activation, inactivation as

well as permanent gene silencing (130, 131). Its effect on gene function and chromatin state depends on, not only the methylated lysine residue, but also the degree of methylation (137-140). Generally, in the active transcript regions, there is an enrichment of H3K4me, H3K36me or H3k79me while silenced genes frequently co-exist with H3K27me or H3K9me (141-144). In addition, H3K9me is tightly associated with stable and permanent gene suppression and therefore is frequently enriched in DNA regions of heterochromatin (145-147). Interestingly, recent studies have indicated some "paradoxical" functions of certain histone methylation; mono-methylation of H3K9me and H3K27me is distributed mostly in euchromatin and linked to gene activation, further reflecting the complexity of histone methylation (145, 147). There are a large number of methyltransferases and demethylase identified to either add or remove methyl groups from the histone.

H3K27me3-associated E-cadherin repression is part of the polycomb repressive complexes (PRCs) originally recruited by EMT-TFs, such as Snail, which is able to physically interact with Ezh2, a subunit of PRC2 that catalyzes H3K27me3 in the surrounding promoters (148, 149). Indeed, overexpression of Ezh2 is associated with an EMT gene expression pattern in breast, prostate and bladder cancer (150-153). In NSCLC, overexpression of Ezh2 enhances *KRAS*-driven adenocarcinoma formation and indicates poor prognosis in patients (154, 155). It is worth noting that there is a bivalent histone modification characterized by presence of both H3K27me3 and H3K4me3 (146, 156-159). Genes residing in these regions are nevertheless poised to become activated upon specific stimulus that lead to removal of the repressive H3K27me3, indicating that these genes are not stably suppressed but remain responsive to dynamic alteration of certain cellular signals (158). Bivalent histone modification is observed in cancer cells with stem-like properties. In the $CD44^{+}$, E-cadherin low stem cell-like population of human mammary epithelial tissue, the *CDH1* promoter is marked by both H3K27me3 and H3K4me3 while there exists only H3K4me3 in $CD24^{+}$, E-cadherin high non-stem cell like

population (160). Therefore, this chromatin configuration allows re-expression of E-cadherin in the $CD44^+$ cells in response to their differentiation into $CD24^+$ epithelial cells. Although it is still unclear whether EMT plasticity largely relies on the bivalent genes, it at least provides an insight of the dynamic regulation of gene expression.

As indicated above, H3K9me2 and H3K9me3 reconstitute heterochromatin that is more resistance to gene activation compared to H3K27me3. Recent work from the Zhou group has demonstrated that in the setting of TGF-β-induced EMT, Snail is able to directly interact with G9a, a major methyltransferase for H3K9me2 (161). They also found that addition of a third methyl group by SUV39H1 to form H3K9me3 confered a more durable repression of E-cadherin (162). Consistent with its role in epithelial gene silencing, cells with abundant SUV39H1 expression display a mesenchymal phenotype (162).

In addition, emerging evidence has suggested that there is a crosstalk between histone and DNA methylation at the level of enzyme interactions. Take G9a for example, its physical interaction by its ankyrin domain with DNMTs leads to stable E-cadherin repression via DNA methylation (161, 163). Similarly, Snail interacts with the SET domain of SUV39H1 to facilitate its localization to the E-cadherin promoter, leading to H3K9me3 and ultimately DNA methylation (162). Knockdown of SUV39H1 is sufficient to restore E-cadherin expression by abolishing H3K9me3 and DNA methylation. Interestingly, biochemistry studies suggest that the interaction of histone methyltransferase with DNMT is carried out by domains not responsible for its methylation function (164). This is suggested by the fact that point mutations in the SET domain of G9a eliminate H3K9me2 without affecting DNA methylation (165, 166). Although Ezh2 is usually exempted from DNA methylation due to protection by PRC, there are a few exceptions. It has been shown that *de novo* methylation occurs in many gene sequences that are initially marked by the PRC during differentiation of embryonic stem cells to neural precursors (146, 167). In addition, genes frequently displaying DNA hypermethylation in adult cancers lack such DNA methylation in

normal embryonic cells where these genes are held in a bivalent state (156). Given the fact that Ezh2 can interact with DNMT3 *in vitro* (168), it is possible that PRC plays a role in mediating the DNA methylation reaction.

In mammalian cells, DNA methylation occurs in the 5' position of the CpG dinucleotides by enzymatic transfer of a methyl group from the methyl donor S-adenosylmethionine to a create methylcytocine (5mC). This reaction is catalyzed by DNA methyltransferases (DNMT) including DNMT1, DNMT3a and DNMT3b (169, 170). DNMT1 is responsible for post-replication restoration of DNA methylation while DNMT3a and DNMT3b are primarily involved in *de novo* DNA methylation (171, 172). Approximately 70% of CpG dinucleotides are methylated in mammalian genome while CpG island, defined as CpG dinucleotide clusters interspersing within approximately 1-kb stretches of DNA sequencing, often locates in the 5' end of genes and remains unmethylated (173, 174). However, methylation of promoter-associated CpG islands is important of transcriptional silencing, demonstrating by some physiological conditions such as genetic imprinting and X chromosome inactivation (174, 175). In the development of cancer, aberrant DNA methylation patterns in cancer cells serve as additional oncogenic mechanisms. For example, hypermethylation of tumor suppressor promoters including *CDKN2*, *APC* and *RB* are frequently seen in NSCLC (176).

The involvement of DNA methylation in EMT has been best studied with TGF-β treatment in multiple different types of malignancy (177-180). Another study examined the DNA methylomes following TGF-β-induced EMT in MDCK cells and identified that hypermethylation of *ITGA5* and *ESYT3* are correlated with mesenchymal cell phenotype and poor survival in breast cancer patients (181). Mechanistically, TGF-β treatment is shown to repress E-cadherin via enrichment of H3K9me2 or H3K9me3 and subsequent DNA methylation (161, 162). The establishment of DNA methylation endows cells with the persistence of the EMT phenotype.

To summarize, the involvement of various histone modifications and DNA methylation are consistent with the highly dynamic transcriptional regulation of the EMT program ranging from fully epithelial to fully mesenchymal state. The repression of epithelial genes may initiate loss of histone acetylation followed by gain of H3K27me3. Co-existence of H3K4me3 and H3K27me3 represents a poised transcription state from which genes can be re-expressed after withdrawal of EMT-inducing signals or under specific physiologic conditions. However, with continuous stimulus of EMT-inducing signals, subsequent loss of H3K4me3 allows the enrichment of more stable repressive histone markers including H3K9me2 and H3K9me3. Protein interaction between histone modification enzymes with DNMTs eventually proceed to DNA methylation in the promoter of epithelial genes, creating a highly stable mesenchymal state that can persist over many cell generations.

References

1. Siegel RL, Miller KD, & Jemal A (2016) Cancer statistics, 2016. *CA: a cancer journal for clinicians* 66(1):7-30.
2. Torre LA, Siegel RL, & Jemal A (2016) Lung Cancer Statistics. *Advances in experimental medicine and biology* 893:1-19.
3. Gould MK (2014) Clinical practice. Lung-cancer screening with low-dose computed tomography. *The New England journal of medicine* 371(19):1813-1820.
4. Usman Ali M*, et al.* (2016) Screening for lung cancer: A systematic review and meta-analysis. *Preventive medicine*.
5. Herbst RS, Heymach JV, & Lippman SM (2008) Lung cancer. *The New England journal of medicine* 359(13):1367-1380.
6. Sholl LM*, et al.* (2015) Multi-institutional Oncogenic Driver Mutation Analysis in Lung Adenocarcinoma: The Lung Cancer Mutation Consortium Experience. *Journal of thoracic oncology : official publication of the International Association for the Study of Lung Cancer* 10(5):768-777.
7. Sullivan I & Planchard D (2016) Treatment modalities for advanced ALK-rearranged non-small-cell lung cancer. *Future oncology* 12(7):945-961.
8. Sullivan I & Planchard D (2016) ALK inhibitors in non-small cell lung cancer: the latest evidence and developments. *Therapeutic advances in medical oncology* 8(1):32-47.
9. Tan CS, Cho BC, & Soo RA (2016) Next-generation epidermal growth factor receptor tyrosine kinase inhibitors in epidermal growth factor receptor -mutant non-small cell lung cancer. *Lung cancer* 93:59-68.
10. Naidoo J & Drilon A (2016) KRAS-Mutant Lung Cancers in the Era of Targeted Therapy. *Advances in experimental medicine and biology* 893:155-178.

11. Chen Z*, et al.* (2012) A murine lung cancer co-clinical trial identifies genetic modifiers of therapeutic response. *Nature* 483(7391):613-617.

12. Skoulidis F*, et al.* (2015) Co-occurring genomic alterations define major subsets of KRAS-mutant lung adenocarcinoma with distinct biology, immune profiles, and therapeutic vulnerabilities. *Cancer discovery* 5(8):860-877.

13. Hemminki A*, et al.* (1997) Localization of a susceptibility locus for Peutz-Jeghers syndrome to 19p using comparative genomic hybridization and targeted linkage analysis. *Nature genetics* 15(1):87-90.

14. Hemminki A*, et al.* (1998) A serine/threonine kinase gene defective in Peutz-Jeghers syndrome. *Nature* 391(6663):184-187.

15. Ylikorkala A*, et al.* (1999) Mutations and impaired function of LKB1 in familial and non-familial Peutz-Jeghers syndrome and a sporadic testicular cancer. *Human molecular genetics* 8(1):45-51.

16. Hemminki A (1999) The molecular basis and clinical aspects of Peutz-Jeghers syndrome. *Cellular and molecular life sciences : CMLS* 55(5):735-750.

17. Koivunen JP*, et al.* (2008) Mutations in the LKB1 tumour suppressor are frequently detected in tumours from Caucasian but not Asian lung cancer patients. *Brit J Cancer* 99(2):245-252.

18. Matsumoto S*, et al.* (2007) Prevalence and specificity of LKB1 genetic alterations in lung cancers. *Oncogene* 26(40):5911-5918.

19. Gill RK*, et al.* (2011) Frequent homozygous deletion of the LKB1/STK11 gene in non-small cell lung cancer. *Oncogene* 30(35):3784-3791.

20. Wingo SN*, et al.* (2009) Somatic LKB1 Mutations Promote Cervical Cancer Progression. *Plos One* 4(4).

21. Sanchez-Cespedes M*, et al.* (2002) Inactivation of LKB1/STK11 is a common event in adenocarcinomas of the lung. *Cancer research* 62(13):3659-3662.

22. Carretero J, Medina PP, Pio R, Montuenga LM, & Sanchez-Cespedes M (2004) Novel and natural knockout lung cancer cell lines for the LKB1/STK11 tumor suppressor gene. *Oncogene* 23(22):4037-4040.

23. Ji H*, et al.* (2007) LKB1 modulates lung cancer differentiation and metastasis. *Nature* 448(7155):807-810.

24. Gleeson FC*, et al.* (2015) Somatic STK11 and concomitant STK11/KRAS mutational frequency in stage IV lung adenocarcinoma adrenal metastases. *Journal of thoracic oncology : official publication of the International Association for the Study of Lung Cancer* 10(3):531-534.

25. Calles A*, et al.* (2015) Immunohistochemical Loss of LKB1 Is a Biomarker for More Aggressive Biology in KRAS-Mutant Lung Adenocarcinoma. *Clinical cancer research : an official journal of the American Association for Cancer Research* 21(12):2851-2860.

26. Shackelford DB & Shaw RJ (2009) The LKB1-AMPK pathway: metabolism and growth control in tumour suppression. *Nature reviews. Cancer* 9(8):563-575.

27. Corradetti MN, Inoki K, Bardeesy N, DePinho RA, & Guan KL (2004) Regulation of the TSC pathway by LKB1: evidence of a molecular link between tuberous sclerosis complex and Peutz-Jeghers syndrome. *Genes & development* 18(13):1533-1538.

28. Inoki K, Zhu T, & Guan KL (2003) TSC2 mediates cellular energy response to control cell growth and survival. *Cell* 115(5):577-590.

29. Shaw RJ*, et al.* (2004) The LKB1 tumor suppressor negatively regulates mTOR signaling. *Cancer cell* 6(1):91-99.

30. Guertin DA & Sabatini DM (2007) Defining the role of mTOR in cancer. *Cancer cell* 12(1):9-22.

31. Almeida A, Moncada S, & Bolanos JP (2004) Nitric oxide switches on glycolysis through the AMP protein kinase and 6-phosphofructo-2-kinase pathway. *Nature cell biology* 6(1):45-51.

32. Carling D, Zammit VA, & Hardie DG (1987) A common bicyclic protein kinase cascade inactivates the regulatory enzymes of fatty acid and cholesterol biosynthesis. *FEBS letters* 223(2):217-222.

33. Marsin AS*, et al.* (2000) Phosphorylation and activation of heart PFK-2 by AMPK has a role in the stimulation of glycolysis during ischaemia. *Current biology : CB* 10(20):1247-1255.

34. Cheng H*, et al.* (2009) SIK1 couples LKB1 to p53-dependent anoikis and suppresses metastasis. *Science signaling* 2(80):ra35.

35. Goodwin JM*, et al.* (2014) An AMPK-independent signaling pathway downstream of the LKB1 tumor suppressor controls Snail1 and metastatic potential. *Molecular cell* 55(3):436-450.

36. Mohseni M*, et al.* (2014) A genetic screen identifies an LKB1-MARK signalling axis controlling the Hippo-YAP pathway. *Nature cell biology* 16(1):108-117.

37. Liu Y*, et al.* (2013) Metabolic and functional genomic studies identify deoxythymidylate kinase as a target in LKB1-mutant lung cancer. *Cancer discovery* 3(8):870-879.

38. Shackelford DB*, et al.* (2013) LKB1 inactivation dictates therapeutic response of non-small cell lung cancer to the metabolism drug phenformin. *Cancer cell* 23(2):143-158.

39. Kim HS*, et al.* (2013) Systematic identification of molecular subtype-selective vulnerabilities in non-small-cell lung cancer. *Cell* 155(3):552-566.

40. Koyama S*, et al.* (2016) STK11/LKB1 Deficiency Promotes Neutrophil Recruitment and Proinflammatory Cytokine Production to Suppress T-cell Activity in the Lung Tumor Microenvironment. *Cancer research* 76(5):999-1008.

41. Dubinett SM (2015) *Inflammation and Lung Cancer* (Springer-Verlag New York).

42. Tichelaar JW*, et al.* (2005) Increased staining for phospho-Akt, p65/RELA and cIAP-2 in pre-neoplastic human bronchial biopsies. *BMC cancer* 5:155.

43. Tang X*, et al.* (2006) Nuclear factor-kappaB (NF-kappaB) is frequently expressed in lung cancer and preneoplastic lesions. *Cancer* 107(11):2637-2646.

44. Liclican EL*, et al.* (2014) Loss of miR125a expression in a model of K-ras-dependent pulmonary premalignancy. *Cancer prevention research* 7(8):845-855.

45. Wislez M*, et al.* (2006) High expression of ligands for chemokine receptor CXCR2 in alveolar epithelial neoplasia induced by oncogenic kras. *Cancer research* 66(8):4198-4207.

46. Qian BZ & Pollard JW (2010) Macrophage diversity enhances tumor progression and metastasis. *Cell* 141(1):39-51.

47. de Visser KE, Eichten A, & Coussens LM (2006) Paradoxical roles of the immune system during cancer development. *Nature reviews. Cancer* 6(1):24-37.

48. Grant JL*, et al.* (2014) A novel molecular pathway for Snail-dependent, SPARC-mediated invasion in non-small cell lung cancer pathogenesis. *Cancer prevention research* 7(1):150-160.

49. Huang W*, et al.* (2016) Small-molecule inhibitors targeting the DNA-binding domain of STAT3 suppress tumor growth, metastasis and STAT3 target gene expression in vivo. *Oncogene* 35(6):802.

50. Qu Z*, et al.* (2015) Interleukin-6 Prevents the Initiation but Enhances the Progression of Lung Cancer. *Cancer research* 75(16):3209-3215.

51. Wang X*, et al.* (2016) Hypermethylated in cancer 1(HIC1) suppresses non-small cell lung cancer progression by targeting interleukin-6/Stat3 pathway. *Oncotarget*.

52. Dalwadi H*, et al.* (2005) Cyclooxygenase-2-dependent activation of signal transducer and activator of transcription 3 by interleukin-6 in non-small cell lung cancer. *Clinical cancer research : an official journal of the American Association for Cancer Research* 11(21):7674-7682.

53. Huang M*, et al.* (1998) Non-small cell lung cancer cyclooxygenase-2-dependent regulation of cytokine balance in lymphocytes and macrophages: up-regulation of interleukin 10 and down-regulation of interleukin 12 production. *Cancer research* 58(6):1208-1216.

54. Baratelli F*, et al.* (2005) Prostaglandin E2 induces FOXP3 gene expression and T regulatory cell function in human CD4+ T cells. *Journal of immunology* 175(3):1483-1490.

55. Krysan K*, et al.* (2014) PGE2-driven expression of c-Myc and oncomiR-17-92 contributes to apoptosis resistance in NSCLC. *Molecular cancer research : MCR* 12(5):765-774.

56. Krysan K*, et al.* (2005) Prostaglandin E2 activates mitogen-activated protein kinase/Erk pathway signaling and cell proliferation in non-small cell lung cancer cells in an epidermal growth factor receptor-independent manner. *Cancer research* 65(14):6275-6281.

57. Liu M*, et al.* (2007) EGFR signaling is required for TGF-beta 1 mediated COX-2 induction in human bronchial epithelial cells. *American journal of respiratory cell and molecular biology* 37(5):578-588.

58. Sharma S*, et al.* (2005) Tumor cyclooxygenase-2/prostaglandin E2-dependent promotion of FOXP3 expression and CD4+ CD25+ T regulatory cell activities in lung cancer. *Cancer research* 65(12):5211-5220.

59. Huang M, Sharma S, Mao JT, & Dubinett SM (1996) Non-small cell lung cancer-derived soluble mediators and prostaglandin E2 enhance peripheral blood lymphocyte IL-10 transcription and protein production. *Journal of immunology* 157(12):5512-5520.

60. Krysan K, Reckamp KL, Sharma S, & Dubinett SM (2006) The potential and rationale for COX-2 inhibitors in lung cancer. *Anti-cancer agents in medicinal chemistry* 6(3):209-220.

61. Mao JT*, et al.* (2005) Chemoprevention strategies with cyclooxygenase-2 inhibitors for lung cancer. *Clinical lung cancer* 7(1):30-39.

62. Kim KK*, et al.* (2006) Alveolar epithelial cell mesenchymal transition develops in vivo during pulmonary fibrosis and is regulated by the extracellular matrix. *Proceedings of the National Academy of Sciences of the United States of America* 103(35):13180-13185.

63. Hall RD, Le TM, Haggstrom DE, & Gentzler RD (2015) Angiogenesis inhibition as a therapeutic strategy in non-small cell lung cancer (NSCLC). *Translational lung cancer research* 4(5):515-523.

64. Yanagawa J*, et al.* (2009) Snail promotes CXCR2 ligand-dependent tumor progression in non-small cell lung carcinoma. *Clinical cancer research : an official journal of the American Association for Cancer Research* 15(22):6820-6829.

65. Coussens LM, Zitvogel L, & Palucka AK (2013) Neutralizing tumor-promoting chronic inflammation: a magic bullet? *Science* 339(6117):286-291.

66. Stolina M*, et al.* (2000) Specific inhibition of cyclooxygenase 2 restores antitumor reactivity by altering the balance of IL-10 and IL-12 synthesis. *Journal of immunology* 164(1):361-370.

67. Gabrilovich DI & Nagaraj S (2009) Myeloid-derived suppressor cells as regulators of the immune system. *Nature reviews. Immunology* 9(3):162-174.

68. Nagaraj S*, et al.* (2009) Regulatory myeloid suppressor cells in health and disease. *Cancer research* 69(19):7503-7506.

69. Talmadge JE & Gabrilovich DI (2013) History of myeloid-derived suppressor cells. *Nature reviews. Cancer* 13(10):739-752.

70. Srivastava MK, Dubinett S, & Sharma S (2012) Targeting MDSCs enhance therapeutic vaccination responses against lung cancer. *Oncoimmunology* 1(9):1650-1651.

71. Srivastava MK*, et al.* (2012) Targeting myeloid-derived suppressor cells augments antitumor activity against lung cancer. *ImmunoTargets and therapy* 2012(1):7-12.

72. Srivastava MK*, et al.* (2012) Myeloid suppressor cell depletion augments antitumor activity in lung cancer. *PloS one* 7(7):e40677.

73. Martens A*, et al.* (2016) Increases in absolute lymphocytes and circulating CD4+ and CD8+ T cells are associated with positive clinical outcome of melanoma patients treated with ipilimumab. *Clinical cancer research : an official journal of the American Association for Cancer Research*.

74. Steven A, Fisher SA, & Robinson BW (2016) Immunotherapy for lung cancer. *Respirology*.

75. Akbay EA*, et al.* (2013) Activation of the PD-1 pathway contributes to immune escape in EGFR-driven lung tumors. *Cancer discovery* 3(12):1355-1363.

76. Xu C*, et al.* (2014) Loss of Lkb1 and Pten leads to lung squamous cell carcinoma with elevated PD-L1 expression. *Cancer cell* 25(5):590-604.

77. Davila JA, Morgan RO, Shaib Y, McGlynn KA, & El-Serag HB (2004) Hepatitis C infection and the increasing incidence of hepatocellular carcinoma: a population-based study. *Gastroenterology* 127(5):1372-1380.

78. de Sanjose S*, et al.* (2010) Human papillomavirus genotype attribution in invasive cervical cancer: a retrospective cross-sectional worldwide study. *The Lancet. Oncology* 11(11):1048-1056.

79. Farraye FA, Odze RD, Eaden J, & Itzkowitz SH (2010) AGA technical review on the diagnosis and management of colorectal neoplasia in inflammatory bowel disease. *Gastroenterology* 138(2):746-774, 774 e741-744; quiz e712-743.

80. Durham AL & Adcock IM (2015) The relationship between COPD and lung cancer. *Lung cancer* 90(2):121-127.

81. Punturieri A, Szabo E, Croxton TL, Shapiro SD, & Dubinett SM (2009) Lung cancer and chronic obstructive pulmonary disease: needs and opportunities for integrated research. *Journal of the National Cancer Institute* 101(8):554-559.

82. Morgner A, Bayerdorffer E, Neubauer A, & Stolte M (2000) Gastric MALT lymphoma and its relationship to Helicobacter pylori infection: management and pathogenesis of the disease. *Microscopy research and technique* 48(6):349-356.

83. Wotherspoon AC, Ortiz-Hidalgo C, Falzon MR, & Isaacson PG (1991) Helicobacter pylori-associated gastritis and primary B-cell gastric lymphoma. *Lancet* 338(8776):1175-1176.

84. Doll R & Hill AB (1950) Smoking and carcinoma of the lung; preliminary report. *British medical journal* 2(4682):739-748.

85. Thun MJ*, et al.* (2013) 50-year trends in smoking-related mortality in the United States. *The New England journal of medicine* 368(4):351-364.

86. Bermudez EA, Rifai N, Buring JE, Manson JE, & Ridker PM (2002) Relation between markers of systemic vascular inflammation and smoking in women. *The American journal of cardiology* 89(9):1117-1119.

87. Churg A, Zhou S, Wang X, Wang R, & Wright JL (2009) The role of interleukin-1beta in murine cigarette smoke-induced emphysema and small airway remodeling. *American journal of respiratory cell and molecular biology* 40(4):482-490.

88. Glossop JR, Dawes PT, & Mattey DL (2006) Association between cigarette smoking and release of tumour necrosis factor alpha and its soluble receptors by peripheral blood mononuclear cells in patients with rheumatoid arthritis. *Rheumatology* 45(10):1223-1229.

89. Zuo L, Otenbaker NP, Rose BA, & Salisbury KS (2013) Molecular mechanisms of reactive oxygen species-related pulmonary inflammation and asthma. *Molecular immunology* 56(1-2):57-63.

90. Paz-Elizur T*, et al.* (2008) DNA repair of oxidative DNA damage in human carcinogenesis: potential application for cancer risk assessment and prevention. *Cancer letters* 266(1):60-72.

91. Aoshiba K, Yasuda K, Yasui S, Tamaoki J, & Nagai A (2001) Serine proteases increase oxidative stress in lung cells. *American journal of physiology. Lung cellular and molecular physiology* 281(3):L556-564.

92. Benhar M, Dalyot I, Engelberg D, & Levitzki A (2001) Enhanced ROS production in oncogenically transformed cells potentiates c-Jun N-terminal kinase and p38 mitogen-activated protein kinase activation and sensitization to genotoxic stress. *Molecular and cellular biology* 21(20):6913-6926.

93. Vaquero EC, Edderkaoui M, Pandol SJ, Gukovsky I, & Gukovskaya AS (2004) Reactive oxygen species produced by NAD(P)H oxidase inhibit apoptosis in pancreatic cancer cells. *The Journal of biological chemistry* 279(33):34643-34654.

94. Rangasamy T*, et al.* (2004) Genetic ablation of Nrf2 enhances susceptibility to cigarette smoke-induced emphysema in mice. *The Journal of clinical investigation* 114(9):1248-1259.

95. Conaway CC*, et al.* (2005) Phenethyl isothiocyanate and sulforaphane and their N-acetylcysteine conjugates inhibit malignant progression of lung adenomas induced by tobacco carcinogens in A/J mice. *Cancer research* 65(18):8548-8557.

96. Fahey JW*, et al.* (2002) Sulforaphane inhibits extracellular, intracellular, and antibiotic-resistant strains of Helicobacter pylori and prevents benzo[a]pyrene-induced stomach tumors. *Proceedings of the National Academy of Sciences of the United States of America* 99(11):7610-7615.

97. Gills JJ*, et al.* (2006) Sulforaphane prevents mouse skin tumorigenesis during the stage of promotion. *Cancer letters* 236(1):72-79.

98. Shen G*, et al.* (2007) Chemoprevention of familial adenomatous polyposis by natural dietary compounds sulforaphane and dibenzoylmethane alone and in combination in ApcMin/+ mouse. *Cancer research* 67(20):9937-9944.

99. DeNicola GM*, et al.* (2011) Oncogene-induced Nrf2 transcription promotes ROS detoxification and tumorigenesis. *Nature* 475(7354):106-109.

100. Solis LM*, et al.* (2010) Nrf2 and Keap1 abnormalities in non-small cell lung carcinoma and association with clinicopathologic features. *Clinical cancer research : an official journal of the American Association for Cancer Research* 16(14):3743-3753.

101. Sporn MB & Liby KT (2012) NRF2 and cancer: the good, the bad and the importance of context. *Nature reviews. Cancer* 12(8):564-571.

102. Wang H*, et al.* (2016) NRF2 activation by antioxidant antidiabetic agents accelerates tumor metastasis. *Science translational medicine* 8(334):334ra351.

103. Kalluri R & Weinberg RA (2009) The basics of epithelial-mesenchymal transition. *The Journal of clinical investigation* 119(6):1420-1428.

104. Thiery JP, Acloque H, Huang RY, & Nieto MA (2009) Epithelial-mesenchymal transitions in development and disease. *Cell* 139(5):871-890.

105. Zeisberg M & Neilson EG (2009) Biomarkers for epithelial-mesenchymal transitions. *The Journal of clinical investigation* 119(6):1429-1437.

106. Dupin E & Sommer L (2012) Neural crest progenitors and stem cells: from early development to adulthood. *Developmental biology* 366(1):83-95.

107. Rastaldi MP*, et al.* (2002) Epithelial-mesenchymal transition of tubular epithelial cells in human renal biopsies. *Kidney international* 62(1):137-146.

108. Zeisberg EM*, et al.* (2007) Endothelial-to-mesenchymal transition contributes to cardiac fibrosis. *Nature medicine* 13(8):952-961.

109. Zeisberg M*, et al.* (2007) Fibroblasts derive from hepatocytes in liver fibrosis via epithelial to mesenchymal transition. *The Journal of biological chemistry* 282(32):23337-23347.

110. Wendt MK, Tian M, & Schiemann WP (2012) Deconstructing the mechanisms and consequences of TGF-beta-induced EMT during cancer progression. *Cell and tissue research* 347(1):85-101.

111. Lamouille S, Xu J, & Derynck R (2014) Molecular mechanisms of epithelial-mesenchymal transition. *Nature reviews. Molecular cell biology* 15(3):178-196.

112. Dohadwala M*, et al.* (2006) Cyclooxygenase-2-dependent regulation of E-cadherin: prostaglandin E(2) induces transcriptional repressors ZEB1 and snail in non-small cell lung cancer. *Cancer research* 66(10):5338-5345.

113. Li CW*, et al.* (2012) Epithelial-mesenchymal transition induced by TNF-alpha requires NF-kappaB-mediated transcriptional upregulation of Twist1. *Cancer research* 72(5):1290-1300.

114. Kumar M*, et al.* (2013) NF-kappaB regulates mesenchymal transition for the induction of non-small cell lung cancer initiating cells. *PloS one* 8(7):e68597.

115. Carretero J*, et al.* (2010) Integrative genomic and proteomic analyses identify targets for Lkb1-deficient metastatic lung tumors. *Cancer cell* 17(6):547-559.

116. Tam WL & Weinberg RA (2013) The epigenetics of epithelial-mesenchymal plasticity in cancer. *Nature medicine* 19(11):1438-1449.

117. Tsai JH & Yang J (2013) Epithelial-mesenchymal plasticity in carcinoma metastasis. *Genes & development* 27(20):2192-2206.

118. Ansieau S*, et al.* (2008) Induction of EMT by twist proteins as a collateral effect of tumor-promoting inactivation of premature senescence. *Cancer cell* 14(1):79-89.

119. Valdes F*, et al.* (2002) The epithelial mesenchymal transition confers resistance to the apoptotic effects of transforming growth factor Beta in fetal rat hepatocytes. *Molecular cancer research : MCR* 1(1):68-78.

120. Mani SA*, et al.* (2008) The epithelial-mesenchymal transition generates cells with properties of stem cells. *Cell* 133(4):704-715.

121. Morel AP*, et al.* (2008) Generation of breast cancer stem cells through epithelial-mesenchymal transition. *PloS one* 3(8):e2888.

122. Pattabiraman DR*, et al.* (2016) Activation of PKA leads to mesenchymal-to-epithelial transition and loss of tumor-initiating ability. *Science* 351(6277):aad3680.

123. Ohkubo T & Ozawa M (2004) The transcription factor Snail downregulates the tight junction components independently of E-cadherin downregulation. *Journal of cell science* 117(Pt 9):1675-1685.

124. Vandewalle C*, et al.* (2005) SIP1/ZEB2 induces EMT by repressing genes of different epithelial cell-cell junctions. *Nucleic acids research* 33(20):6566-6578.

125. Hwang WL*, et al.* (2011) SNAIL regulates interleukin-8 expression, stem cell-like activity, and tumorigenicity of human colorectal carcinoma cells. *Gastroenterology* 141(1):279-291, 291 e271-275.

126. Lyons JG*, et al.* (2008) Snail up-regulates proinflammatory mediators and inhibits differentiation in oral keratinocytes. *Cancer research* 68(12):4525-4530.

127. Onder TT*, et al.* (2008) Loss of E-cadherin promotes metastasis via multiple downstream transcriptional pathways. *Cancer research* 68(10):3645-3654.

128. Bae GY*, et al.* (2013) Loss of E-cadherin activates EGFR-MEK/ERK signaling, which promotes invasion via the ZEB1/MMP2 axis in non-small cell lung cancer. *Oncotarget* 4(12):2512-2522.

129. Luger K, Mader AW, Richmond RK, Sargent DF, & Richmond TJ (1997) Crystal structure of the nucleosome core particle at 2.8 A resolution. *Nature* 389(6648):251-260.

130. Consortium EP*, et al.* (2007) Identification and analysis of functional elements in 1% of the human genome by the ENCODE pilot project. *Nature* 447(7146):799-816.

131. Jenuwein T & Allis CD (2001) Translating the histone code. *Science* 293(5532):1074-1080.

132. Talbert PB & Henikoff S (2006) Spreading of silent chromatin: inaction at a distance. *Nature reviews. Genetics* 7(10):793-803.

133. Feinberg AP & Tycko B (2004) The history of cancer epigenetics. *Nature reviews. Cancer* 4(2):143-153.

134. Peinado H, Ballestar E, Esteller M, & Cano A (2004) Snail mediates E-cadherin repression by the recruitment of the Sin3A/histone deacetylase 1 (HDAC1)/HDAC2 complex. *Molecular and cellular biology* 24(1):306-319.

135. Lin Y*, et al.* (2010) The SNAG domain of Snail1 functions as a molecular hook for recruiting lysine-specific demethylase 1. *The EMBO journal* 29(11):1803-1816.

136. Nagathihalli NS, Massion PP, Gonzalez AL, Lu P, & Datta PK (2012) Smoking induces epithelial-to-mesenchymal transition in non-small cell lung cancer through HDAC-mediated downregulation of E-cadherin. *Molecular cancer therapeutics* 11(11):2362-2372.

137. Miao F & Natarajan R (2005) Mapping global histone methylation patterns in the coding regions of human genes. *Molecular and cellular biology* 25(11):4650-4661.

138. Kouzarides T (2007) Chromatin modifications and their function. *Cell* 128(4):693-705.

139. Guenther MG, Levine SS, Boyer LA, Jaenisch R, & Young RA (2007) A chromatin landmark and transcription initiation at most promoters in human cells. *Cell* 130(1):77-88.

140. Berger SL (2007) The complex language of chromatin regulation during transcription. *Nature* 447(7143):407-412.

141. Steger DJ*, et al.* (2008) DOT1L/KMT4 recruitment and H3K79 methylation are ubiquitously coupled with gene transcription in mammalian cells. *Molecular and cellular biology* 28(8):2825-2839.

142. Poncet V*, et al.* (2007) Development of genomic microsatellite markers in Coffea canephora and their transferability to other coffee species. *Genome / National Research Council Canada = Genome / Conseil national de recherches Canada* 50(12):1156-1161.

143. Krivtsov AV*, et al.* (2008) H3K79 methylation profiles define murine and human MLL-AF4 leukemias. *Cancer cell* 14(5):355-368.

144. Edmunds JW, Mahadevan LC, & Clayton AL (2008) Dynamic histone H3 methylation during gene induction: HYPB/Setd2 mediates all H3K36 trimethylation. *The EMBO journal* 27(2):406-420.

145. Vakoc CR, Sachdeva MM, Wang H, & Blobel GA (2006) Profile of histone lysine methylation across transcribed mammalian chromatin. *Molecular and cellular biology* 26(24):9185-9195.

146. Meissner A*, et al.* (2008) Genome-scale DNA methylation maps of pluripotent and differentiated cells. *Nature* 454(7205):766-770.

147. Barski A*, et al.* (2007) High-resolution profiling of histone methylations in the human genome. *Cell* 129(4):823-837.

148. Herranz N*, et al.* (2008) Polycomb complex 2 is required for E-cadherin repression by the Snail1 transcription factor. *Molecular and cellular biology* 28(15):4772-4781.

149. Bracken AP, Dietrich N, Pasini D, Hansen KH, & Helin K (2006) Genome-wide mapping of Polycomb target genes unravels their roles in cell fate transitions. *Genes & development* 20(9):1123-1136.

150. Kleer CG*, et al.* (2003) EZH2 is a marker of aggressive breast cancer and promotes neoplastic transformation of breast epithelial cells. *Proceedings of the National Academy of Sciences of the United States of America* 100(20):11606-11611.

151. Collett K*, et al.* (2006) Expression of enhancer of zeste homologue 2 is significantly associated with increased tumor cell proliferation and is a marker of aggressive breast cancer. *Clinical cancer research : an official journal of the American Association for Cancer Research* 12(4):1168-1174.

152. Chang CJ*, et al.* (2011) EZH2 promotes expansion of breast tumor initiating cells through activation of RAF1-beta-catenin signaling. *Cancer cell* 19(1):86-100.

153. Cao Q*, et al.* (2008) Repression of E-cadherin by the polycomb group protein EZH2 in cancer. *Oncogene* 27(58):7274-7284.

154. Wang X, *et al.* (2016) Prognostic Significance of EZH2 Expression in Non-Small Cell Lung Cancer: A Meta-analysis. *Scientific reports* 6:19239.

155. Serresi M, *et al.* (2016) Polycomb Repressive Complex 2 Is a Barrier to KRAS-Driven Inflammation and Epithelial-Mesenchymal Transition in Non-Small-Cell Lung Cancer. *Cancer cell* 29(1):17-31.

156. Ohm JE, *et al.* (2007) A stem cell-like chromatin pattern may predispose tumor suppressor genes to DNA hypermethylation and heritable silencing. *Nature genetics* 39(2):237-242.

157. Mikkelsen TS, *et al.* (2007) Genome-wide maps of chromatin state in pluripotent and lineage-committed cells. *Nature* 448(7153):553-560.

158. Bernstein BE, *et al.* (2006) A bivalent chromatin structure marks key developmental genes in embryonic stem cells. *Cell* 125(2):315-326.

159. Voigt P, Tee WW, & Reinberg D (2013) A double take on bivalent promoters. *Genes & development* 27(12):1318-1338.

160. Maruyama R, *et al.* (2011) Epigenetic regulation of cell type-specific expression patterns in the human mammary epithelium. *PLoS genetics* 7(4):e1001369.

161. Dong C, *et al.* (2012) G9a interacts with Snail and is critical for Snail-mediated E-cadherin repression in human breast cancer. *The Journal of clinical investigation* 122(4):1469-1486.

162. Dong C, *et al.* (2013) Interaction with Suv39H1 is critical for Snail-mediated E-cadherin repression in breast cancer. *Oncogene* 32(11):1351-1362.

163. Feldman N, *et al.* (2006) G9a-mediated irreversible epigenetic inactivation of Oct-3/4 during early embryogenesis. *Nature cell biology* 8(2):188-194.

164. Epsztejn-Litman S, *et al.* (2008) De novo DNA methylation promoted by G9a prevents reprogramming of embryonically silenced genes. *Nature structural & molecular biology* 15(11):1176-1183.

165. Tachibana M, Matsumura Y, Fukuda M, Kimura H, & Shinkai Y (2008) G9a/GLP complexes independently mediate H3K9 and DNA methylation to silence transcription. *The EMBO journal* 27(20):2681-2690.

166. Dong KB*, et al.* (2008) DNA methylation in ES cells requires the lysine methyltransferase G9a but not its catalytic activity. *The EMBO journal* 27(20):2691-2701.

167. Mohn F*, et al.* (2008) Lineage-specific polycomb targets and de novo DNA methylation define restriction and potential of neuronal progenitors. *Molecular cell* 30(6):755-766.

168. Vire E*, et al.* (2006) The Polycomb group protein EZH2 directly controls DNA methylation. *Nature* 439(7078):871-874.

169. Chen T & Li E (2004) Structure and function of eukaryotic DNA methyltransferases. *Current topics in developmental biology* 60:55-89.

170. Bestor TH (2000) The DNA methyltransferases of mammals. *Human molecular genetics* 9(16):2395-2402.

171. Okano M, Bell DW, Haber DA, & Li E (1999) DNA methyltransferases Dnmt3a and Dnmt3b are essential for de novo methylation and mammalian development. *Cell* 99(3):247-257.

172. Li E, Bestor TH, & Jaenisch R (1992) Targeted mutation of the DNA methyltransferase gene results in embryonic lethality. *Cell* 69(6):915-926.

173. Smith ZD & Meissner A (2013) DNA methylation: roles in mammalian development. *Nature reviews. Genetics* 14(3):204-220.

174. Laird PW (2003) The power and the promise of DNA methylation markers. *Nature reviews. Cancer* 3(4):253-266.

175. Jones PA & Baylin SB (2007) The epigenomics of cancer. *Cell* 128(4):683-692.

176. Lu F & Zhang HT (2011) DNA methylation and nonsmall cell lung cancer. *Anatomical record* 294(11):1787-1795.

177. Lee C*, et al.* (2012) TGF-beta mediated DNA methylation in prostate cancer. *Translational andrology and urology* 1(2):78-88.

178. Cardenas H*, et al.* (2014) TGF-beta induces global changes in DNA methylation during the epithelial-to-mesenchymal transition in ovarian cancer cells. *Epigenetics* 9(11):1461-1472.

179. Bu F*, et al.* (2015) TGF-beta1 induces epigenetic silence of TIP30 to promote tumor metastasis in esophageal carcinoma. *Oncotarget* 6(4):2120-2133.

180. Papageorgis P*, et al.* (2010) Smad signaling is required to maintain epigenetic silencing during breast cancer progression. *Cancer research* 70(3):968-978.

181. Carmona FJ*, et al.* (2014) A comprehensive DNA methylation profile of epithelial-to-mesenchymal transition. *Cancer research* 74(19):5608-5619.

CHAPTER TWO: Regulation of CXCR2 ligands by LKB1 in the development of NSCLC

Abstract

Loss of *LKB1/STK11*, a tumor suppressor gene, characterizes approximately 30% of primary non-small cell lung cancers (NSCLC). In a murine model of lung carcinogenesis with inducible *Kras* activation, concurrent mutation of *Lkb1* (*Kras*^{G12D}; *Lkb1*$^{-/-}$) yields a higher frequency of NSCLC tumors and metastasis. *In vitro* studies have shown that following *LKB1* loss, tumor cells acquire the capacity for increased migration and invasion through activation of the SRC kinase family. Although these previous findings offer a possible explanation for LKB1-dependent tumorigenesis and progression, the involved mechanisms are still largely unknown. In this study, we utilize human bronchial epithelial cells (HBECs) that are immortalized in the absence of viral onco-proteins to study the stepwise events in lung carcinogenesis. Knockdown of LKB1 in HBECs leads to enhanced secretion of multiple inflammatory factors, most prominent of which are CXCL1 and CXCL8, belonging to the CXCR2 ligands. By binding to their common receptor CXCR2 which is universally expressed by neutrophils, macrophages, endothelial cells and pulmonary epithelial cells, CXCR2 ligands are thereby involved in chemotaxis, angiogenesis, tumorigenicity and metastasis. Our data indicate that knockdown of LKB1 leads to transcriptional upregulation of CXCR2 ligands in HBECs and conversely, re-introduction of wild-type LKB1 in LKB1-null NSCLC tumor cells decreases CXCR2 ligand production. In addition, gene expression analysis indicates that human NSCLC cell lines with *KRAS* and *LKB1* mutation have higher levels of CXCR2 ligands. Importantly, lung tumors from *Kras*^{G12D};*Lkb1*$^{-/-}$ mice also demonstrate heightened expression levels of CXCR2 ligands compared to that from *Kras*^{G12D} tumors. We

further show that the NF-κB and WNT pathways are activated and mediate the increased production of CXCR2 ligands following LKB1 loss. Surprisingly, the ability of LKB1 to regulate the NF-κB pathway is independent of AMPK, but instead requires the microtubule affinity-regulating kinase (MARK) family. Knockdown of MARKs or inhibition of MARK function recapitulates LKB1 loss-induced CXCR2 ligand expression in HBECs. In summary, our findings suggest that LKB1 deficiency drives augmentation of CXCR2 ligands in the developing tumor microenvironment via NF-κB and WNT signaling. Investigating the contribution of CXCR2 ligands to LKB1-depedent malignancy may aid in the development of novel therapeutic strategies against LKB1-null NSCLC.

Introduction

Lung cancer is the leading cause of cancer-related death; the majority of patients die due to metastatic disease (1, 2). Treatment against advanced stage NSCLC has improved due to successful targeting of the aberrant pathways led by driver mutations, such as EGFR mutation and ALK fusion. Therefore, there is an increasing recognition that these genetic aberrations and pathways must be better defined to foster both a personalized medicine approach for patients with established NSCLC, and importantly, a similar targeted chemoprevention approach for those at risk for the development of lung cancer (3).

Loss of the tumor suppressor *LKB1* accounts for approximately 30% of NSCLC patients and it is frequently co-mutated with *KRAS* (4, 5). The aggressive phenotypes in NSCLC caused by LKB1

loss have been attributed to several mechanisms including dysregulation of the AMPK-mTOR signaling, hyperactivation of SRC kinase, suppression of the Hippo pathway and induction of EMT-promoting transcription factors (6-10). However, few attempts have been successfully translated into the clinic, suggesting that better delineation of the molecular profile underlying LKB1-dependent carcinogenesis is still an urgent need.

To better study the function of LKB1, we utilized human bronchial epithelial cells (HBECs) as a pre-clinical model of pulmonary premalignancy. The HBECs were obtained from the bronchi of patients with or without lung cancer and immortalized in the absence of viral onco-proteins via ectopic expression of human telomerase and cyclin-dependent kinase 4 (11). The gene expression pattern of these cells is distinct from that of lung cancer cells and clusters more tightly with the parental non-immortalized pulmonary epithelial cells; the cells test negative for all mutations evaluated thus far, including *LKB1*, *KRAS*, *TP53*, *EGFR*, and *MYC*. This evaluation suggests that HBECs carry minimal naturally acquired oncogenic mutations and resemble normal pulmonary epithelial cells. In addition, functional assays indicate that HBECs can differentiate into each of the major cell types of the normal pseudo-stratified columnar bronchial epithelium in a 3D organotypic air-liquid interface (ALI) culture system, suggesting that these cells bear progenitor-like characteristics that allow modeling of the pulmonary airways and their associated malignant transformation (12). In this regard, utilizing the cell-based HBEC model allows us to evaluate pathway intermediaries in isolation and to study early abnormal cellular events precipitating pulmonary carcinogenesis.

The association between unresolved inflammation and cancer has been increasingly documented in the past decade (13). The inflammatory niche is capable of fostering the development of pre-neoplasia into full-blown cancers (14, 15). Important pro-tumor effects of inflammation facilitate angiogenesis and reshape the biological functions of tumor-infiltrating immunocytes in the tumor microenvironment. Tumor cells are known to secret multiple angiogenic chemokines and growth factors to promote tumor neovascularization. Moreover, immunocytes recruited to premalignant lesions or tumor sites not only trip the angiogenic switch in previously quiescent tissue but also may suppress anti-tumor immune responses (16). CXCR2 ligands, including CXCL1, CXCL2, CXCL3, CXCL5 and CXCL8, are chemokines highly expressed in NSCLC (17-19). These chemokines belong to the CXC family with an NH2-terminal Glu-Leu-Arg (ELR) motif and function by binding to their common G-protein-coupled receptor CXCR2, which is ubiquitously expressed by endothelial cells, neutrophils, macrophages and lymphocytes (20, 21). We and others have demonstrated the important contribution of CXCR2 ligands in lung cancer pathogenesis; antagonizing CXCR2 at the level of receptor or ligands is sufficient to reduce tumor burden *in vivo*, concurrently with reduced angiogenesis and neutrophil infiltration (18, 22-24). In addition, tumors with higher levels of these ligands positively correlate with higher clinical stages and significantly poorer prognosis (19, 25, 26). Therefore, CXCR2 ligands play important roles in the development and progression of NSCLC, making blockade of CXCR2 an intriguing therapeutic strategy.

Here, we discover that LKB1 loss in HBECs leads to a dysregulation of the inflammatory profile, among which CXCR2 ligands are most predominant. The level of CXCR2 ligands is also increased in human NSCLC cell lines and in lung tumors from genetically engineered murine models. We further identify that the MARKs-dependent NF-kB pathway mediates CXCR2 expression following LKB1 loss. The ultimate goal of this study is to determine the mechanisms underlying the contribution of LKB1 loss to the induction of CXCR2 ligands and to evaluate the role of CXCR2 inhibition in the prevention and therapy of LKB1-deficient lung cancer.

Results

Regulation of CXCR2 ligands by LKB1 in HBECs

To investigate whether there is a dysregulation of inflammatory factors following LKB1 loss in HBECs, we utilized a Luminex assay which is a Bio-plex bead-based multiplex immunoassay characterized by its high sensitivity and capacity to measure multiple proteins simultaneously. Forty-six different inflammatory proteins were examined, including cytokines, chemokines and growth factors. These marker proteins were selected based on our own investigations of lung cancer pathogenesis as well as the results of others. Because *LKB1* is frequently co-mutated with *KRAS*, we examined the result of LKB1 knockdown by short-hairpin RNA (shRNA) in supernatants from HBEC3 cells transduced with either a control (βgal) or $Kras^{V12}$ (Kras) construct (**Fig 2.1**) and showed that the majority of the examined proteins were upregulated following LKB1 loss in both control and Kras HBEC3 cells (**Fig 2.2**). We chose to focus on IL-8 (CXCL8) and Gro-α (CXCL1) because they were most abundantly expressed in these HBECs

and belong to the same CXC chemokine family known to facilitate lung cancer progression through the common receptor CXCR2 (**Fig 2.2**). We further validated the increased levels of CXCL1 and CXCL8 in these supernatants by ELISA (**Fig 2.3**). To assess whether this observation is more broadly applicable, we examined the production of CXCR2 ligands in four parental HBEC cell lines (H2, H3, H4 and H7) following transient knockdown of LKB1 via siRNA. CXCL8 production was increased in all the HBECs and the transcription levels of three other CXCR2 ligands were also elevated following LKB1 loss in the H2 and H7 cell lines (**Fig 2.4**). Interestingly, we also observed slower cell proliferation with large and flat cell morphology following LKB1 loss in βgal HBECs, consistent with previous descriptions of senescence-associated phenotypes (**Fig 2.5**). Senescence cells are associated with heightened inflammatory secretome including CXCR2 ligands (27, 28). However, because we also observed increased secretion of CXCL8 in the Kras HBECs (H2, H3 and H7) without evidence of senescence-associated phenotypes, as noted above, we reasoned that the elevation of CXCR2 ligands in HBECs is not primarily due to cell senescence (**Fig 2.3, 2.5, 2.6**). Taken together, these data indicate that LKB1 loss increases CXCR2 ligand expression in the HBECs.

Regulation of CXCR2 ligands by LKB1 in NSCLC cells

It is possible that *LKB1* mutation is a later stage event in lung cancer development. Therefore, we sought to assess whether the LKB1-CXCR2 ligand regulation occurs in established NSCLC cell lines. First, we chose cancer cells with intact LKB1 expression, including H322, H1693 and H1793 (**Fig 2.7**). Knockdown of LKB1 in these cancer cell lines increased the expression of

certain CXCR2 ligands at the transcription level (**Fig 2.8**). On the other hand, we selected four NSCLC cell lines harboring intrinsic *LKB1* mutations including A549, H838, H1568 and H2126 (**Fig 2.7**) and re-expressed wild type LKB1 in these cells via retroviral transduction (**Fig 2.9**). We showed that there was less CXCL8 produced following re-expression of LKB1 and the transcription levels of other CXCR2 ligands also decreased compared to the vector control in both A549 and H838 cell lines (**Fig 2.10**). However, we did not observe consistent downregulation of these ligands in H1568-LKB1 cells and we were not able to generate the H2126-LKB1 isogenic cell line due to repeated loss of LKB1 expression in these cells (**Fig 2.7, 2.11**). Compared to the consistent results from different HBEC lines, the discrepancy in established cancer cell lines may reflect their genetic complexity that could potentially disturb LKB1-CXCR2 ligand regulation. To test whether this regulation is dependent on LKB1 kinase function, we also re-expressed LKB1 with a mutated kinase domain (kinase dead) in these cancer cells. The results showed that kinase dead LKB1 decreased the expression of some CXCR2 ligands, however to a much less extent compared to wild type LKB1, indicating that LKB1 kinase activity is important in the regulation of CXCR2 ligands (**Fig 2.10**). In addition, we determined whether *LKB1* mutation could predict high level of CXCR2 ligands in human NSCLC cell lines. We performed a non-supervised clustering analysis on forty-three NSCLC cell lines using the expression of CXCR2 ligands from the CCLE database. These cell lines were automatically divided into either Cluster 1 with low ligand expression or Cluster 2 with high ligand expression. We showed that cell lines with *LKB1* mutation randomly distributed in the two

clusters while 9 out of 11 cell lines with both *KRAS* and *LKB1* mutations were stratified into Cluster Two, indicating that *KRAS*/*LKB1* double mutation but not *LKB1* mutation alone predicts high levels of CXCR2 ligands (**Fig 2.12**). Taken together, these data suggest that *LKB1* regulates CXCR2 ligand expression in some human NSCLC cells and its co-mutation with *KRAS* can potentially serve as a genetic biomarker for high ligand expression.

The expression of CXCR2 ligands in mouse lung tumor

To measure CXCR2 ligands *in vivo*, we obtained lung tumors that spontaneously developed in our GEMM and compared CXCR2 ligand expression between *Kras*^{G12D} (K) mice and *Kras*^{G12D};*Lkb1*$^{lox/lox}$ (KL) mice. Results from RT-PCR revealed that four out of five examined CXCR2 ligands increased in KL mouse tumors from both adenocarcinoma and squamous cell carcinoma compared to K tumors (**Fig 2.13**). To exclude the possibility higher CXCR2 expression in KL mice is due to greater tumor burden or more advanced tumor grade histology, we also utilized lung tumors from *Kras*^{G12D};*Tp53*$^{lox/lox}$ (KP) mice. We found that CXCR2 ligands in KP tumors were lower than those in KL tumors, despite the fact that KP tumors are similarly aggressive (**Fig 2.13**). As CXCR2 ligands have similar biological functions through the same receptor, we combined their relative expression in individual tumors as the CXCR2 ligand score and showed that the score from KL lung tumors is more than 100 times higher than that from either K tumors or KP tumors (**Fig 2.14**). As the tumor taken from GEMM is a mixture of multiple cell types, we sought to generate syngeneic murine lung tumor cell lines for precise measurement of CXCR2 ligands in tumor cells. As KL tumor cells did not grow *in vitro*, we

introduced *Tp*53 mutation in these cells and showed that KPL cells tended to express higher level of CXCR2 ligands compared to their KP counterparts (**Fig 2.15**).

Mechanisms of LKB1-dependent regulation of CXCR2 ligands

Next, we sought to explore the mechanisms underlying LKB1-CXCR2 ligand regulation. We first examined the NF-κB pathway because it is the master regulator of inflammatory proteins. Indeed, we found increased phosphorylation of p65 following LKB1 loss in HBECs, indicating increased activity of the NF-κB pathway (**Fig 2.16**). We further confirmed this finding by showing enhanced localization of p65 into the nucleus upon LKB1 knockdown (**Fig 2.16**). Importantly, inhibition of the NF-κB pathway either by a chemical inhibitor BMS345541 or genetic knockdown of IKKB decreased the secretion of CXCL8 and the transcription of CXCL1 and CXCL2 in HBECs (**Fig 2.17**). Furthermore, we also observed LKB1-dependent alteration of NF-κB signaling in cancer cells. Knockdown of LKB1 in H1793 cells increased p65 phosphorylation while re-introduction of wild type LKB1 decreased p65 nucleus localization in A549 cells (**Fig 2.18**).

Although regulation of different CXCR2 ligands converge through the NF-κB pathway, individual ligands can also be regulated by different pathways (29). Specifically, we found that CXCL8 is also regulated by the WNT pathway. We first demonstrated that knockdown of LKB1 in HBECs increased β-catenin phosphorylation and its nuclear localization, indicating increased activity of WNT signaling (**Fig 2.19**). In contrast, LKB1 re-introduction decreased β-catenin phosphorylation and its nuclear localization in A549 cells (**Fig 2.20**). Decreased WNT activity by wild type LKB1 re-introduction was further confirmed by decreased luciferase intensity in LEF/LCF luciferase

reporter assay (**Fig 2.21**). However, kinase dead LKB1, seemed to have a minor effect on the WNT pathway determined by these assays (**Fig. 2.20, 2.21**). Importantly, blockade of the WNT pathway either by chemical inhibitor XAV939 or knockdown of β-catenin impaired CXCL8 production in HBECs (**Fig 2.22**).

Identification of MARKs as the connection between LKB1 and NF-κB signaling.

Regulation of the WNT pathway by LKB1 has been well documented in previous studies (30-33). Therefore, we focused on elucidating the mechanism by which LKB1 regulates the NF-κB pathway. LKB1 is known to directly phosphorylate at least 14 downstream proteins that belong to six sub-families, including the AMPKs (**Fig 2.23**). To screen the proteins that participate in the regulation of the NF-κB signaling, we knocked down these downstream proteins in individual subfamilies in HBECs and found that loss of MARK but not other sub-family proteins increased p-65 phosphorylation (**Fig 2.24**). Further evaluation of individual MARK proteins revealed that loss of each MARK protein isoform was able to activate the NF-κB pathway to various extents, suggesting that MARKs regulate the NF-κB pathway in a highly redundant manner (**Fig 2.25**). In addition, we treated the HBECs with compound 39621, a MARK inhibitor that could inhibit the kinase function of all MARKs by competing their ATP binding sites and found that 72-hour inhibitor treatment increased the level of p-65 phosphorylation and subsequently led to increased CXCL8 production (**Fig 2.26**). Taken together, these results reveal that LKB1 regulation of the NF-κB signaling is mediated by MARKs, independent of AMPKs.

Discussion

In this study, we discover that LKB1 loss alters the inflammatory secretomes in pulmonary epithelial cells. In our initial screening, we show more than two thirds of the ligands under evaluation are upregulated upon LKB1 knockdown in both βgal HBEC and Kras HBEC cell lines. We choose CXCR2 ligands as our focus due to their abundance and known significance in the pathogenesis of NSCLC. Although we do not exclude LKB1 loss-induced cell senescence in βgal HBECs, we do not observe senescence phenotypes in Kras HBECs, indicating that upregulation of CXCR2 ligands is an event primarily due to LKB1 loss rather than an effect of cell senescence. Utilizing HBECs allows us to study the effect of LKB1 in a relatively uncomplicated genetic background because these immortalized but normal pulmonary epithelial cells bear minimal somatic mutations. We obtained consistent upregulation of CXCR2 ligands by LKB1 loss across different HBECs.

We further reveal the LKB1-CXCR2 ligand regulation in established human NSCLC cell lines. Although knockdown of LKB1 in cancer cell lines also increases CXCR2 ligands, some of these ligands remain unchanged. Re-introduction of wild type LKB1 into cancer cells carrying intrinsic *LKB1* mutations regulates CXCL2 ligand expression differently depending on the individual cell line. We suspect this discrepancy among different cancer cells is the result of their complicated genomic backgrounds, which may interrupt this regulation at the transcriptional, translational, or post-translational levels. Nevertheless, we find that *KRAS* and *LKB1* double mutation in human NSCLC cell lines is associated with higher expression of these ligands, which serves as a genetic marker for patients who may be potentially suitable for CXCR2 blockade therapy.

Notably, *LKB1* mutation alone is not sufficient to predict high levels of CXCR2 ligand, possibly due to its insufficiency to overcome distinct genetic backgrounds among different cell lines, which may be also involved in the regulation of CXCR2 ligands. However, it is possible that these cancer cell lines still express higher level of CXCR2 ligands compared to their normal epithelial counterparts. We experimentally prove this hypothesis by using two sets of HBEC/cancer cell pairs. Each pair is obtained from the same patient, minimizing the genetic variation between individuals. We demonstrate that both cancer cell lines, HCC4058 and HCC4087, secrete higher levels of CXCL8 compared to their normal epithelial counterparts both at the basal level and following LKB1 knockdown, although HCC4058 produces five-fold less CXCL8 than does HCC4087. Notably, compared to the epithelial cells, both cancer cell lines express lower amounts of LKB1 (**Fig 2.27**).

We validated our *in vitro* findings in the genetically engineered murine models. Although we tested CXCR2 ligand expression in the entire tumor mass which is comprised of many different cell types, the result still suggests an inflammatory microenvironment with higher levels of CXCR2 ligands in KL tumors. This is also consistent with the previously reported gene expression profile of these tumors (34). Importantly, we show these ligands are lower in pulmonary tumors with *Kras* and *Tp53* mutation, which grow and metastasize at a similar rate compared to the KL tumors. This comparison suggests that the higher expression of CXCR2 ligands in KL tumors is not primarily due to tumor burden or aggressive behavior.

As the major CXCR2 ligand, CXCL8 is mostly regulated by the NF-κB and MAPK pathways (29). Indeed, we show that the NF-κB pathway is activated upon LKB1 loss in both HBECs and cancer cells while re-introduction of wild type LKB1 reduces its signaling in cancer cells. Importantly, NF-κB inhibition impairs LKB1-induced CXCR2 ligand expression. We also assessed the MAPK pathway and did not observe consistent change following LKB1 loss in different HBEC lines, suggesting the MAPK pathway may not be important in this regulation (**Fig 2.28**). In addition, we reveal that the WNT signaling is involved in LKB1-dependent CXCL8 regulation, consistent with previous findings showing that the WNT pathway is downstream of LKB1 and upstream of CXCL8 (35). However, we do not observe any alterations of the other CXCR2 ligands after WNT signaling blockade, possibly due to the fact that there are no binding sites for the WNT signaling in their promoter regions.

The microtubule affinity-regulating kinases (MARKs) belong to a subfamily of LKB1 substrates and are originally identified to phosphorylate microtubule-associated proteins in regulation of microtubule dynamics (9, 36, 37). Although MARKs have been studied, for example, in the pathogenesis of Alzheimer's disease for decades, their roles in cancer are just beginning to be understood (7, 8, 38, 39). Recent studies show that MARKs connect LKB1 with the Hippo pathway and are functionally important for the tumor suppression of LKB1 (8). Loss of MARKs also promotes tumor metastasis by upregulating the epithelial-to-mesenchymal transition transcription factor Snail (7). However, contributions of MARK to inflammation are as yet unknown. We identify MARKs as downstream of LKB1 regulating the NF-κB pathway and further

show that inhibition of MARK function or knockdown of individual MARK proteins is able to activate the NF-κB pathway and increase CXCL8 production. This regulation, however, is likely indirect because components from the NF-κB pathway are phosphorylated for activation. Surprisingly, although AMPK is known to suppress the NF-κB pathways through multiple mechanisms (40), we do not find consistent repression of the AMPK signaling upon LKB1 loss in HBECs and loss of AMPK does not induce p65 phosphorylation (**Fig 2.28**). It is possible that cells in standard culture condition do not have adequate energy stress, and under these circumstances AMPK is not sufficiently activated by LKB1.

In conclusion, this study demonstrates a dysregulation of inflammation induced by LKB1 loss in tumorigenesis and progression of NSCLC and identifies CXCR2 ligands as major targets. Further mechanistic experiments reveal the MARKs-dependent NF-κB pathway as the control point mediating levels of CXCR2 ligands. These data suggest that CXCR2 blockade may be a particularly effective therapy against LKB1-deficient tumors. Based on these findings and as these agents are being developed, a personalized, targeted approach may be utilized to define the patient population in which CXCR2 blockade will be most effective.

Materials and Methods

Cell lines and cell culture

Immortalized HBEC lines and HBEC-cancer cell pairs were gifts kindly provided by Dr. John D. Minna from University of Texas Southwestern Medical Center. The establishment of these cell lines is as previously described (11). All cell lines were authenticated in the UCLA Genotyping and Sequencing Core and routinely tested for the presence of Mycoplasma using the MycoAlert Mycoplasma Detection Kit (Lonza). HBEC lines were cultured in Keratinocyte serum-free media supplemented with 30ug/ml bovine pituitary extract and 0.2ng/ml recombinant epidermal growth factor (Life Technologies). NSCLC cell lines A549, H838, H1568, H322, H1693, H1793 and H2126 were purchased from ATCC and cultured in RPMI1640 (Corning) with 10% fetal bovine serum. Cells were growing in a 5% CO_2 atmosphere at 37°C and cultured within 10 passages of genotyping. The syngeneic murine tumor cell lines were gifts from Dr. David Shackelford and were cultured in the same conditions as were NSCLC cell lines.

Gene knockdown by RNA interference

Cells were plated and allowed sufficient attachment overnight in a 6-well plate. They were then transfected with small interfering RNA (siRNA) using Lipofectamine RNAiMAX (Life Technologies) at final concentration of 15 nmol/L for 72h. siRNAs against LKB1, CTNNB1, IKKB and scramble control were pooled siRNA purchased from Dharmacon GE healthcare. Small interfering RNAs against LKB1 substrates were from Sigma. Stable isogenic cell lines were

made via transduction with retro- or lenti-virus and selected with puromycin (EMD chemicals) for 10 to 14 days as previously described (41). Short-hairpin RNAs against LKB1 were purchased from Sigma. Plasmids carrying empty vector, wild type LKB1 or kinase dead LKB1 were purchased from Addgene.

Luminex-based multiplex assay

We performed a fluorescence-based cytokine screen using the Luminex-based multiplex system from Bio-Rad. HBEC cells were cultured until 20% confluence and then washed twice with PBS before fresh medium was added. Cells were incubated for an additional 72 hours, after which the supernatants were collected and centrifuged to remove floating cells. Lysates were prepared from the adherent cells, and the BCA assay was performed to determine protein concentration. A customized panel of forty-six human cytokine/growth factors (Bio-Rad) was used, and all samples were run in triplicate. Results were normalized to protein concentration from the matched lysates and then expressed as fold-change over control cell cytokine secretion (after normalization). We used ANOVA to compare cell populations for each analyte, and adjusted for multiple testing by computing the false-discovery rate using the q value method implemented in R. Cytokines differentially produced by the cells were verified by enzyme-linked immunosorbent assay (ELISA) or RT-PCR

Proliferation assay

As an indication of cell viability and proliferation, cellular ATP levels were measured using the ATPlite 1 step Luminescence Assay Kit (Perkin Elmer). Briefly, HBEC cells were plated in 96-well plates at 1500 cells per well. Eight replicates for each condition were plated for each independent experiment. ATP luminescence was assessed every 24 hours up to 96 hours. Readings at each time point were normalized to the 0 hour readings as control for plating differences.

Inhibitor treatment

Cells were treated with indicated concentration of the inhibitors for 72 hours. Inhibitors were dissolved in DMSO and stored in -20°C at 20mM stock. Cycles of freeze and thaw are no more than 3 times. The NF-κB pathway inhibitor BMS345541 was purchased from Sigma. The WNT pathway inhibitor XAV939 and MARK inhibitor compound 39621 were purchased from Calbiochem.

Luciferase reporter assay

The A549 isogenenic cell lines were plated in 96-well plates at 5000 cells per well and allowed overnight attachment. Topflash or Fopflash plasmid (Addgene) was transfected into each well using Lipofectamine 2000 (Life Technologies). The plate was read by BioTak using the Firefly Luciferase Assay Kit (Promega) after 24-hour transfection. Each condition had six replicates and values from Fopflash served as an internal control for normalization.

Protein extraction and Western Blot

Cells grown to 80% confluence in 6-well plate were washed with ice-cold PBS and lysed with RIPA buffer using standard methods. Ten μg of each cell lysate was loaded per lane, and proteins were resolved by 10% SDS-PAGE and transferred to an Immobilon-P Transfer Membrane (Millipore, Danvers, MA). The membranes were blocked with 5% milk and then incubated with primary antibodies diluted in blocking solution according to the manufacturer's recommendations. Horseradish peroxidase-conjugated secondary antibodies (Bio-Rad, Hercules, CA) and enhanced chemiluminescence (ECL) reagent (Amersham Biosciences, Piscataway, NJ) were used for protein detection. Antibodies against LKB1, p65, phosphorylated-p65 (S536), AMPK, phosphorylated-AMPK (T172), β-Catenin, phosphorylated-β-Catenin (S552), p-MAPK (T202/Y204), Lamin A/C, β-Actin, α-Tubulin were purchased from Cell Signaling Technology. GAPDH was from Advanced Immunochemical Inc.

RNA extraction and Quantitative reverse transcription PCR

Total RNA was isolated using the Quick-RNA MiniPrep (Zymo), and cDNA for mRNA analysis was prepared using the High Capacity RNA-to-cDNA Kit (Life Technologies). Transcript levels of CXCR2 ligands were measured by quantitative reverse transcription PCR (qRT-PCR) using the Syber Green-based Gene Expression System (Life Technologies) in a MyiQ Cycler (Bio-Rad). Primers were adapted from Primerbank (http://pga.mgh.harvard.edu). Amplification was carried out for 40 cycles of 15 seconds at 95°C, 30 seconds at 55°C and 30 seconds at 72°C. All samples were run in triplicate, and relative gene expression levels were determined by normalizing their expression to GAPDH. Expression data are presented as fold-change values

relative to normalized expression levels in a reference sample using the following equation: RQ ¼ $2^{-\Delta\Delta Ct}$.

Enzyme-linked immunosorbent assay

Cells were plated in 6-well plates at 20% confluence per well. Following overnight attachment, old medium was replaced by 1.1ml of fresh regular medium. After 72 hours, supernatants were collected and protein levels of CXCL1 and CXCL8 were quantified using a DuoSet ELISA Development System (R&D Systems). In siRNA transfection studies, cells were transfected with siRNA against IKKB or CTNNB1 one day after LKB1 siRNA knockdown. Supernatants were collected 72 hours post-transfection and assayed as above. In MARK inhibitor studies, treatment with MARK inhibitor (40µmol/L) or the DMSO control started following overnight attachment. Supernatants were collected 72 hours after treatment initiation. Lysates were prepared from the adherent cells, and the BCA assay was performed to determine protein concentration. Results were normalized to protein concentration from the matched lysates.

Bioinformatic analysis of CXCR2 ligand expression using CCLE database

Expression data was downloaded from GEO accession GSE36139. Data was normalized by RMA approach. The expressions of CXCR2 ligands, which are CXCL1, CXCL2, CXCL3, CXCL5, and CXCL8, were extracted and transformed to z-scores. The unsupervised hierarchical cluster analysis was used to stratify cell lines based on the ligand expressions.

Genetically engineered murine model

We performed the *in vivo* studies by using Lox-Stop-Lox $Kras^{G12D}$, $Lkb1^{Lox/Lox}$, Rosa26-Lox-Stop-Lox-Luc mice (KL), Lox-Stop-Lox $Kras^{G12D}$, $Tp53^{Lox/Lox}$, Rosa26-Lox-Stop-Lox-Luc mice (KL) and Lox-Stop-Lox $Kras^{G12D}$, Rosa26-Lox-Stop-Lox-Luc mice (K) that were obtained from Reuben Shaw at Salk Institute for Biological Studies. All mice were on a FVB background. Lung tumors were induced by intranasal administration of 2.5×10^6 plaque forming units of Adeno-Cre (Gene Transfer Vector Core, University of Iowa) as previously described. Mice were sacrificed at 10 to 12 weeks after tumor induction. For the early stage studies, 2.5×10^7 plaque forming units of Adeno-Cre was administrated via nasal inhalation and mice were sacrificed at 2, 4 and 6 weeks. Mice were housed in pathogen-free facilities at UCLA and all experimental procedures performed on mice were approved by the UCLA Animal Research Committee.

Statistical analysis

Samples were plated and run in triplicate, unless otherwise indicated, and all experiments were performed at least three times. Statistical analyses were performed on all data sets, and results from one representative experiment or image are shown. All statistical analyses were performed in Prism 6 (GraphPad, La Jolla, CA) unless noted. All results are reported as mean ± SEM, unless indicated. The statistical significance of these data was determined using an unpaired, parametric *t*-test with 95% confidence interval. The statistical significance of the viability data set was determined using the Mann-Whitney test (two-tailed, 95% confidence interval). Data were reported significant as follows: * if $p \leq 0.05$, ** if $p \leq 0.01$, and *** if $p \leq 0.001$.

Figures

Figure 2.1: The expression of LKB1 after shRNA knockdown in βgal and Kras HBEC3 lines.

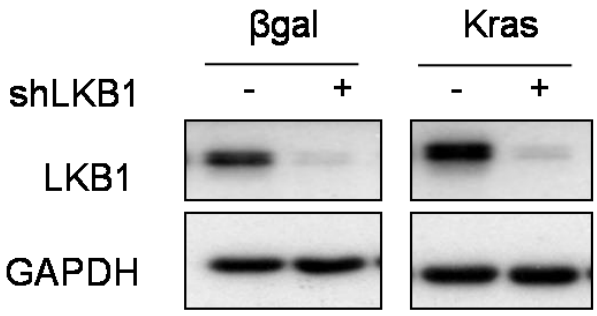

Figure 2.2: The heat map shows the relative production of the secreted inflammatory proteins due to LKB1 knockdown in both βgal and Kras HBEC3 lines using a Log2 scale (left). Red denotes a high level of production and green denotes a low level of production. The absolute amounts of the examined proteins are displayed in a dot plot (right). The red circle denotes CXCL8, the blue triangle denotes CXCL1, and the green diamond denotes G-CSF.

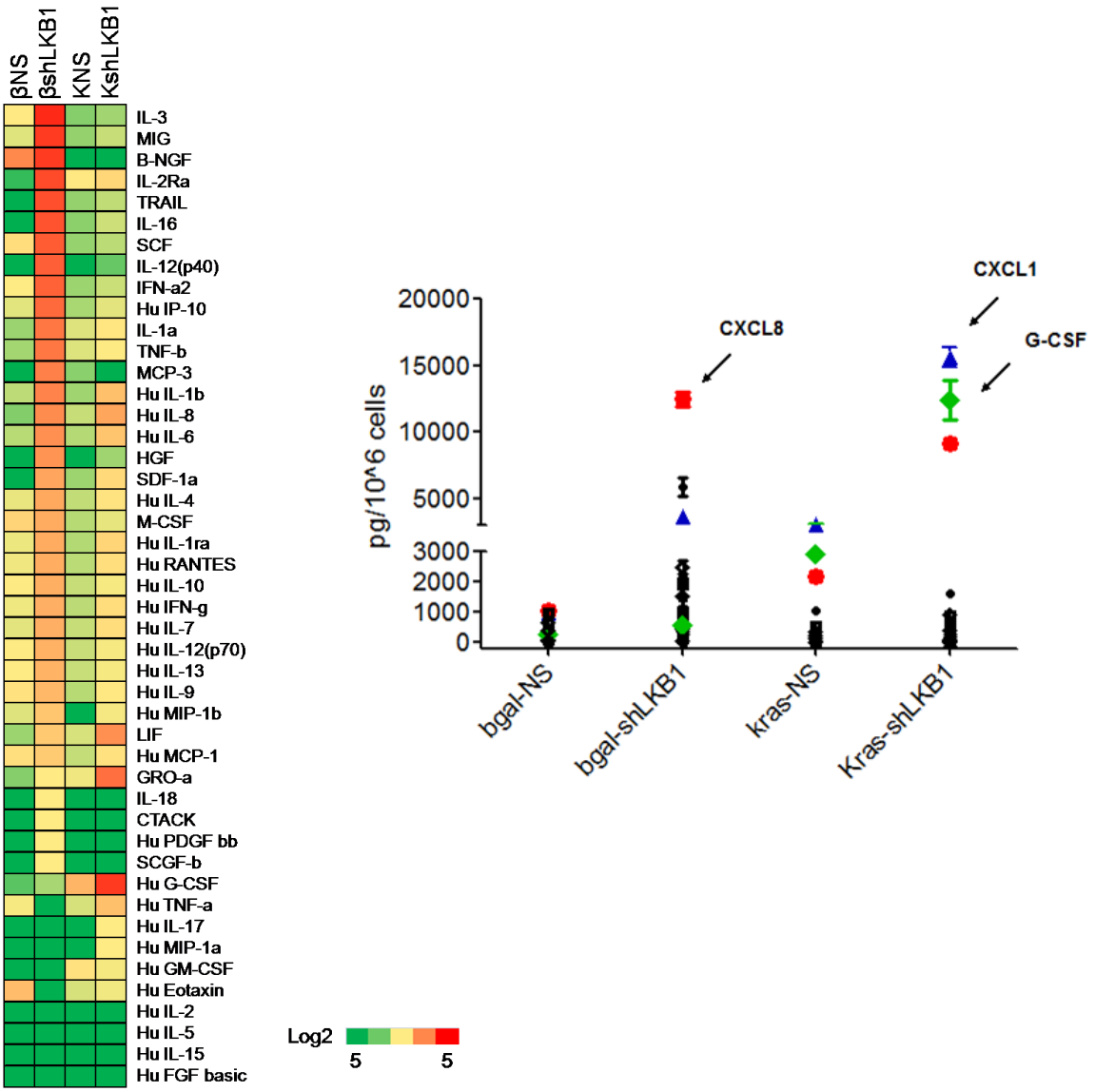

Figure 2.3: Validation of the increased production of CXCL1 and CXCL8 following LKB1 knockdown in βgal and Kras HBEC3 lines by ELISA. NS, non-silencing control.

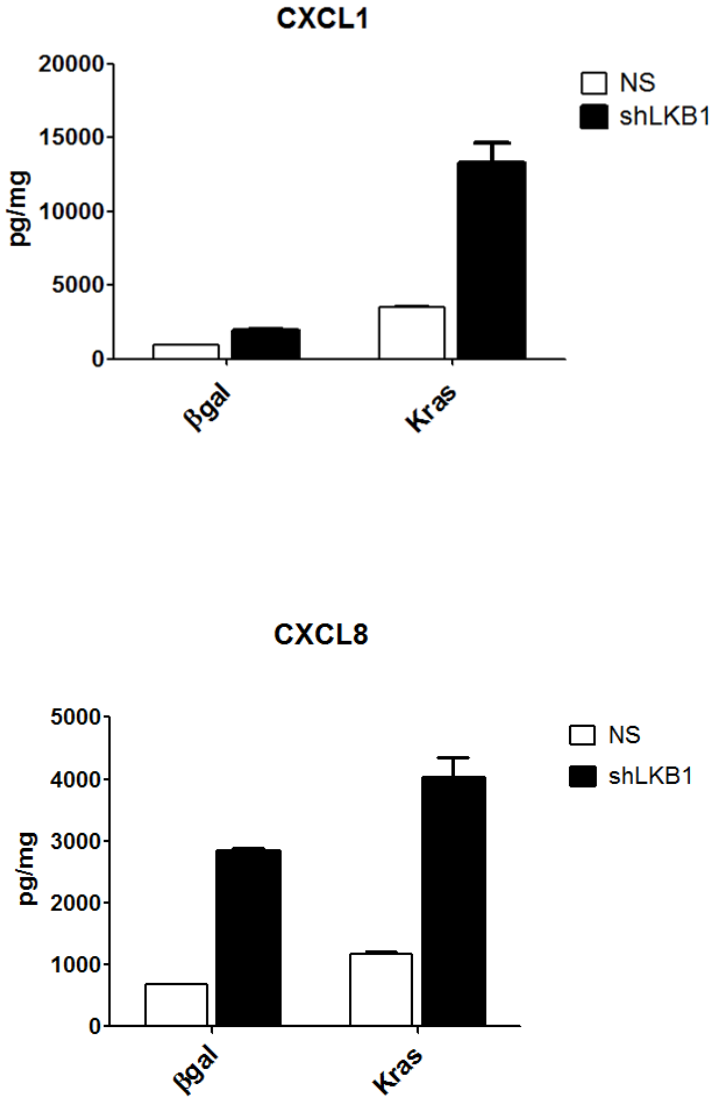

Figure 2.4: Evaluation of the transcription and protein levels of CXCR2 ligands in multiple HBEC lines (H2, H3, H4 and H7) following transient LKB1 knockdown via siRNA. Top: the level of CXCL8 determined by ELISA. Bottom: transcription levels of other CXCR2 ligands in H2 and H7.

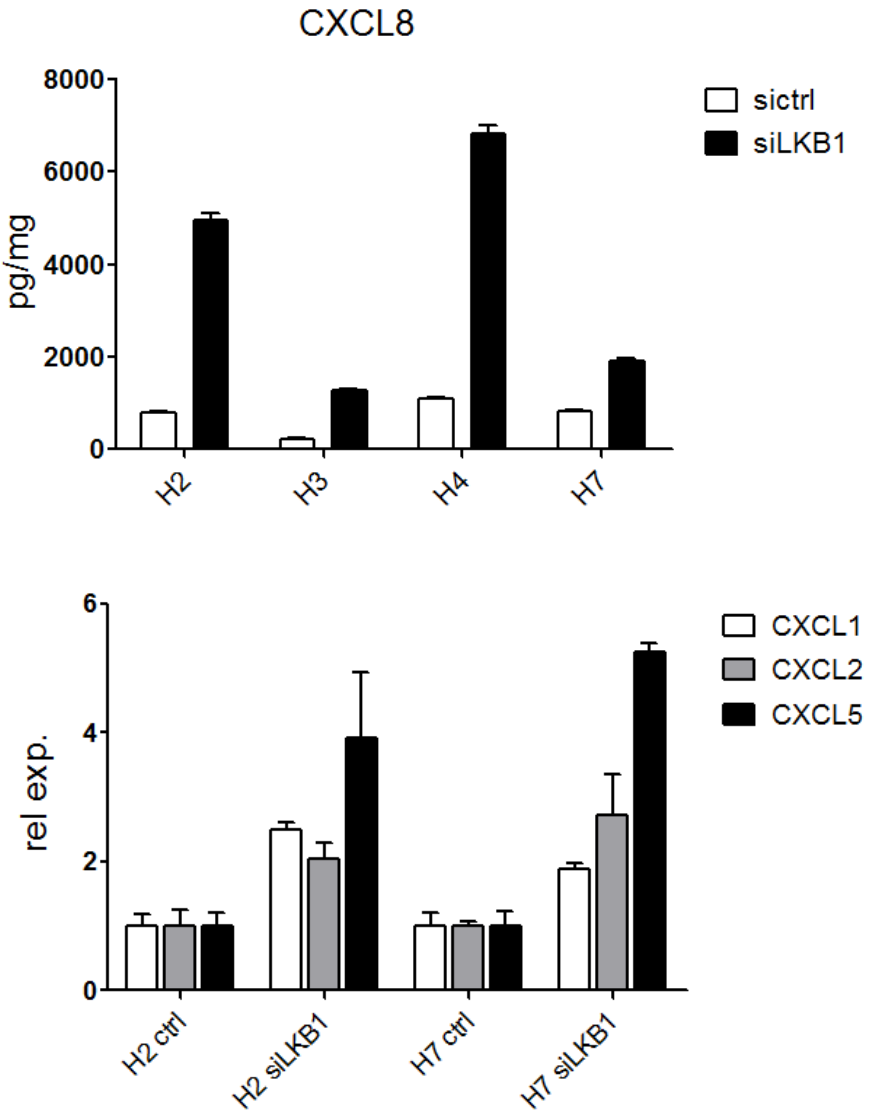

Figure 2.5: Bright field microscopy shows the morphological change of H3 cells with stable LKB1 knockdown (10x magnification) (top). Cell proliferation was evaluated by ATPlite in indicated isogenic HBEC lines (bottom). NS, non-silencing control.

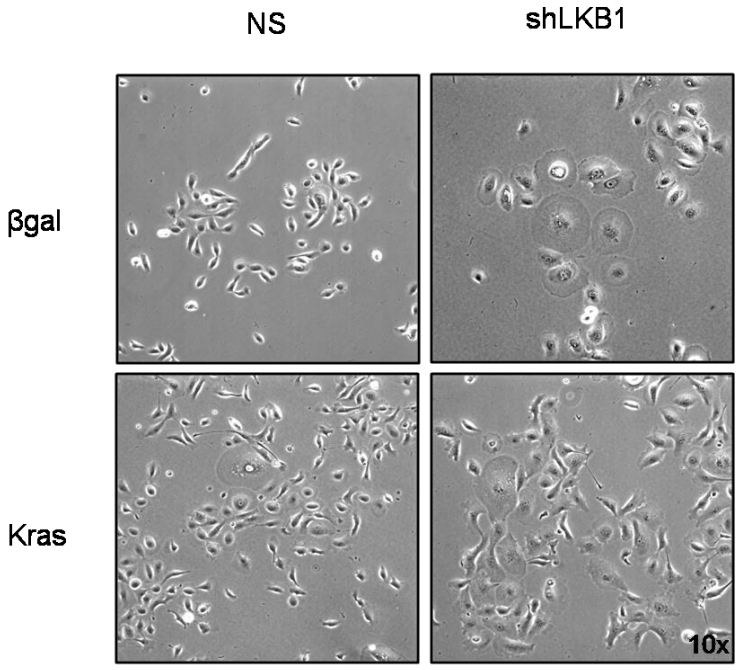

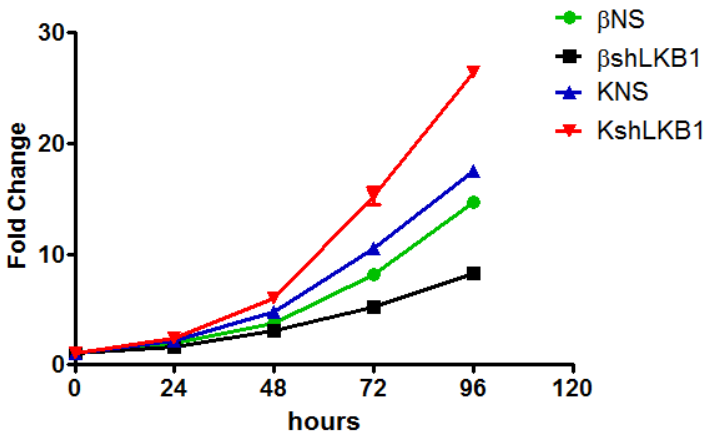

Figure 2.6: CXCL8 production upon LKB1 knockdown in H2 and H7 cells with overexpression of $Kras^{V12}$.

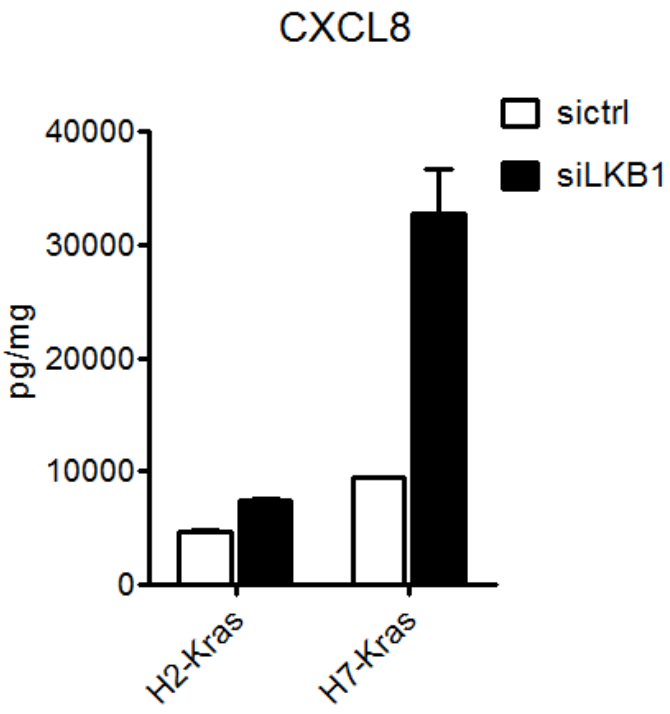

Figure 2.7: LKB1 expression in various NSCLC cell lines shown by immunoblot analysis.

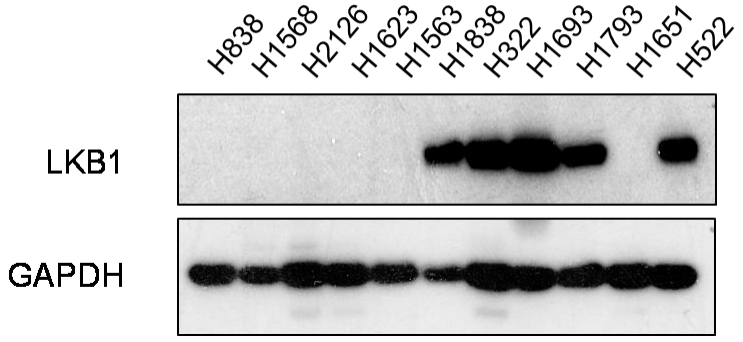

Figure 2.8: CXCR2 ligand expression upon LKB1 knockdown in the NSCLC cell lines H322, H1693, and H1793, as determined by RT-PCR. CXCL1 in H322 and CXCL3 in all the examined cell lines were not detectable. N.D., not detectable.

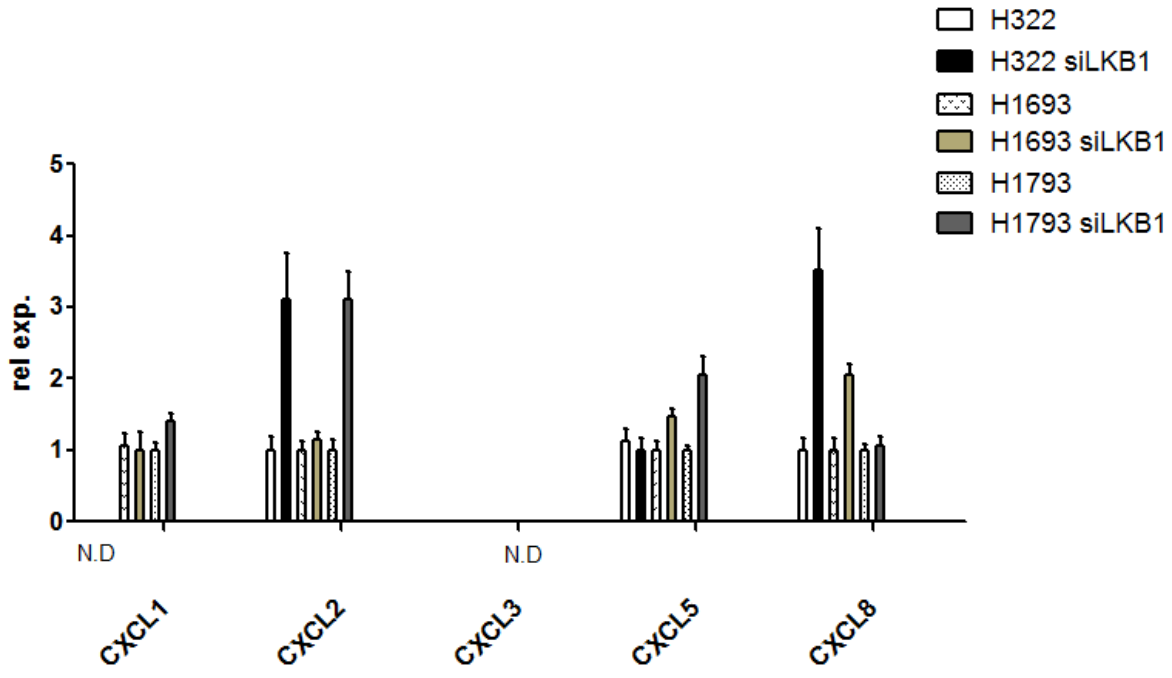

Figure 2.9: Expression of LKB1 in various isogenic cancer cell lines after transduction of the retrovirus carrying the empty control (v), wild-type LKB1 (L), or kinase dead LKB1 (KD) plasmid.

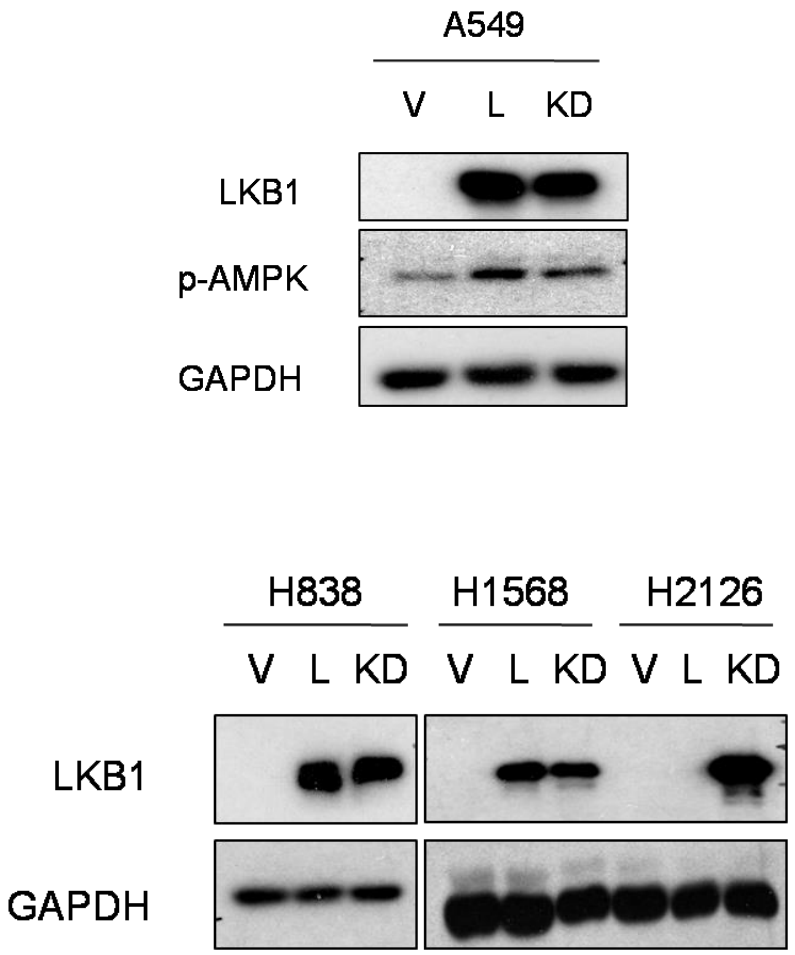

Figure 2.10: Protein level of CXCL8 determined by ELISA in A549 isogenic cell lines (top left). Transcription levels of CXCR2 ligands determined by RT-PCR in A549 (top right) and H838 (bottom) isogenic cell lines. V, empty control; L, wild-type LKB1; KD, kinase dead LKB1.

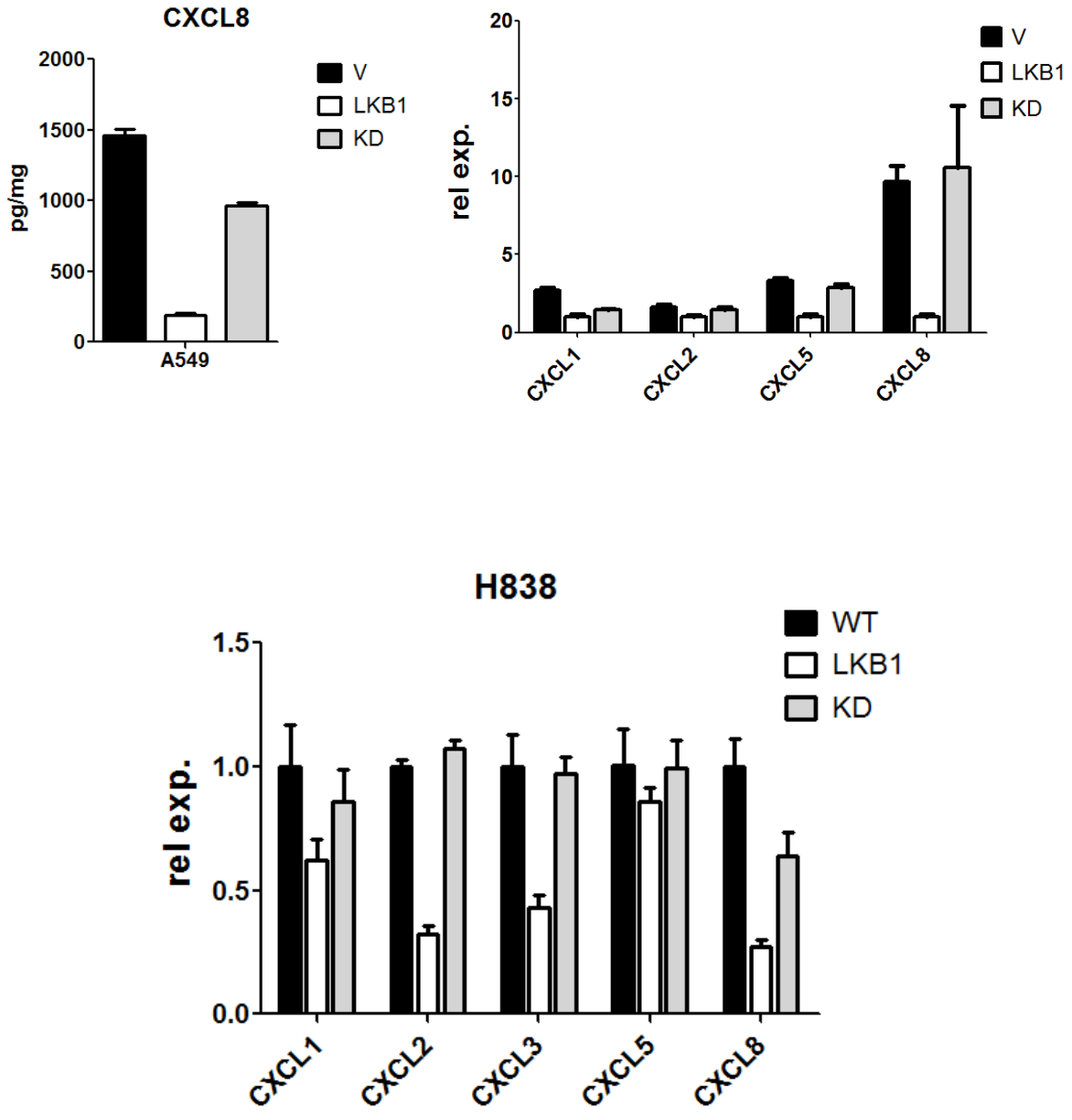

Figure 2.11: Transcription levels of CXCR2 ligands determined by RT-PCR in H1568 isogenic cell lines. V, empty control; L, wild-type LKB1; KD, kinase dead LKB1. N.D., not detectable

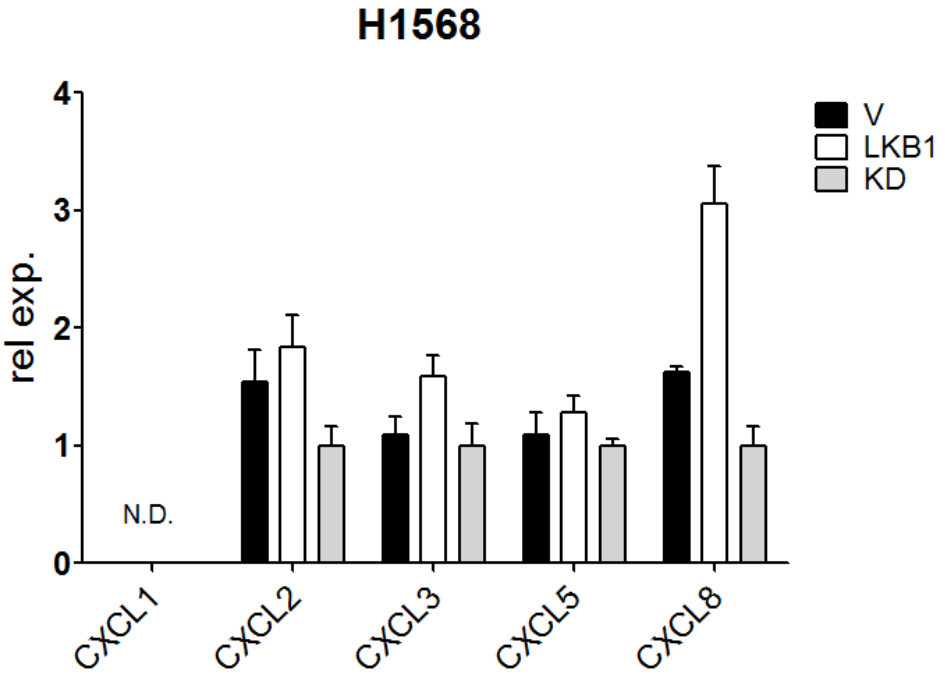

Figure 2.12: Non-supervised clustering analysis of CXCR2 ligands divides NSCLC cell lines into two clusters. Cluster one: low ligand expression. Cluster Two: high ligand expression. The red areas at the bottom of the heat map indicate *KRAS* and *LKB1* mutation status. Red arrows dictate cell lines with both *KRAS* and *LKB1* mutation.

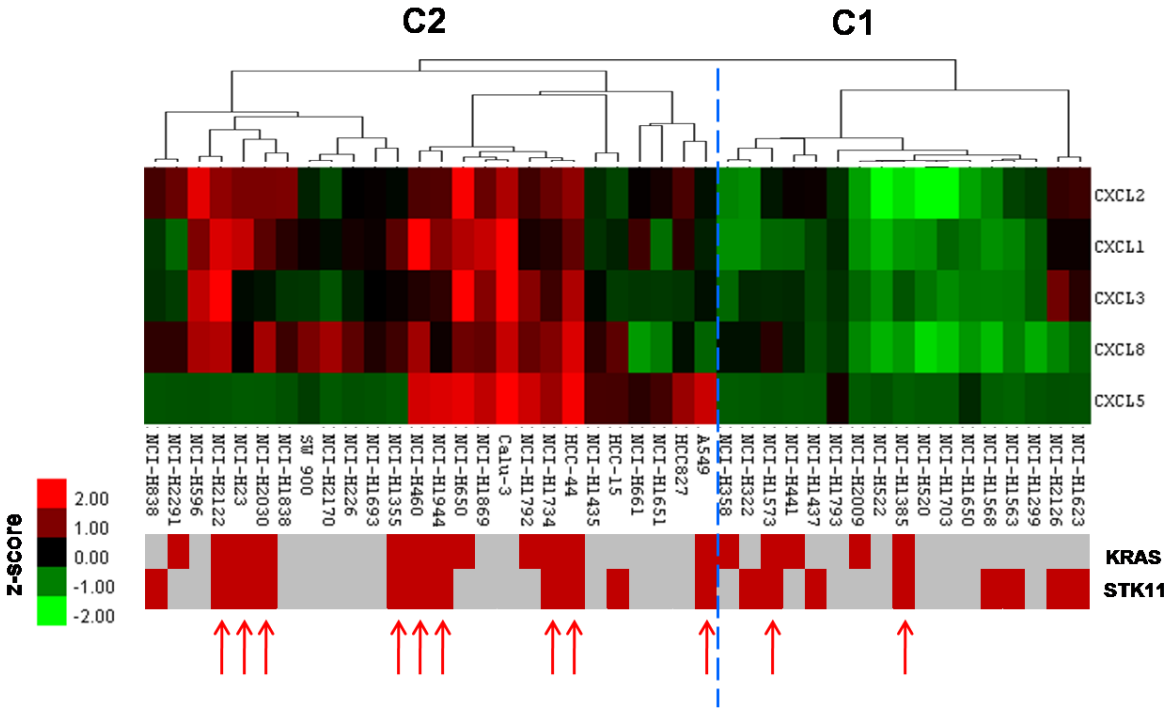

Figure 2.13: Relative gene expression of CXCR2 ligands in murine lung tumors with different genetic backgrounds and histological types. Values are in terms of the fold change determined by RT-PCR. Red denotes an increase in fold change while green denotes a decrease in fold change. K, *Kras*^{G12D}; KP, *Kras*^{G12D};*Tp53*$^{lox/lox}$; KL, *Kras*^{G12D};*Lkb1*$^{lox/lox}$. Ad, adenocarcinoma; Sq, Squamous carcinoma.

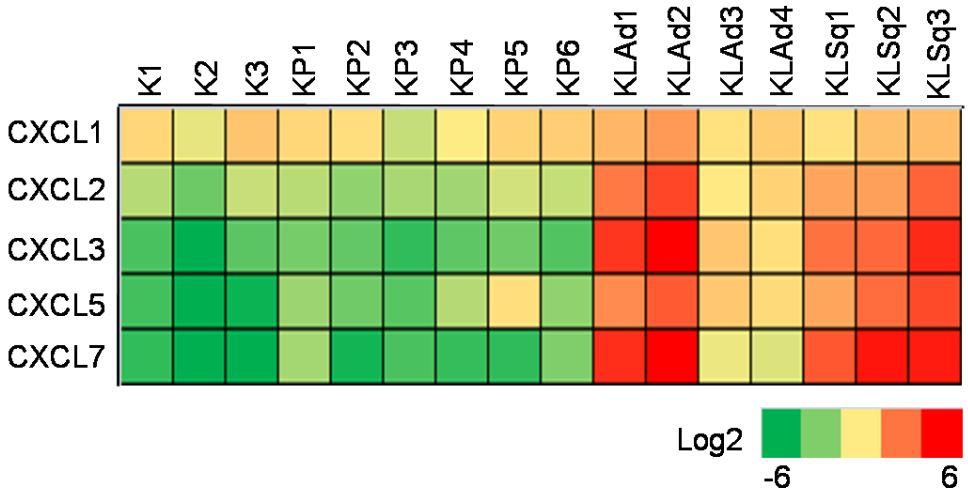

Figure 2.14: CXCR2 ligand score was generated by combining the relative expression values from all the examined CXCR2 ligands in individual tumors and then normalized to the average score of the three *Kras*^{G12D} tumors. The score is displayed using a log10 scale in a dot plot. K, *Kras*^{G12D}; KP, *Kras*^{G12D};*Tp53*$^{lox/lox}$; KL, *Kras*^{G12D};*Lkb1*$^{lox/lox}$.

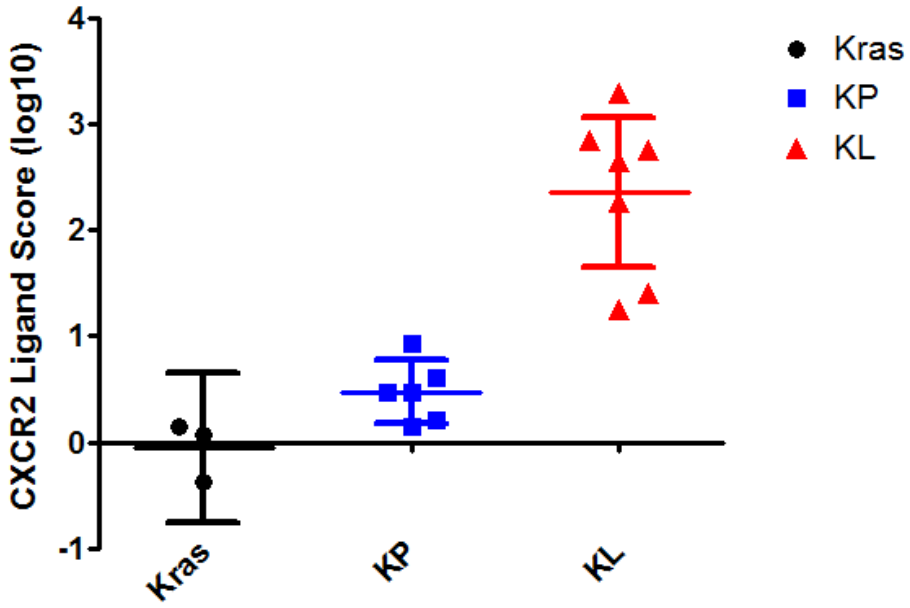

Figure 2.15: LKB1 expression in the syngeneic cell lines was determined by immunoblot analysis (top). Relative gene expression of CXCR2 ligands determined by RT-PCR is displayed in the heat map (bottom). LKB1-long, long exposure time. KPL, *Kras*^{G12D}; LKB $^{lox/lox}$; *Tp53*$^{+/lox}$. KP, *Kras*^{G12D}; *Tp53*$^{lox/lox}$

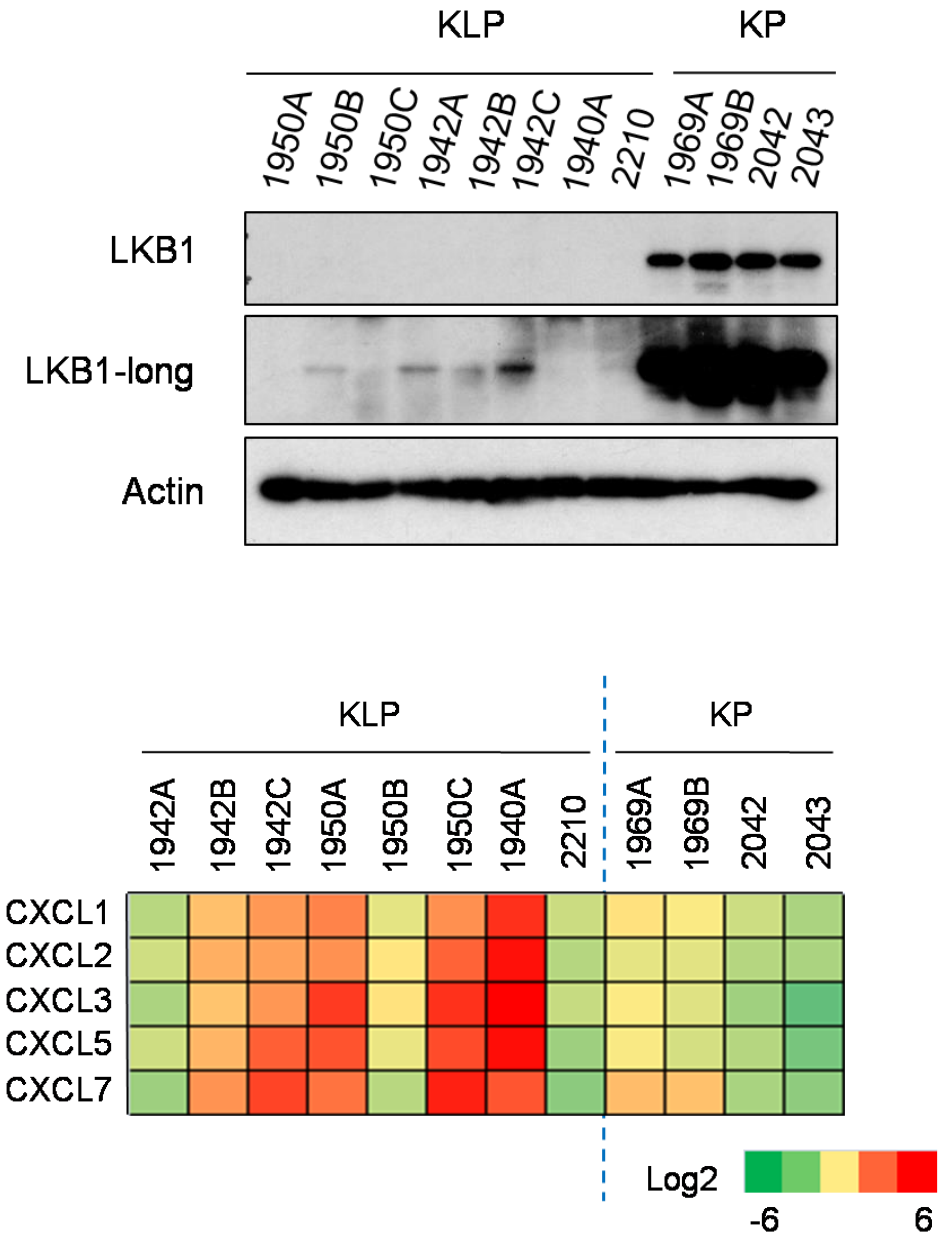

Figure 2.16: Immunoblotting of phosphorylated p65 (top) and nuclear p65 (bottom) in HBECs following LKB1 knockdown. Lamin A/C serves as the loading control for nuclear protein and Tubulin serves as the loading control for cytoplasmic protein.

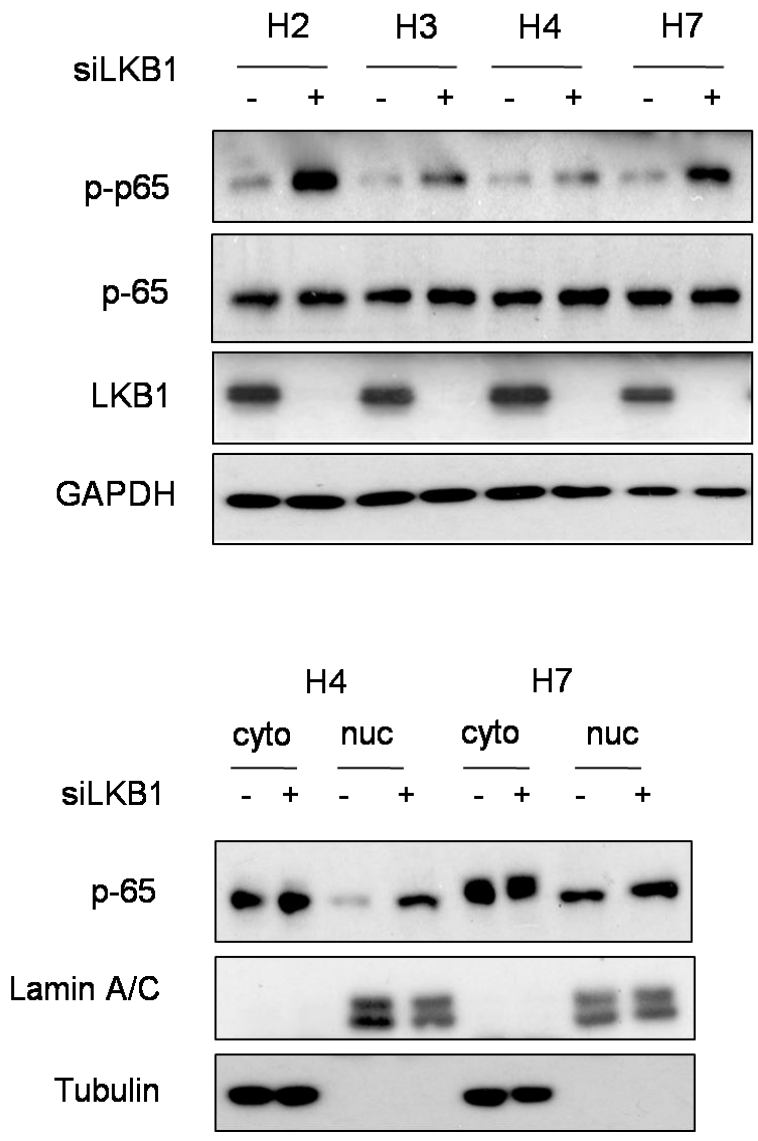

Figure 2.17: CXCR2 ligand levels were measured after 72-hour inhibition of the NF-κB pathway either by chemical inhibition using BMS345541 (1μM) or by siRNA knockdown of IKKB. CXCL8 production was determined by ELISA (top); CXCL1 and CXCL2 levels were determined by RT-PCR.

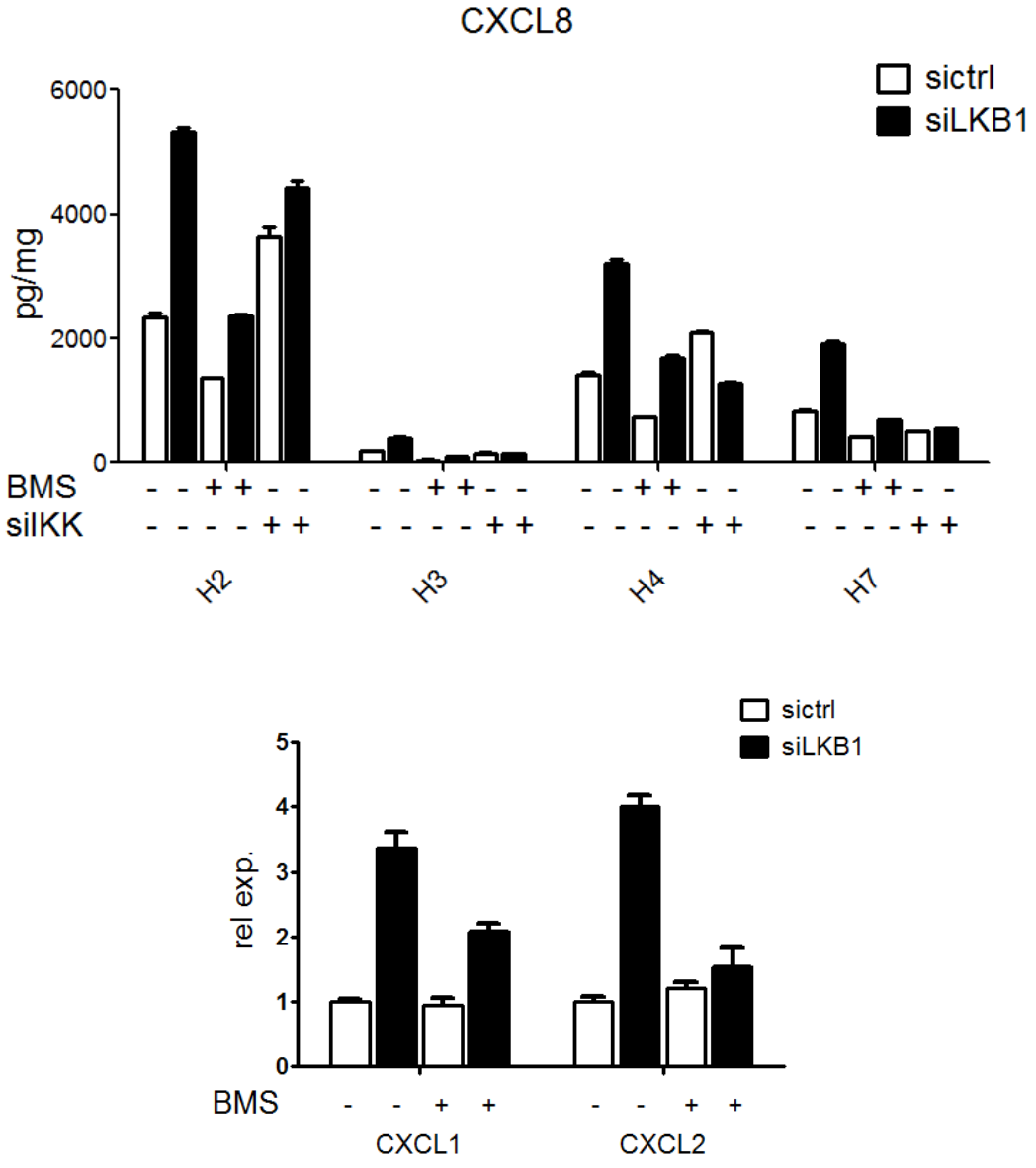

Figure 2.18: Immunoblot analysis of phosphorylated p65 following LKB1 knockdown by two shRNAs in H1793 cells (top). P65 nuclear localization in isogenic A549 cells (bottom).V, empty control; L, wild-type LKB1; KD, kinase dead LKB1. Lamin A/C serves the loading control for nuclear protein and Tubulin serves as the loading control for cytoplasmic protein.

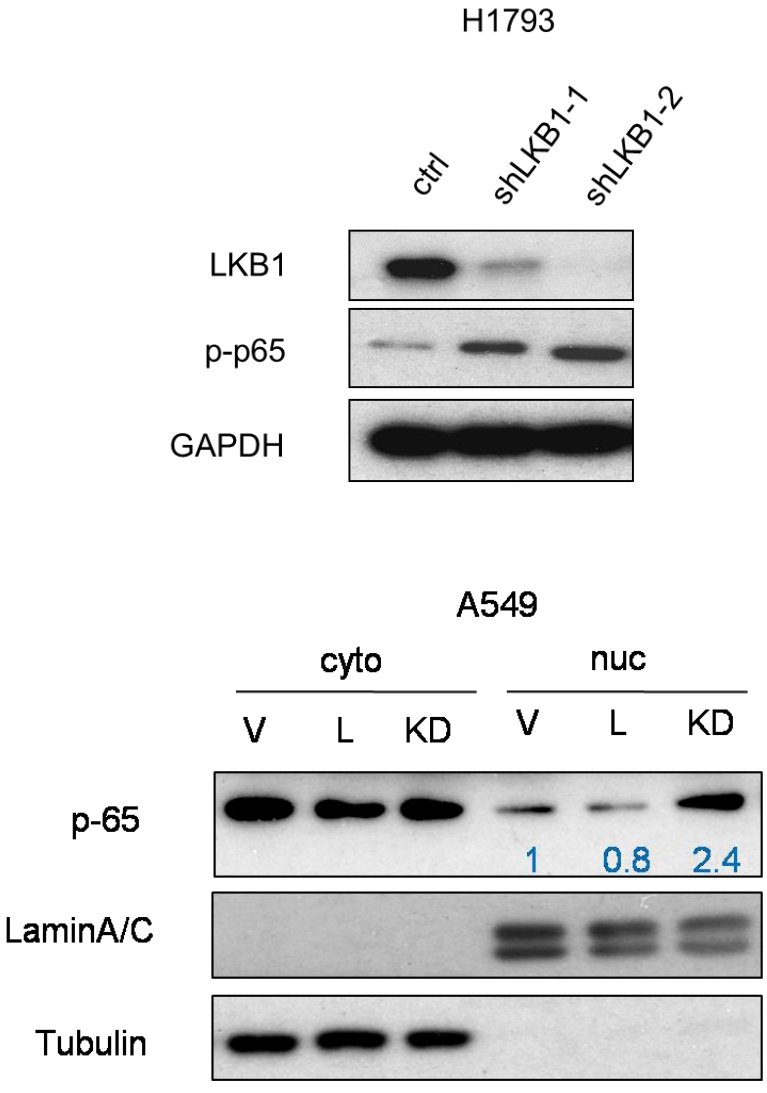

Figure 2.19: Immunoblot analysis of phosphorylated β-catenin, phosphorylated GSK-3β (top) and β-catenin nuclear localization (bottom) in HBECs following LKB1 knockdown. Two independent siRNAs were used to knockdown LKB1. Lamin A/C serves as the loading control for nuclear protein and Tubulin serves as the loading control for cytoplasmic protein.

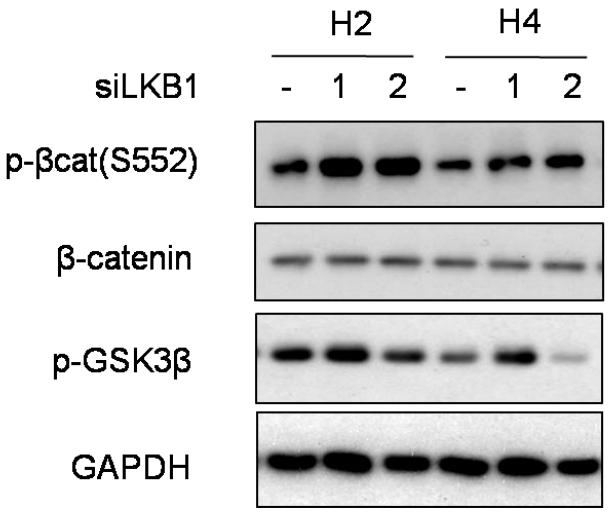

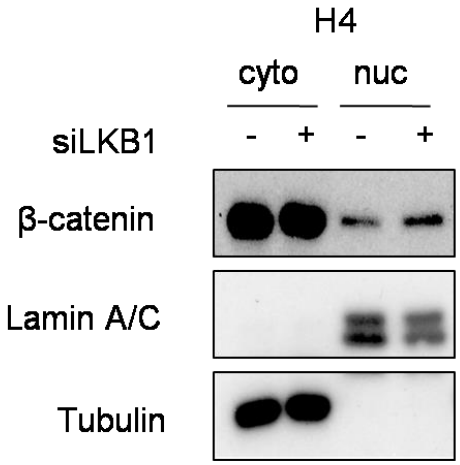

Figure 2.20: Immunoblot analysis of phosphorylated β-catenin (top) and β-catenin nuclear localization (bottom) in isogenic A549 cells. V, empty control; L, wild-type LKB1; KD, kinase dead LKB1. Lamin A/C serves as the loading control for nuclear protein and Tubulin serves as the loading control for cytoplasmic protein.

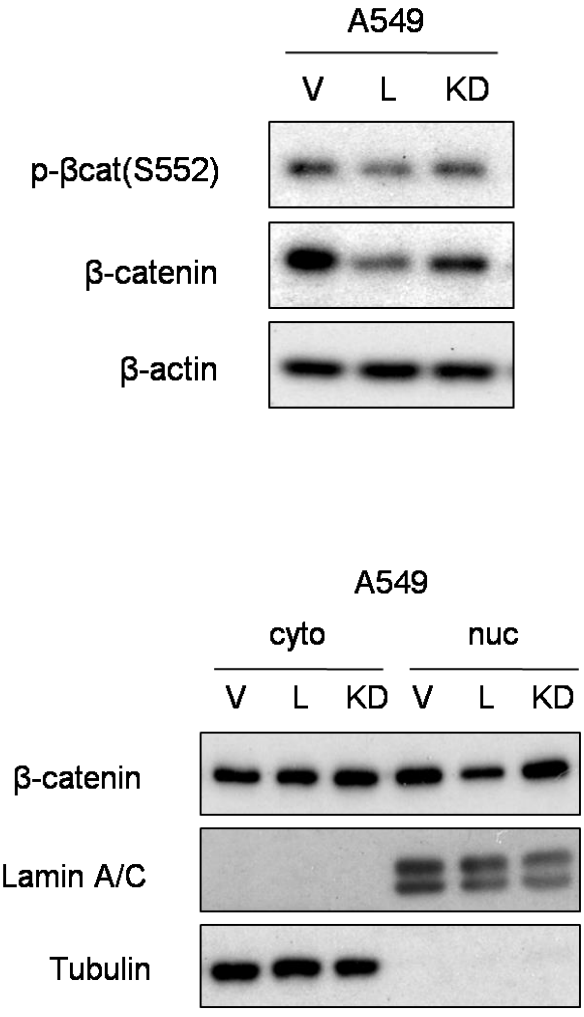

Figure 2.21: Luciferase reporter assay performed in isogenic A549 cells after transfection of either the Topflash or Fopflash plasmid. Fopflash contains mutated TCF/TEF binding sites and serves as the internal control for normalization. V, empty control; L, wild-type LKB1; KD, kinase dead LKB1.

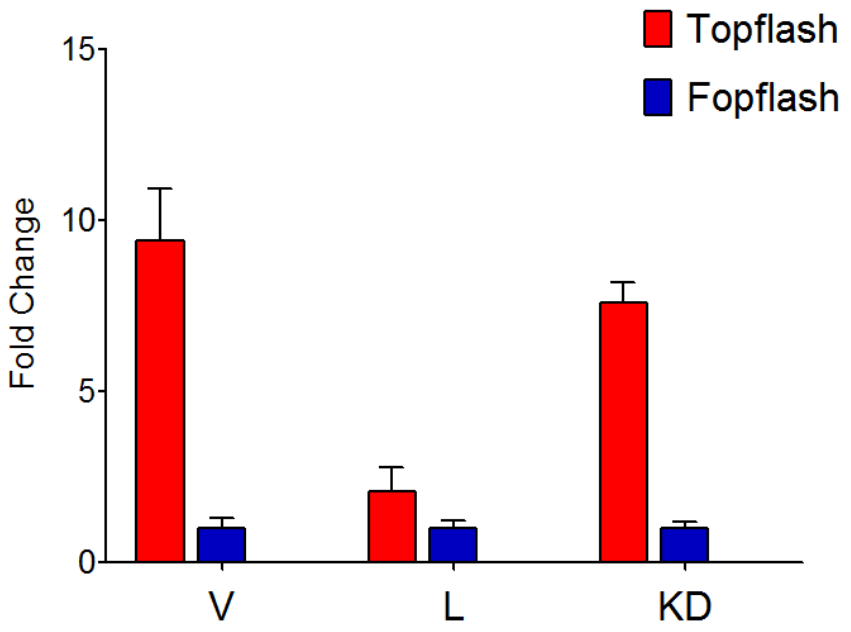

Figure 2.22: CXCL8 production after inhibition of the WNT pathway either by the chemical drug XAV939 (5 µM) or by siRNA knockdown of β-catenin for 72 hours in HBECs.

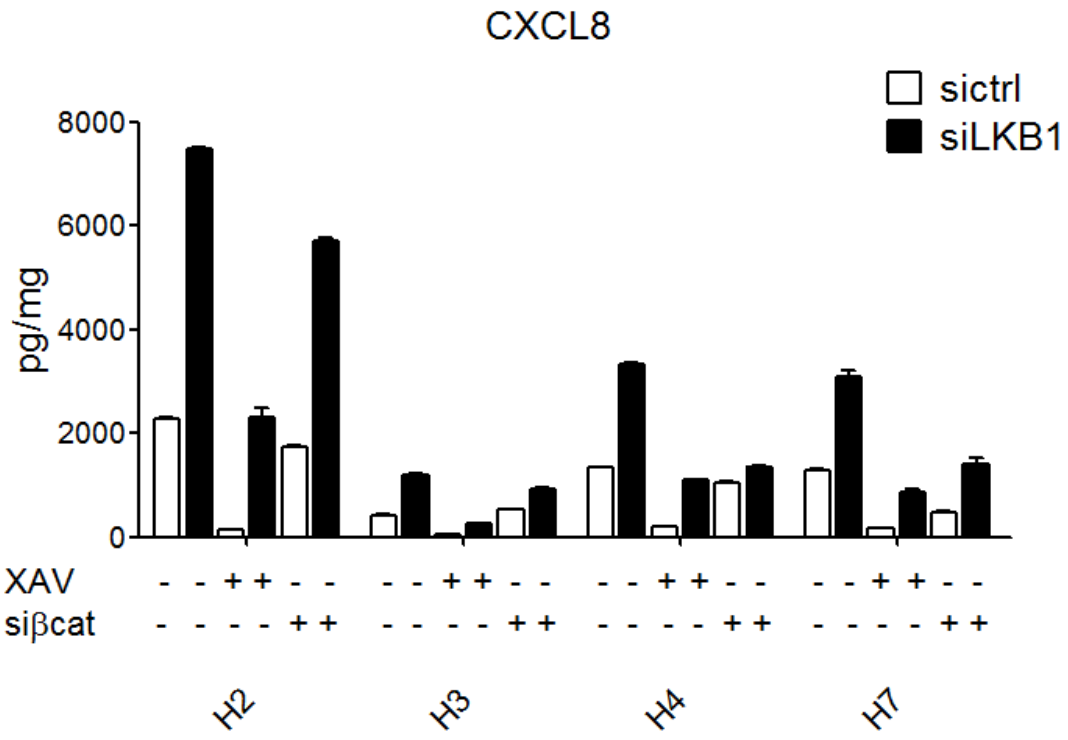

Figure 2.23: Schematic model of LKB1 substrates.

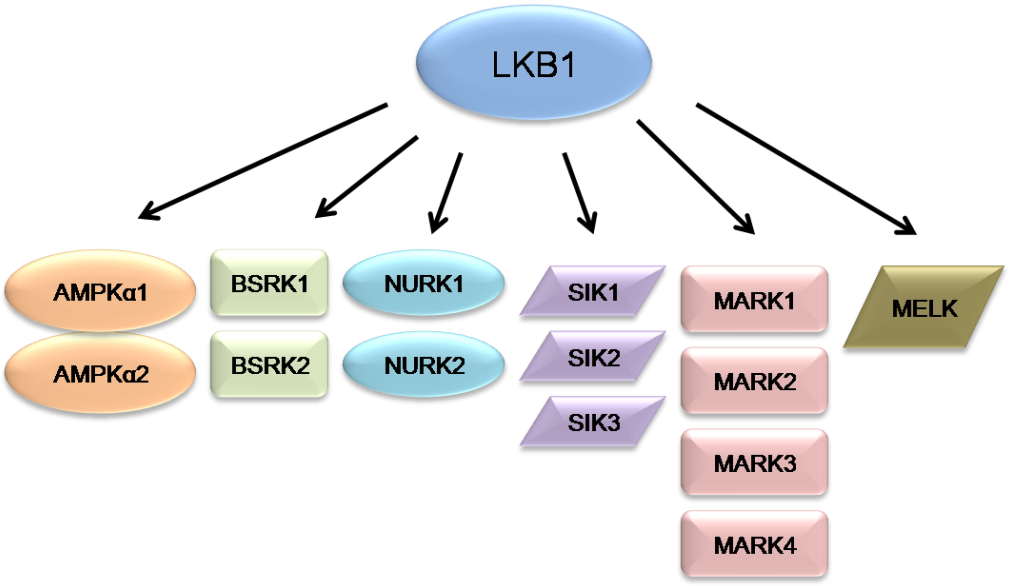

Figure 2.24: Phosphorylation of p65 was measured via immunoblotting after knocking down individual subfamilies of LKB1 substrates in H4 cells. Knockdown of LKB1 serves as the positive control.

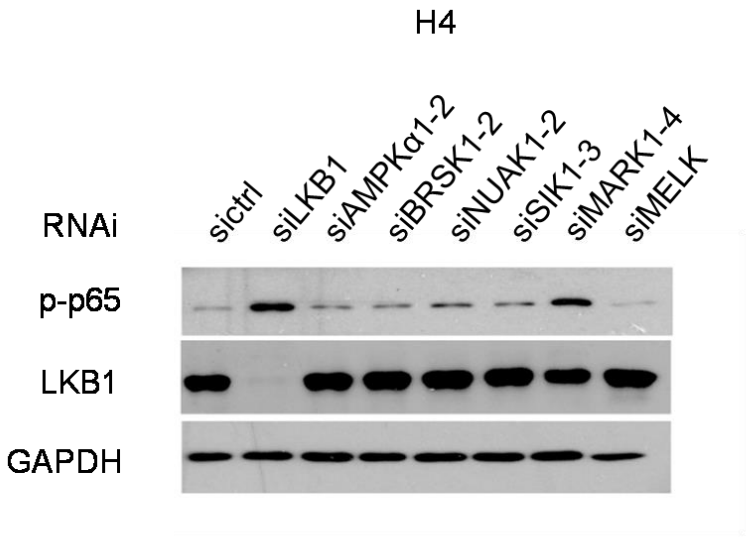

Figure 2.25: Phosphorylation of p65 was measured via immunoblotting after individual MARK proteins were knocked down in H4 (top) and H7 (bottom). Knockdown of LKB1 serves as the positive control.

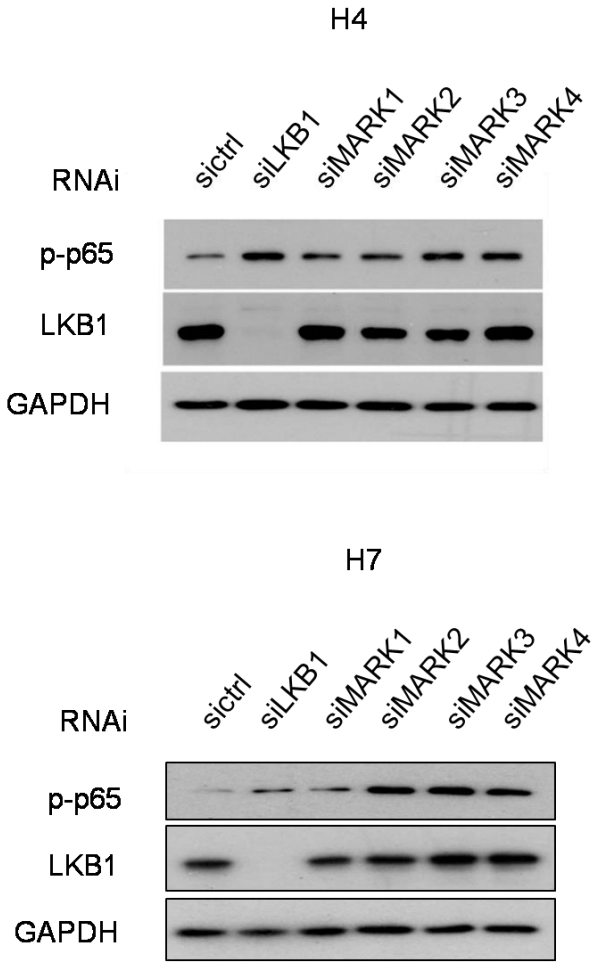

Figure 2.26: Phosphorylation of p65 was measured via immunoblotting after treatment with the MARK inhibitor (40 µM) (top). CXCL8 production was determined after treatment with increasing doses of the MARK inhibitor (bottom). MARKI, MARK inhibitor.

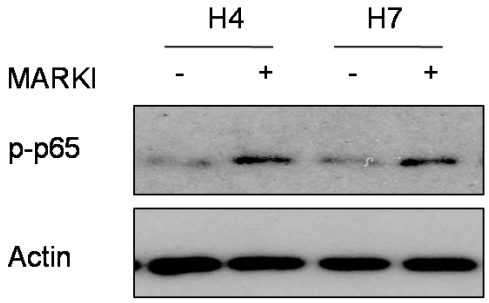

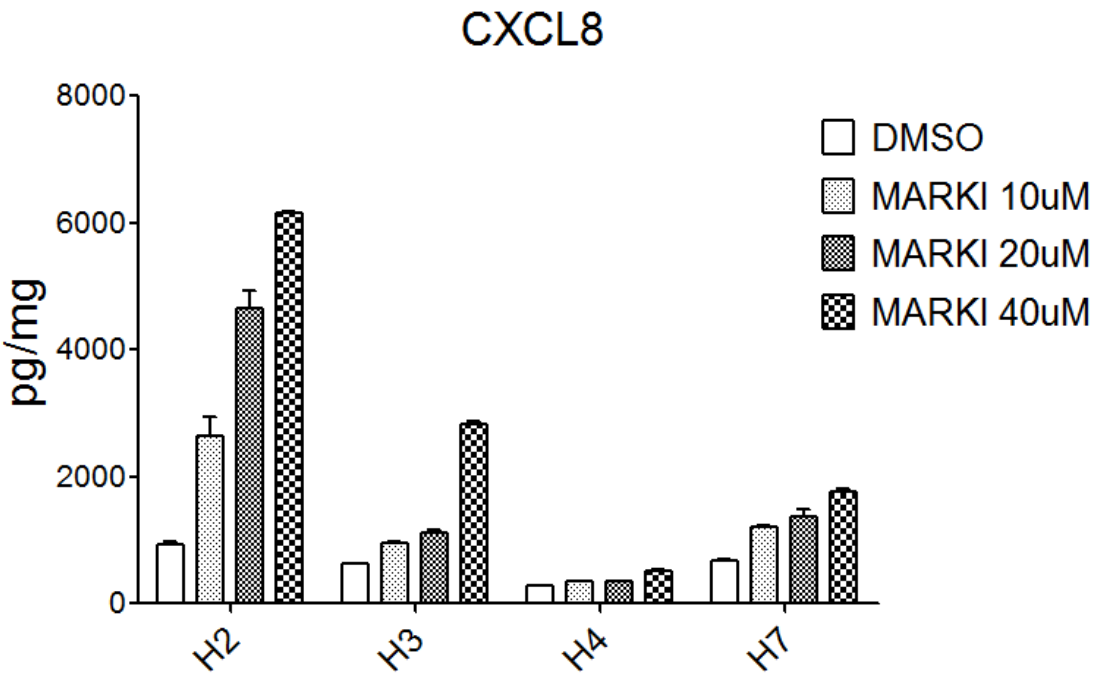

Figure 2.27: CXCL8 production (top) and phosphorylation of p65 (bottom) were determined in two pairs of HBEC-cancer cells.

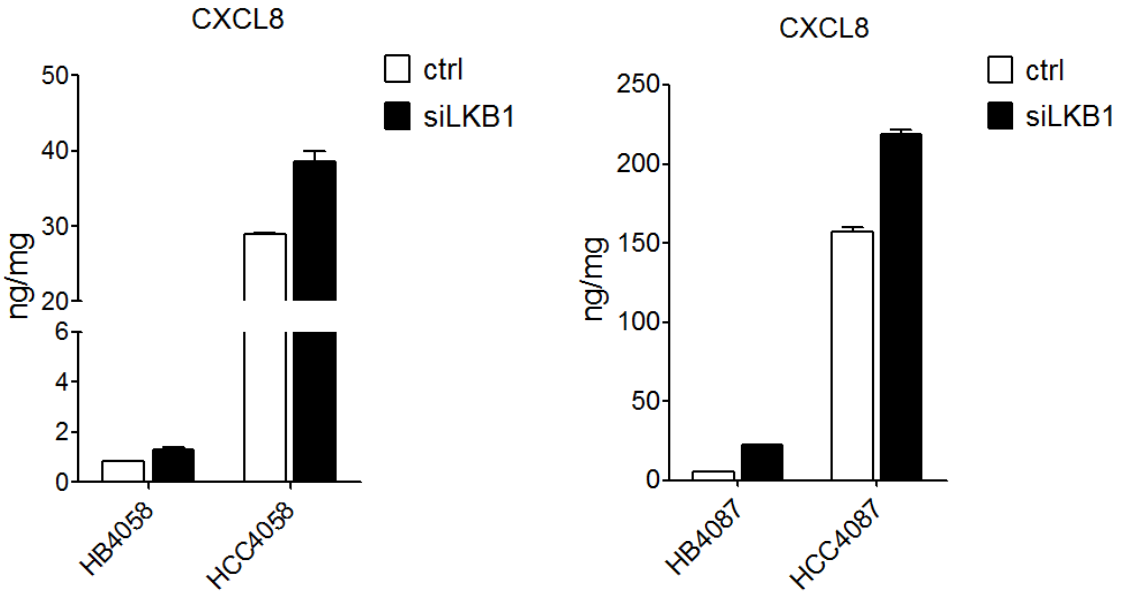

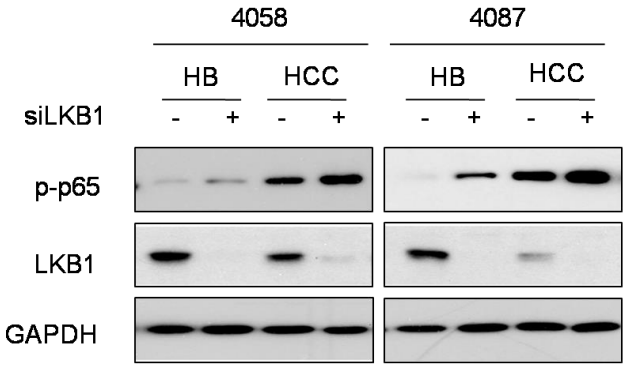

Figure 2.28: ERK1/2 and AMPK phosphorylation were determined by immunoblot analysis following LKB1 knockdown in HBECs.

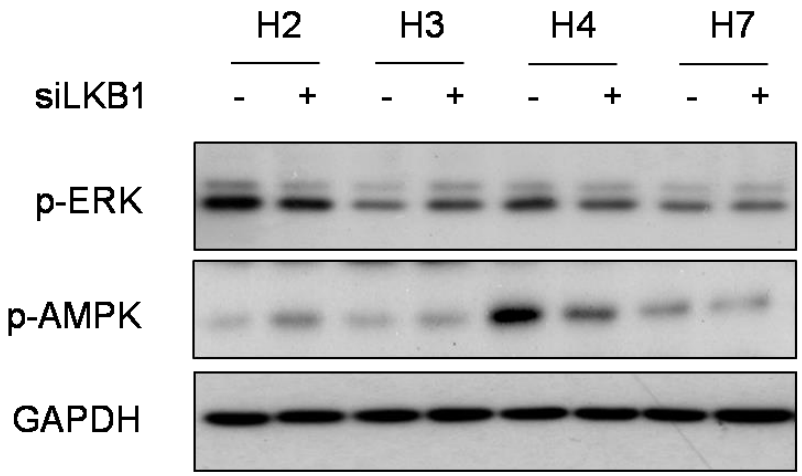

References

1. Siegel RL, Miller KD, & Jemal A (2016) Cancer statistics, 2016. *CA: a cancer journal for clinicians* 66(1):7-30.
2. Torre LA, Siegel RL, & Jemal A (2016) Lung Cancer Statistics. *Advances in experimental medicine and biology* 893:1-19.
3. Dubinett SM & Spira A (2013) Challenge and opportunity of targeted lung cancer chemoprevention. *Journal of clinical oncology : official journal of the American Society of Clinical Oncology* 31(33):4169-4171.
4. Matsumoto S*, et al.* (2007) Prevalence and specificity of LKB1 genetic alterations in lung cancers. *Oncogene* 26(40):5911-5918.
5. Carretero J, Medina PP, Pio R, Montuenga LM, & Sanchez-Cespedes M (2004) Novel and natural knockout lung cancer cell lines for the LKB1/STK11 tumor suppressor gene. *Oncogene* 23(22):4037-4040.
6. Carretero J*, et al.* (2010) Integrative genomic and proteomic analyses identify targets for Lkb1-deficient metastatic lung tumors. *Cancer cell* 17(6):547-559.
7. Goodwin JM*, et al.* (2014) An AMPK-independent signaling pathway downstream of the LKB1 tumor suppressor controls Snail1 and metastatic potential. *Molecular cell* 55(3):436-450.
8. Mohseni M*, et al.* (2014) A genetic screen identifies an LKB1-MARK signalling axis controlling the Hippo-YAP pathway. *Nature cell biology* 16(1):108-117.

9. Shackelford DB & Shaw RJ (2009) The LKB1-AMPK pathway: metabolism and growth control in tumour suppression. *Nature reviews. Cancer* 9(8):563-575.

10. Shaw RJ*, et al.* (2004) The LKB1 tumor suppressor negatively regulates mTOR signaling. *Cancer cell* 6(1):91-99.

11. Ramirez RD*, et al.* (2004) Immortalization of human bronchial epithelial cells in the absence of viral oncoproteins. *Cancer research* 64(24):9027-9034.

12. Vaughan MB, Ramirez RD, Wright WE, Minna JD, & Shay JW (2006) A three-dimensional model of differentiation of immortalized human bronchial epithelial cells. *Differentiation; research in biological diversity* 74(4):141-148.

13. Hanahan D & Weinberg RA (2011) Hallmarks of cancer: the next generation. *Cell* 144(5):646-674.

14. Qian BZ & Pollard JW (2010) Macrophage diversity enhances tumor progression and metastasis. *Cell* 141(1):39-51.

15. de Visser KE, Eichten A, & Coussens LM (2006) Paradoxical roles of the immune system during cancer development. *Nature reviews. Cancer* 6(1):24-37.

16. Marquez JP, Stanton SE, & Disis ML (2015) The antigenic repertoire of premalignant and high-risk lesions. *Cancer prevention research* 8(4):266-270.

17. Wislez M*, et al.* (2006) High expression of ligands for chemokine receptor CXCR2 in alveolar epithelial neoplasia induced by oncogenic kras. *Cancer research* 66(8):4198-4207.

18. Yanagawa J*, et al.* (2009) Snail promotes CXCR2 ligand-dependent tumor progression in non-small cell lung carcinoma. *Clinical cancer research : an official journal of the American Association for Cancer Research* 15(22):6820-6829.

19. Saintigny P*, et al.* (2013) CXCR2 expression in tumor cells is a poor prognostic factor and promotes invasion and metastasis in lung adenocarcinoma. *Cancer research* 73(2):571-582.

20. Strieter RM*, et al.* (2006) Cancer CXC chemokine networks and tumour angiogenesis. *European journal of cancer* 42(6):768-778.

21. Strieter RM*, et al.* (2004) CXC chemokines: angiogenesis, immunoangiostasis, and metastases in lung cancer. *Annals of the New York Academy of Sciences* 1028:351-360.

22. Keane MP, Belperio JA, Xue YY, Burdick MD, & Strieter RM (2004) Depletion of CXCR2 inhibits tumor growth and angiogenesis in a murine model of lung cancer. *Journal of immunology* 172(5):2853-2860.

23. Pold M*, et al.* (2004) Cyclooxygenase-2-dependent expression of angiogenic CXC chemokines ENA-78/CXC Ligand (CXCL) 5 and interleukin-8/CXCL8 in human non-small cell lung cancer. *Cancer research* 64(5):1853-1860.

24. Gong L*, et al.* (2013) Promoting effect of neutrophils on lung tumorigenesis is mediated by CXCR2 and neutrophil elastase. *Molecular cancer* 12(1):154.

25. Sanmamed MF*, et al.* (2014) Serum interleukin-8 reflects tumor burden and treatment response across malignancies of multiple tissue origins. *Clinical cancer research : an official journal of the American Association for Cancer Research* 20(22):5697-5707.

26. Sunaga N*, et al.* (2014) Clinicopathological and prognostic significance of interleukin-8 expression and its relationship to KRAS mutation in lung adenocarcinoma. *British journal of cancer* 110(8):2047-2053.

27. Acosta JC & Gil J (2009) A role for CXCR2 in senescence, but what about in cancer? *Cancer research* 69(6):2167-2170.

28. Acosta JC*, et al.* (2008) Chemokine signaling via the CXCR2 receptor reinforces senescence. *Cell* 133(6):1006-1018.

29. Waugh DJ & Wilson C (2008) The interleukin-8 pathway in cancer. *Clinical cancer research : an official journal of the American Association for Cancer Research* 14(21):6735-6741.

30. Jacob LS*, et al.* (2011) Genome-wide RNAi screen reveals disease-associated genes that are common to Hedgehog and Wnt signaling. *Science signaling* 4(157):ra4.

31. Jian SF*, et al.* (2014) Utilization of liquid chromatography mass spectrometry analyses to identify LKB1-APC interaction in modulating Wnt/beta-catenin pathway of lung cancer cells. *Molecular cancer research : MCR* 12(4):622-635.

32. Lai C*, et al.* (2011) Elevation of WNT5A expression in polyp formation in Lkb1+/- mice and Peutz-Jeghers syndrome. *The Journal of pathology* 223(5):584-592.

33. Spicer J, *et al.* (2003) Regulation of the Wnt signalling component PAR1A by the Peutz-Jeghers syndrome kinase LKB1. *Oncogene* 22(30):4752-4756.

34. Ji H, *et al.* (2007) LKB1 modulates lung cancer differentiation and metastasis. *Nature* 448(7155):807-810.

35. Levy L, *et al.* (2002) Transcriptional activation of interleukin-8 by beta-catenin-Tcf4. *The Journal of biological chemistry* 277(44):42386-42393.

36. Drewes G, *et al.* (1995) Microtubule-associated protein/microtubule affinity-regulating kinase (p110mark). A novel protein kinase that regulates tau-microtubule interactions and dynamic instability by phosphorylation at the Alzheimer-specific site serine 262. *The Journal of biological chemistry* 270(13):7679-7688.

37. Illenberger S, *et al.* (1996) Phosphorylation of microtubule-associated proteins MAP2 and MAP4 by the protein kinase p110mark. Phosphorylation sites and regulation of microtubule dynamics. *The Journal of biological chemistry* 271(18):10834-10843.

38. Chan KT, *et al.* (2014) LKB1 loss in melanoma disrupts directional migration toward extracellular matrix cues. *The Journal of cell biology* 207(2):299-315.

39. Hubaux R, *et al.* (2015) Microtubule affinity-regulating kinase 2 is associated with DNA damage response and cisplatin resistance in non-small cell lung cancer. *International journal of cancer* 137(9):2072-2082.

40. Salminen A, Hyttinen JM, & Kaarniranta K (2011) AMP-activated protein kinase inhibits NF-kappaB signaling and inflammation: impact on healthspan and lifespan. *Journal of molecular medicine* 89(7):667-676.

41. Grant JL*, et al.* (2014) A novel molecular pathway for Snail-dependent, SPARC-mediated invasion in non-small cell lung cancer pathogenesis. *Cancer prevention research* 7(1):150-160.

CHAPTER THREE: Study of the dynamics in cytokine-induced EMT in NSCLC

Abstract

Dysregulated inflammation is associated with the development and progression of lung cancer. Pulmonary diseases characterized by increased inflammation, including chronic obstructive pulmonary disease, occupational lung diseases and pulmonary fibrosis, are strongly related to heightened risk of lung cancer. EMT, an important phenotype during cancer metastasis can be induced by a variety of inflammatory proteins such as cytokines, chemokines and growth factors. However, the underlying mechanisms have not been fully understood. In this study, we find that acute IL-1β exposure (within 7 days) induces EMT via the activator protein 1 (AP-1) components Fra-1 and c-Jun, which occurs concomitantly with increased cell migration and invasion. AP-1 functions downstream of the ERK1/2 and JNK signaling and resides upstream of the transcription factors Slug and Zeb2. Importantly, inhibition of Slug, Zeb2, Fra-1 or the ERK1/2 and JNK signaling is sufficient to abolish EMT induced by the acute IL-1β exposure. Unexpectedly, following prolonged IL-1β exposure (21 days), cells do not revert back to the epithelial state despite the inhibition of these mediators of acute EMT. We have also found that following IL-1β withdrawal after the prolonged exposure, the treated cells are able to maintain their mesenchymal phenotype for more than 30 days when they continue proliferating. Similar phenomenon are also observed with chronic TNF-α and TGF-β exposure. We refer to this prolonged but reversible EMT program that can persist in the absence of the original inflammatory stimulus as EMT memory. Further studies show that Fra-1 is required to establish

the initial EMT program but not to maintain EMT memory. Intriguingly, chemical inhibition of a variety of enzymes involved in histone modifications and DNA methylation indicates that the repression of E-cadherin is mediated by dynamic epigenetic modifications depending on the duration of IL-1β exposure. ChIP and MSP analysis further confirm that H3K27me3 and histone deacetylation mediate E-cadherin repression during acute EMT. In contrast, H3K9me2/3 methylation and DNA methylation occur and function as the dominant repression mechanism in EMT memory. *In vitro* functional studies show that EMT memory endows cancer cells with enhanced motility yet impaired proliferation. These findings reveal dynamic epigenetic modifications as the cause of EMT memory upon chronic inflammation exposure, which may create a time window for cancer cells to migrate to distant organs and eventually undergo MET to form macro-metastatic clones. We also demonstrate different metastatic phenotypes following acute versus chronic inflammation exposure.

Introduction

Lung cancer is still the leading cause of cancer-associated mortality. The overall survival of lung cancer patients is approximately 18% and the majority of patients succumb due to metastatic disease (1, 2). Cigarette smoking is the single strongest risk factor and accounts for more than 80% of lung cancers (3, 4). Smoking-induced chronic pulmonary inflammation is considered to facilitate tumorigenesis via high levels of reactive oxygen species (ROS) and promotion of DNA damage, leading to persistent tissue damage and gene mutations (5). Other unresolved

inflammatory conditions such as chronic obstructive lung disease or occupational lung diseases are also characterized by heightened risk of lung cancer (6, 7). In addition, high levels of inflammation are negatively correlated with lung cancer patient survival (8-11). It has been well documented that the inflammatory proteins including cytokines, chemokines and growth factors promote cancer progression through a variety mechanisms such as angiogenesis, proliferation, apoptosis resistance, immunosuppression and EMT induction (12). It is important to note that acute inflammatory conditions generally do not increase cancer risk, although numerous *in vitro* studies have shown that acute inflammation also induces a variety of malignant phenotypes in established cancer cells. The functional and mechanistic differences between acute and chronic inflammation in cancer progression have not yet been resolved.

The epithelial-to-mesenchymal transition (EMT) is regarded as an important process during tumor metastasis, when invasive cells detach from their neighboring cells and acquire the capability to degrade basement membrane and extracellular matrix (13, 14). The enhanced migration and invasion allow the cells to disseminate into blood vessels and be transported to distant organs. Although numerous studies have documented the existence of mesenchymal cells in primary invasive tumors and in the circulation, tumors cells growing from macrometastatic sites are largely epithelial, thus giving rise to controversy regarding the role of EMT during cancer metastasis (15-18). EMT plasticity offers a possible explanation for such a discrepancy, indicating that mesenchymal-to-epithelial (MET) is necessary for the outgrowth of metastatic

clones at distant organ sites (19, 20). Recently, several studies have demonstrated the importance of EMT plasticity *in vivo* (21, 22). For example, utilizing an inducible Twist1 expressing murine skin tumor, Tsai *et al*. have shown that Twist1-induced EMT facilitates the early steps of metastasis, including local invasion, intravasation and extravasation. However, loss of Twist1 and EMT at the distant site is essential for the proliferation of metastatic clones (22). Questions remain regarding how cells maintain the mesenchymal phenotype during dissemination and then revert to an epithelial phenotype at metastatic sites. Relevant models of EMT plasticity may help address these gaps.

The reversibility of EMT requires a dynamic genome-wide reprogramming of gene expression and implies epigenetic regulators are important in this process. Histone modifications and DNA methylation play important roles in epigenetic regulation of gene expression (19, 23). For example, the active transcription of epithelial genes is controlled by histone markers such as H3K9ac and H3K4me3 (24, 25). In the process of EMT, the epithelial genes gradually become inaccessible to transcription due to loss of those active histone markers and gain of repressive histone modifications such as H3K27me3 and H3K9me2/3 (26-29). EMT transcription factors including Snail and Slug have been shown to mediate these histone modifications by interacting with the enzymes that catalyze acetylation and methylation. Interestingly, compared to H3K27me3, H3K9me2/3 and DNA methylation are associated with more profound repression of epithelial genes, and subsequently, a more stable mesenchymal phenotype (26, 27). However,

mechanisms underlying these dynamics and the selectivity of different repressive epigenetic modifications in EMT are largely unknown.

In this study, we establish a model of EMT plasticity *in vitro* by chronic cytokine exposure. We have discovered that chronic cytokine exposure endows cells with a prolonged mesenchymal phenotype, referred to as EMT memory that occurs through epigenetic modifications. Subsequently, the memorized mesenchymal phenotype is independent of the transcription factors that are otherwise indispensible in acute inflammation-induced EMT. Cells with EMT memory are also endowed with the capacity for enhanced migration.

Results

Acute IL-1β exposure induces EMT in a subset of NSCLC cell lines

IL-1β expression is elevated in the lungs of smokers, and increased expression of IL-1β characterizes a number of malignancies, including lung cancer (30-34). To determine the effect of IL-1β in lung cancer, we treated the NSCLC cell line A549 with IL-1β for 48 hours and found that the cells became elongated and spread, forming a fibroblast-like morphology (**Fig 3.1**). Immunoblotting revealed that expression of the epithelial markers E-cadherin and Cytokeratin 18 (CK18) decreased while the mesenchymal marker Vimentin increased, indicating cells was undergoing EMT (**Fig 3.2**). Phase-contract microscopy showed that IL-1β-treated cells had more membrane ruffling and cytoplasmic protrusions indicative of enhanced cell motility (**Fig 3.3**).

Indeed, upon IL-1β treatment cells migrated faster to close the wound in the scratch assay (**Fig 3.4**). However, IL-1β treatment decreased cell proliferation, consistent with the "grow or go" concept that mesenchymal cells migrate faster but grow slower (**Fig 3.5**). In addition, we also observed IL-1β-induced EMT in two other NSCLC cell lines A427 and H460 (**Fig. 3.6**).

The mechanism of EMT upon acute IL-1β exposure

Next, we sought to dissect the mechanism of EMT induced by acute IL-1β exposure. IL-1β treatment activated the MAPKs (p38, ERK and JNK), AKT and NF-κB pathways within 48 hours (**Fig 3.7**). Chemical inhibition of individual pathways revealed that pre-treatment of cells with only JNK or ERK inhibitor impaired E-cadherin repression following IL-1β exposure and there was a dose-dependent response (**Fig 3.8**). We also found two individual components of heterodimer transcription factor AP-1, namely Fra-1 and c-Jun, were phosphorylated and upregulated by the MAPK signaling pathway upon acute IL-1β treatment (**Fig 3.9**). AP-1 has been reported to induce EMT via upregulation of the EMT-TFs such as Snail and Zeb (35, 36). RT-PCR showed Slug and Zeb2, but not Snail, Zeb1 or Twist, were significantly elevated following the acute IL-1β treatment. Knockdown of Fra-1 completely abolished Slug upregulation (**Fig 3.10, 3.11**). Importantly, Slug, Zeb2 or Fra-1 silencing by RNA interference was sufficient to block the repression of E-cadherin and subsequent EMT (**Fig 3.11**). Other AP-1 components including JunB, c-Fos, FosB and Fra-2 did not increase upon acute IL-1β exposure (**Fig 3.12**). Taken together, these data suggest that IL-1β-induced EMT is attributed to activation of the ERK/JNK

pathway, which phosphorylates and upregulates Fra-1 and c-Jun to increase the expression of Slug and Zeb2 (**Fig 3.13**).

Chronic cytokine exposure leads to EMT memory

Although IL-1β is one of the predominant cytokines induced in acute inflammation, it can be persistently elevated in diseases characterized by chronic inflammation, such as COPD and chronic gastritis (37, 38). Patients with these two chronic conditions have higher risk of cancer incidence. As such, we suspected that chronic exposure to IL-1β might have some unique pro-tumor effects. To mimic the chronic inflammatory condition, we treated A549 cells with IL-1β for 21 days *in vitro* and found that the cells displayed mesenchymal cell-like growth pattern as they did following the acute IL-1β exposure. Surprisingly, after IL-1β was withdrawn from the culture, the treated cells did not immediately revert back to the epithelial state but were able to maintain the mesenchymal cell-growth pattern for more than 30 days as the cells continued proliferating (**Fig 3.14**). Immunoblotting of EMT markers confirmed the mesenchymal phenotype by showing that E-cad and CK-18 were low and Vimentin was high compared to the untreated cells (**Fig 3.15**). These data suggest that cells can "remember" the mesenchymal phenotype following chronic IL-1β exposure. We refer to this prolonged but reversible EMT program that persists in the absence of the original inflammatory stimulus as EMT memory. We further found that EMT memory could be established upon IL-1β exposure only after at least 14 days, indicating that the establishment of EMT memory is dependent on exposure duration (**Fig 3.16**).

Next, we sought to determine whether higher dose of IL-1β could decrease the minimal required duration for establishing EMT memory and found that a high dose of IL-1β exposure did not accelerate the process of EMT or EMT memory (**Fig 3.17**). We also observed EMT memory in two other NSCLC cell lines, A427 and H460, following chronic IL-1 β treatment (**Fig 3.18**). To determine whether EMT memory is unique to chronic IL-1β exposure, we treated A549 with TNF-α and TGF-β chronically and observed similar phenomenon in both conditions (**Fig 3.19**).

Distinct mechanisms in acute EMT versus EMT memory

To dissect the molecular pathway of EMT memory, we examined the expression levels of Slug, Zeb2, c-Jun and Fra-1 because they are indispensible to induce EMT following the acute IL-1β exposure. RT-PCR results showed that their transcription levels continuously increased up to 10-fold in the presence of IL-1β and decreased gradually with IL-1β withdrawal, in parallel with the mesenchymal state (**Fig 3.20**). In addition, the ERK pathway was also activated over the course of the experiment (**Fig 3.21**), suggesting a feed forward mechanism. However, transient inhibition of the ERK/JNK pathway or knockdown of Fra-1 did not impair EMT memory (**Fig 3.22**). To confirm this result, we prolonged Fra-1 silencing for 12 days by repeated siRNA transfection and did not observe any reversion of EMT (**Fig 3.22**). To assess the possibility of trans-activation of other EMT-inducing pathways and proteins in the chronic IL-1β exposure, we sought to determine whether the initiation of EMT memory requires Fra-1. Therefore, Fra-1 was silenced beginning at day 9 after initial IL-1β treatment when EMT memory was not yet established and

was continuously repressed by repetitive siRNA transfection. Following 21-day IL-1β treatment, there was no EMT phenotype observed (**Fig 3.23**). These data suggest that Fra-1 is required to initiate and establish the EMT program but it is not important to maintain the EMT memory.

Dynamic epigenetic modifications in EMT

Because EMT memory is heritable and independent of the acute EMT mediators, epigenetic modification was hypothesized as an alternative mechanism to maintain the mesenchymal state. It is known that gene expression is controlled by the overall effects of different histone modifications including active markers such as H3K9ac and H3K4me3, as well as repressive markers such H3K27me3 and H3K9me2/3. Enrichment of the repressive modifications such as H3K9me2/3 is commonly associated with DNA methylation (26, 27). In addition, using a tamoxifen-controlled Snail induction system, Javaid *et al.* demonstrated that histone modifications dynamically changed in the process of EMT (39). Therefore, to assess the importance of epigenetic modifications during EMT, we treated cells with small molecular chemicals inhibiting the key enzymes involving in histone deacetylation, H3K4me3, H3K27me3, H3K9me2/3 and DNA methylation. To further dissect their roles in different stages of EMT, we also divided EMT into four stages based on the presence of IL-1β and the duration of IL-1β treatment (**Fig 3.24**): EMT induction (pre-IL-1β exposure), acute EMT (IL-1β exposure within 7 days), chronic EMT (IL-1β exposure for at least 21 days) and EMT memory (IL-1β withdrawal after chronic EMT). Inhibitor treatment for 72 hours in these distinct stages showed that the

H3K27me3 inhibitor EPZ-6438 and the pan histone deacetylation inhibitor TSA were able to prevent E-cadherin downregulation in EMT induction and acute EMT (**Fig 3.25, 3.26**) while DNA methylation inhibitor 5'-Aza reversed E-cadherin repression in EMT memory (**Fig 3.27**). Surprisingly, none of these inhibitors were able to impair E-cadherin repression in chronic EMT (**Fig 3.28**). In further studies, we confirmed the previous experiments by genetic knockdown of EZH2, an enzyme mediating H3K27me3 and showed that EZH2 loss was sufficient to disinhibit E-cadherin expression in EMT induction and acute EMT (**Fig 3.29**). To verify that these epigenetic modifications do exist in the E-cadherin promoter, we performed ChIP-PCR and Methylation specific PCR (MSP) in these different stages of EMT. The results showed that H3K27me3 was rapidly enriched and increased up to 7 fold in response to IL-1β treatment while H3K9me2/3 was only enriched with chronic IL-1β treatment. The activation marker H3K9ac decreased after 3 days of IL-1β treatment while H3K4me3 only displayed transient reduction (**Fig 3.30**). We also found that the level of DNA methylation in the E-cadherin promoter increased in EMT memory but not acute EMT (**Fig 3.31**). However, these changes gradually returned to the basal level in the absence of IL-1β. Taken together, these data suggest that there is a dynamic alteration in histone modifications and DNA methylation during IL-1β-induced EMT. H3K27me3 mediates E-cadherin repression in the early stages of EMT while DNA methylation is required for EMT memory.

Mechanism of dynamic epigenetic modifications in EMT

Next, we sought to understand the mechanism underlying this dynamics of epigenetic modification. Previous studies have demonstrated that Snail-mediated E-cadherin repression is attributed to the recruitment of EZH2 and subsequent enrichment of H3K27me3 (29). In our system, we showed that H3K27me3 is the initially responsive histone methylation that mediates the transient repression of E-cadherin. In addition, the level of H3K27me3 continued rising upon IL-1β exposure, parallel with the Slug dynamics. Therefore, we hypothesized that the accumulation of Slug-induced H3K27me3 leads to H3K9me2/3 and DNA methylation during the chronic IL-1β exposure. To manipulate the level of Slug expression, we generated A549 cells with a doxycycline-controlled system so that Slug can be induced stepwise when doxycycline concentration gradually decreases. We observed Slug-dependent E-cadherin repression within 48 hours (**Fig 3.32**). Indeed, maximum induction of Slug for 21 days repressed E-cadherin and increased DNA methylation in the E-cadherin promoter (**Fig 3.33**). Taken together, our data suggest that the dynamic epigenetic modifications of E-cadherin are consequences of the accumulation of Slug and that high Slug levels are important for more stable repression of E-cadherin by DNA methylation.

Functional characterization of cells with EMT memory

Because EMT is associated with enhanced metastasis, we tested whether cells with EMT memory also inherit metastasis-associated traits. Transwell migration assays demonstrated that cells with EMT memory moved with greater velocity compared to the control cells but as these

cells reverted back to the epithelial state, the migration rate decreased to the basal line (data not shown). In addition, consistent with the “grow or go” theory, the EMT memory cells lower rates of proliferation and also formed fewer and smaller colonies in AIG assays (**Fig 3.34**).

Discussion

In this study, we discover that the pro-inflammatory cytokine IL-1β induces EMT in a subset of NSCLC cell lines. We further dissect the molecular pathway in A549 cells and reveal that the activator protein 1 (AP-1), comprised of Fra-1 and c-Jun, is required in this process. Two transcription repressors Slug and Zeb2, downstream of AP-1, are responsible for the repression of E-cadherin upon acute IL-1β exposure. Cells undergoing EMT display enhanced migration but decreased proliferation *in vitro*.

Chronic rather than acute inflammation is tightly associated with cancer incidence in a variety of conditions. In addition, in a physiologic tumor microenvironment tumor cells are exposed to inflammatory factors for months rather than a few hours or days. Therefore, we hypothesize that chronic inflammation may have a unique impact on tumor cells that is distinct from acute exposure. By extending IL-1β treatment up to 21 days, we mimic chronic inflammation *in vivo* and find that chronic IL-1β exposure endows cells with a more profound mesenchymal phenotype that can be maintained even after IL-1β is withdrawn. We refer to this response as “EMT memory.” We also observe EMT memory after chronic TNF-α and TGF-β treatment and in

another two NSCLC cell lines treated with IL-1β, suggesting that EMT memory may be a common phenomenon.

As we show that proteins mediating the acute EMT are still upregulated following chronic IL-1β exposure, we were expecting that blockade of these acute mediators would reverse EMT memory. Quite surprisingly, knockdown of Fra-1 is not sufficient to impair EMT memory, although it is required for the initiation of EMT memory. This result indicates that EMT is a requisite for its memory phenotype but distinct mechanisms are involved in the initiation/establishment and the maintenance of EMT memory. This is also the first report indicating that tumor cells can utilize distinct mechanisms in EMT following acute versus chronic inflammatory stimuli.

It has been proposed that the epigenetic profile controls EMT plasticity. Gain of an increasingly stable mesenchymal phenotype is accompanied by more profound silence of the epithelial genes via epigenetic modifications such as H3K9me3 and DNA methylation (19). Consistent with this association, our data show that H3K9me2/3 and DNA methylation increase in alignment with the establishment of EMT memory following chronic IL-1β exposure. Importantly, inhibition of DNA methylation reverses E-cadherin repression in EMT memory. In contrast, H3K27me3, the histone marker associated with PRC-mediated repression, is immediately enriched in the E-cadherin promoter in response to IL-1β treatment and mediates EMT induction and acute EMT. Our data suggest that sustained presence of EMT-promoting signals alters the epigenetic modifications which lead to a switch from transient to stable repression of epithelial genes.

However, we do not exclude the possibility that accumulation of H3K27me3 in the chronic IL-1β exposure is also important for stable repression of E-cadherin because high level of H3K27me3 may be the trigger to recruit H3K9me2/3 and subsequently induces DNA methylation. Interesting, we do not observe any reversion of E-cadherin expression in chronic EMT treated with the epigenetic inhibitors, indicating that multiple epigenetic modifications may reinforce the repression of E-cadherin transcription.

Although studies have shown that Snail represses E-cadherin by either H3K27me3 or H3K9me2/3 via recruitment of the corresponding enzymes, the selectivity of these epigenetic markers in these different scenarios are not clearly defined (26, 27, 29). In our model, H3K9me2/3 and DNA methylation are unique to chronic IL-1β treatment and parallel high Slug expression, suggesting a possible mechanism whereby the level of Slug may be the determinant of the epigenetic switch. In addition, the enzymes involved in these epigenetic modifications including *SETDB1*, *SUV39H1*, *EHMT1*, *EHMT2, DNMT1, DNMT3A* and *DNMT3B* did not increase following IL-1β treatment and many of them actually decreased (**Fig 3.35**). Therefore, it is hypothesized that in the chronic IL-1β exposure, the accumulation of Slug leads to increasing level of H3K27me3 and subsequent formation of more stable repressive modifications including H3K9me2/3 and DNA methylation. The preliminary MSP analysis of high Slug expression cells supports our hypothesis but examination of histone modification by ChIP assay is needed for further validation.

During metastasis, increased cell migration and invasion enable tumor cells to move away from the primary tumor site, which also separates them from EMT-promoting stimuli such as inflammation. In order to increase the chance of successful intravasation, survival in the circulation and extravasation at distant organ sites, these cells need to maintain their mesenchymal phenotypes. The *in vitro* phenotypic characterization of EMT memory demonstrates concurrent sustainability of enhanced migration.

Inflammation has multiple deleterious interactions with cancer and it is unclear how chronic inflammation facilitates cancer progression. The current studies provide evidence for potential pathways mediating EMT plasticity and emphasize the different EMT phenotypes induced by acute versus chronic IL-1β exposure. It also provides detailed interrogation of the underlying mechanisms which could form the rationale for epigenetic modification as a therapeutic strategy to prevent metastasis.

Materials and Methods

Cell lines and recombinant cytokines

NSCLC cell lines A549, H460 and A427 were purchased from ATCC and cultured in RPMI1640 (Corning) with 10% fetal bovine serum. Cells were growing in a 5% CO2 atmosphere at 37°C and cultured within 10 passages of genotyping. Recombinant IL-1β, TNF-α and TGF-β were purchased from BD Pharmingen. IL-1β, TNF-α and TGF-β were used as 1ng/ml, 10ng/ml and 5ng/ml respectively unless stated otherwise. For chronic cytokine treatment, cells were split every 3 to 4 days and fresh medium and cytokines were replenished.

Generation of doxycycline-controlled Slug expression cell lines

Slug was subcloned into the doxycycline-repressible lentiviral vector pLVX-Tight-Puro (Clontech) and then transduced into A549 cells. Briefly, HEK293T kidney cells (ATCC) were transfected with pLVX-Tet-Off Advanced Vector along with VSVG (Addgene) envelope protein and pDeltavpr (Addgene) packaging protein plasmids using lipofectamine 2000 (Life Technologies) according to the manufacturer's protocol. The cells were given fresh DMEM media with 10% FBS 6 hours after the transfection and maintained in culture under standard condition. Viral supernatants were collected over 48-72 hours, pooled and filtered using a 0.45μm filter to remove any cells. Viral transduction was carried in 1ml of viral supernatant with 10μg/ml polybrene (Sigma), incubating with A549 cells for 6 hours. Transduced A549 cells were further selected via

neomycin (1mg/ml) over the next 10-14 days. Viral supernatant containing the Slug-Tight-Puro plasmid (clontech) was made as mentioned above and further added to the neomycin-selected A549 cells. Single clones were picked under the selection of puromycin (100ug/ml).

Inhibitor treatment

Cells were treated with indicated concentration of the inhibitors for 72 hours. Inhibitors were dissolved in DMSO and stored in -20°C at 20mM stock. Cycles of freeze and thaw are no more than 3 times. ERK inhibitor U0126 was purchased from Cell Signaling Technology; NF-κB inhibitor BMS345541, histone deacetylase inhibitor Trichostatin A (TSA) and DNA methylation inhibitor 5'-Aza-2'-deoxycytidine (5'-Aza) were from Sigma; AKT inhibitor LY294002, JNK inhibitor II, p38 inhibitor SB203580 (SB) were from Calbiochem; LSD1 inhibitor OG-L002, G9a inhibitor BIX01294 and EZH2 inhibitor EPZ-6438 were purchased from Selleckchem. The treatment concentrations for these inhibitors are 50nM for TSA, 1uM for BMS345541 and BIX01294, 5uM for U0126, SB203580 and 5'-Aza, 10uM for JNK inhibitor II and LY294002, 20uM for EPZ-6438 and 50uM for OG-L002, or indicated otherwise.

Gene knockdown by siRNA transfection

Cells were plated in a 6-well plate and allowed overnight attachment. They were transfected with small interfering RNA (siRNA) using Lipofectamine RNAiMAX (Life Technologies) at final concentration of 15 nmol/L. The transfection lasted up to 96 hours for transient gene repression.

For prolonged gene repression, cells were split and repeatedly transfected with indicated siRNA every 4 days. Small interfering RNAs against Slug, ZEB2, FOSL1, EZH2 were pooled siRNA and purchased from GE Healthcare Dharmacon.

Protein extraction and immunoblotting

Cells grown to 80% confluence in T25 flasks were washed with ice-cold PBS and lysed with RIPA buffer using standard methods. Twenty μg of each cell lysate was loaded per lane, and proteins were resolved by SDS-PAGE and transferred to an Immobilon-P Transfer Membrane (Millipore, Danvers, MA). The membranes were blocked with 5% milk and then incubated with primary antibodies diluted in blocking solution according to the manufacturer's recommendations. Horseradish peroxidase-conjugated secondary antibodies (Bio-Rad, Hercules, CA) and enhanced chemiluminescence (ECL) reagent (Amersham Biosciences, Piscataway, NJ) were used for protein detection. Antibodies against phosphorylated-p65 (S536), p-MAPK (T202/Y204), p-Jun (S73), p-p38 (T180/Y182), p-Fra-1 (S265), Fra-1, Slug, β-actin, α-tubulin were purchased from Cell Signaling Technology. Antibodies against E-cadherin and Vimentin were purchased from BD Pharmingen. Antibody against CK18 was from Abcam and GAPDH was from Advanced Immunochemical Inc.

RNA extraction and RT-PCR

Total RNA was isolated using the Quick-RNA MiniPrep (Zymo), and cDNA for mRNA analysis was prepared using the High Capacity RNA-to-cDNA Kit (Life Technologies). Transcript levels of *SNAI1, SNAI2, ZEB1, ZEB2, TWIST1, CJUN, JUNB, CFOS, FOSL1, FOSL2, B2M* were measured by quantitative reverse transcription PCR (qRT-PCR) using the Taqman Probe-based Gene Expression System (Life Technologies) in a MyiQ Cycler (Bio-Rad). Transcript levels of *EZH2, SETDB1, EHMT1, EHMT2, SUV39h1, DNMT1, DNMT3A, DNMT3B* and *ACTB* were measured using Syber green master mix (Life Technologies). The primers for these genes were adopted from Primerbank. Amplification was carried out for 40 cycles of 15 seconds at 95°C, 30 seconds at 55°C and 30 seconds at 72°C. All samples were run in triplicate, and relative gene expression levels were determined by normalizing their expression to *B2M* or *ACTB*. Expression data are presented as fold-change values relative to normalized expression levels in a reference sample using the following equation: RQ ¼ $2^{-\Delta\Delta Ct}$.

Proliferation assay

As an indication of cell viability and proliferation, cellular ATP levels were measured using the ATPlite 1 step Luminescence Assay Kit (Perkin Elmer). A549 cells with indicated IL-1β treatment were plated in 96-well plates at 1000 cells per well. Eight replicates were plated for each experiment condition. ATP luminescence was assessed every 24 hours up to 72 hours. Zero time point was defined after overnight attachment of the initial plating. Readings at each time point were normalized to the 0 hour readings to control plating differences.

Scratch assay

Cells were plated in 12-well plates and allowed to grow until confluent. A 200μl pipet tip was used to make a scratch across the center of each well. The wells were rinsed to remove detached cells and media containing relevant treatments was added. Plates were photographed at time 0 and 24 hours post-treatment. Percentage of closed distance at 24 hours was normalized to that at 0 time point.

AIG assay

We used a modified high-throughput cell transformation assay for evaluation of soft agar colony growth. Briefly, the cells are suspended in 0.4% agar and plated atop a thick layer of solidified 0.6% agar. A549 cells with indicated IL-1β treatment were plated in 96-well plates at 750 cells per well. Cells were cultured in complete media for a total of 14 days. Three-dimensional projection images (x100 total magnification) of the colonies in each sample were obtained by assembling Z-stacks comprised of 30 optical sections, at an interval of approximately 50 mm, using the Nikon Eclipse Ti microscope. The 30 images were then focused into a single representative image per well using the extended depth of focus function of the Nikon Elements AR software, and the total number of colonies in each focused image was manually counted. Ten replicates for each condition were plated for each independent experiment.

ChIP-PCR

ChIP assays were performed based on the manufacturer's protocol (Millipore). Briefly, $5*10^6$ cells were collected and cross-linked with 1% of formaldehyde at RT followed by cell nucleus extraction. The cell lysate was subjected to sonication and then incubate with 1ug of antibody overnight in the presence of magnetic protein A/G beads. Bound DNA-protein complexes were eluted and reversely cross-linked after a series of washes. Quantitative-PCR assays were performed under standard condition. The primers for E-cadherin promoter were 5'- CCACGCACCCCCTCTCAGT -3' and 5'- GAGCGGGCTGGAGTCTGAAC -3'; for negative control loci were 5'- TCTTGACCTCTCCGCATC -3'and 5'-CAACAGGACGAATGTGACTG -3'

Methylation specific PCR (MSP)

MSP was performed using bisulfate-modified DNA on conditions that has been previously described. Briefly, genome DNA was extracted using Genome DNA Extraction Kit (Zymo Research) and subjected to bisulfate conversion following the manufacturer's protocol (Zymo Reseach). The primers for E-cadherin promoter were: 5'- TTAGGTTAGAGGGTTATCGCGT -3' and 5'- TAACTAAAAATTCACCTACCGAC -3' for methylated DNA; 5'- TAATTTTAGGTTAGAGGGTTATTGT -3' and 5'- CACAACCAATCAACAACACA -3' for unmethylated DNA. PCR products were electrophoresed on 2% agarose gels, stained with ethidium bromide and visualized under UV illumination.

RNA sequencing and bioinformatic analysis

A549 cells were cultured in 6-well plates with proper treatment. Lysates were harvested using 400 µLQiazole (Qiagen) and RNA extracted according to manufacturer's protocol (Zymo Research). Total RNA was provided to the UCLA Clinical sequencing Core, where library preparation and sequencing was performed on Illumina Hiseq3000. Single-end transcriptome reads were mapped to the Ensemble GRCh37 reference genome using Tophat2. HTSeq-count (PMID: 25260700) was used to count reads for each gene. EdgeR was then used to normalize expression to CPM (count per million) and to identify differentially expressed genes based on negative binomial distribution. A gene was defined as differentially expressed between two conditions if its p-value was less than 0.05 and fold change was more than 1.5. Cluster 3.0 was used for clustering analysis.

Statistical analysis

Samples were plated and run in triplicate, unless otherwise indicated, and all experiments were performed at least three times. Statistical analyses were performed on all data sets, and results from one representative experiment or image are shown. All statistical analyses were performed in Prism 6 (GraphPad, La Jolla, CA) unless noted. All results are reported as mean ± SEM, unless indicated. The statistical significance of these data was determined using an unpaired, parametric *t*-test with 95% confidence interval. The statistical significance of the viability data set was determined using the Mann-Whitney test (two-tailed, 95% confidence interval). Data were reported significant as follows: * if $p \leq 0.05$, ** if $p \leq 0.01$, and *** if $p \leq 0.001$.

Figures

Figure 3.1: Changes in cell morphology and growth pattern upon IL-1β treatment under bright light microscope at 4x magnification.

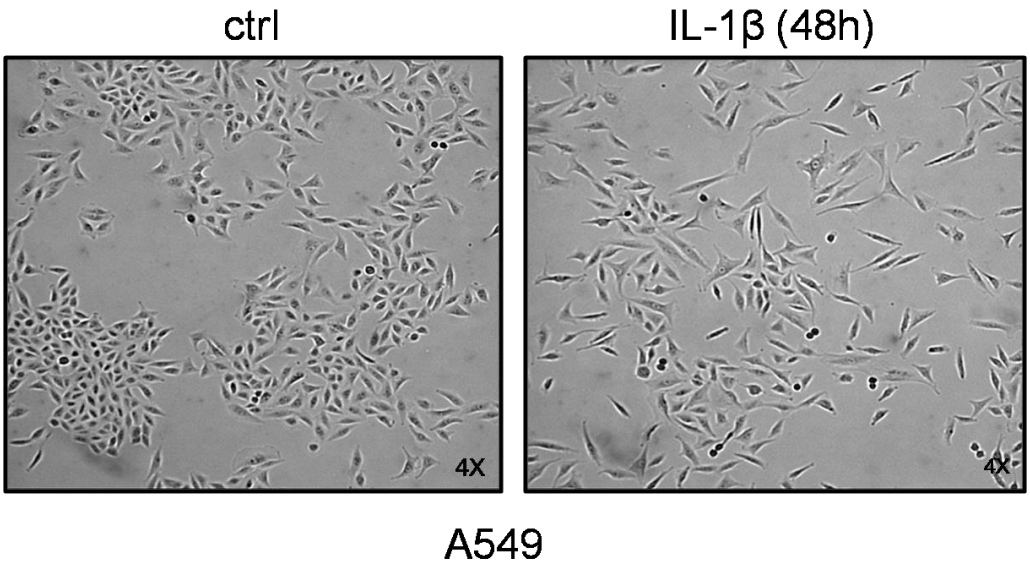

Figure 3.2: Expression levels of EMT markers determined by immunoblotting after 48-hour IL-1β treatment in A549 cells.

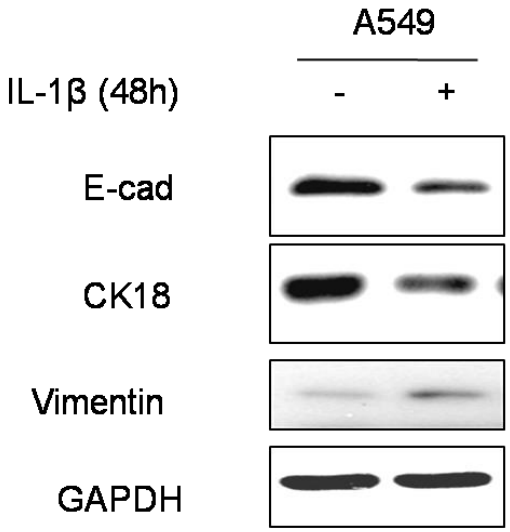

Figure 3.3: There are more membrane ruffling and cytoplasmic protrusions (indicated by arrows) in IL-1β-treated cells than in control cells. Images were taken at 400x magnification using a phase-contrast microscope.

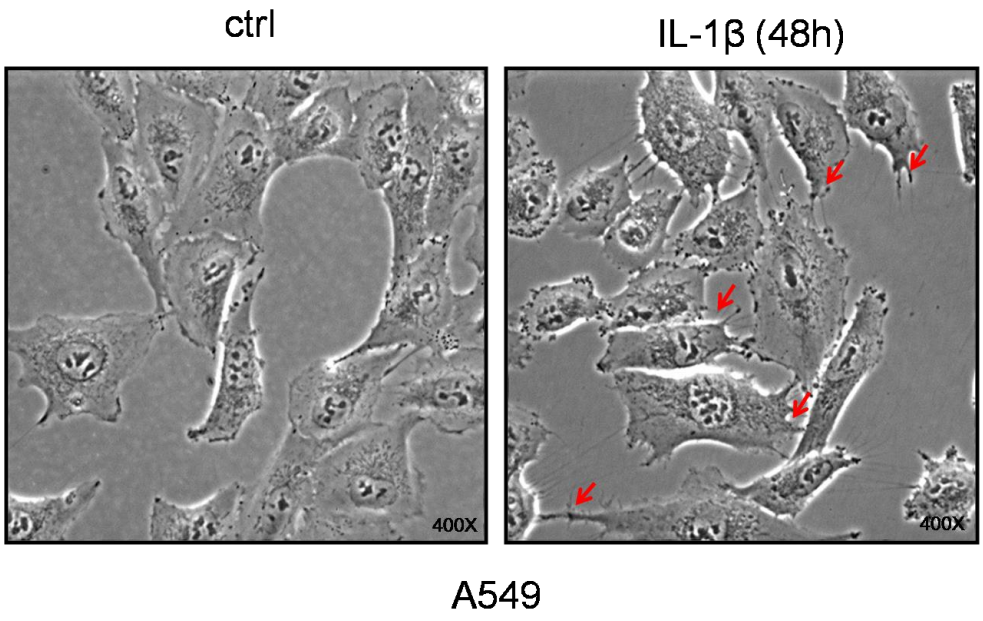

Figure 3.4: Cell migration demonstrated by scratch assay. Images were taken 24 hours after a scratch was created (top). Statistical analysis of the percentage of closed distance compared to that at the zero time point (bottom).

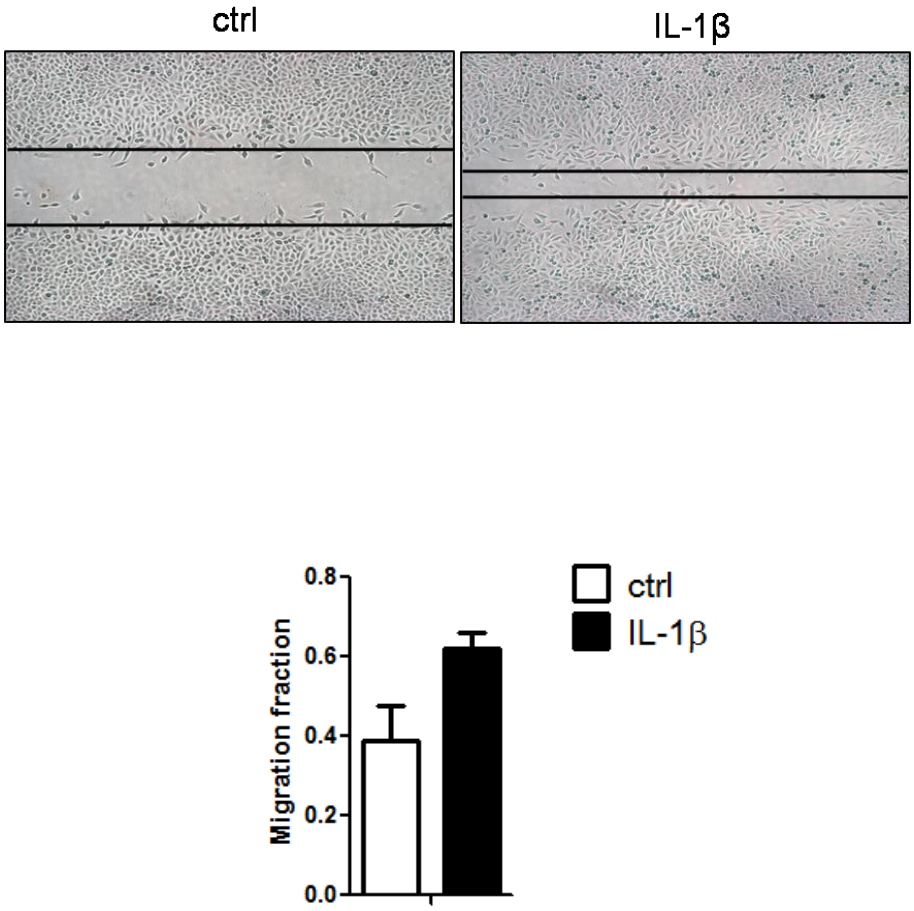

Figure 3.5: IL-1β treatment decreases cell proliferation in a 72-hour time frame.

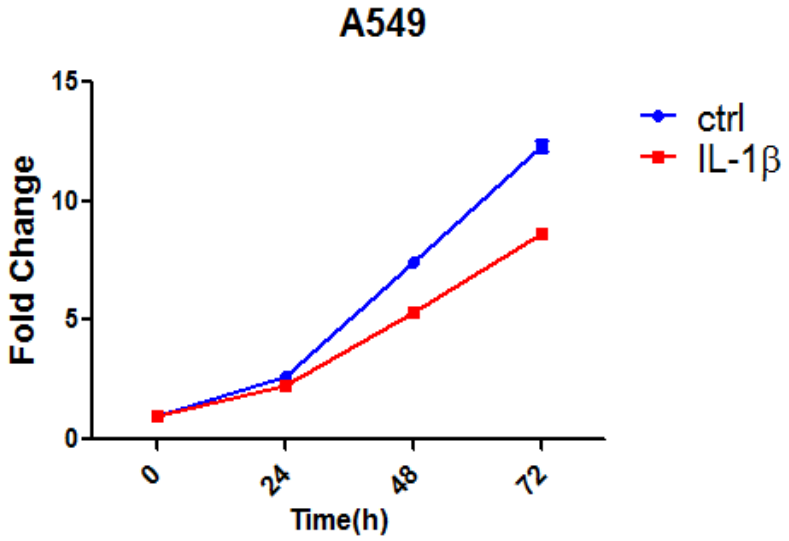

Figure 3.6: The expression levels of EMT markers determined by immunoblotting after 48-hour IL-1β treatment in A427 and H460 cell lines.

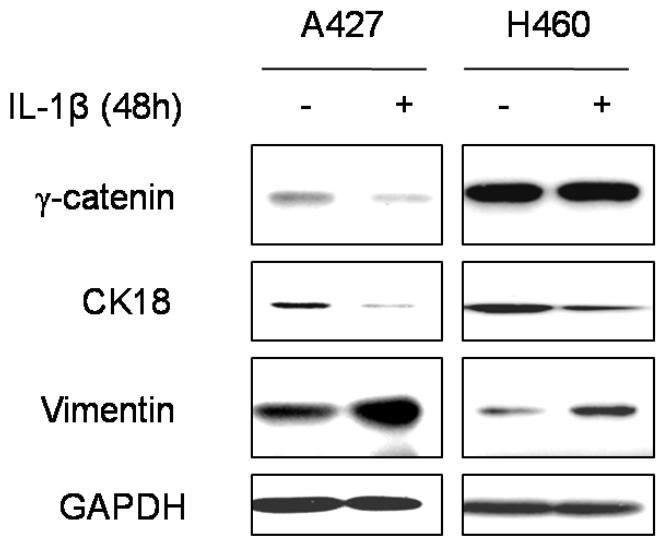

Figure 3.7: Immunoblotting shows the pathways activated by IL-1β treatment at the indicated time points (15 minutes, 30 minutes, 1 hour, 8 hours, 24 hours and 48 hours).

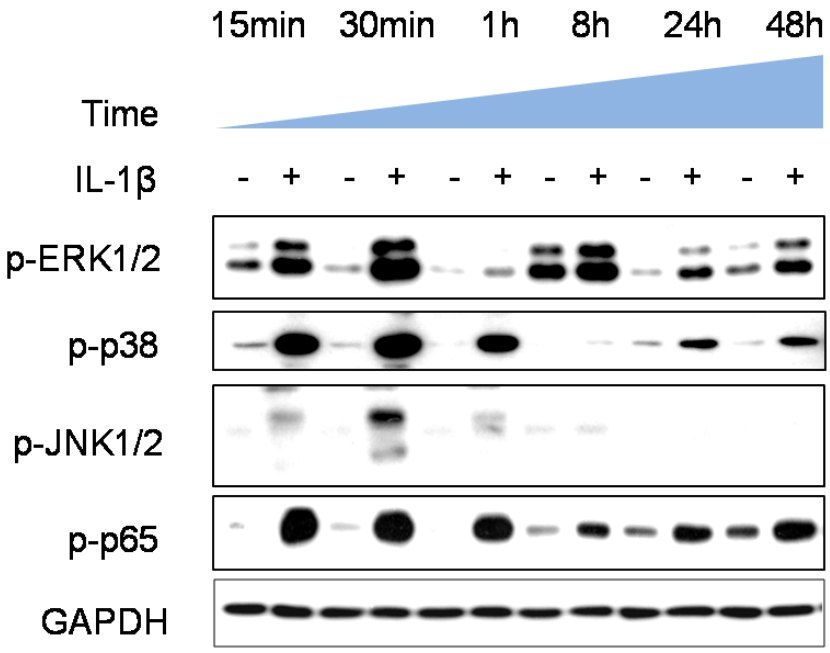

Figure 3.8: Immunoblot analysis of EMT markers after inhibition of the indicated pathways (top) and dose-dependent inhibition of the ERK and JNK pathways (bottom). JNKi, JNK inhibitor; ERKi, ERK inhibitor.

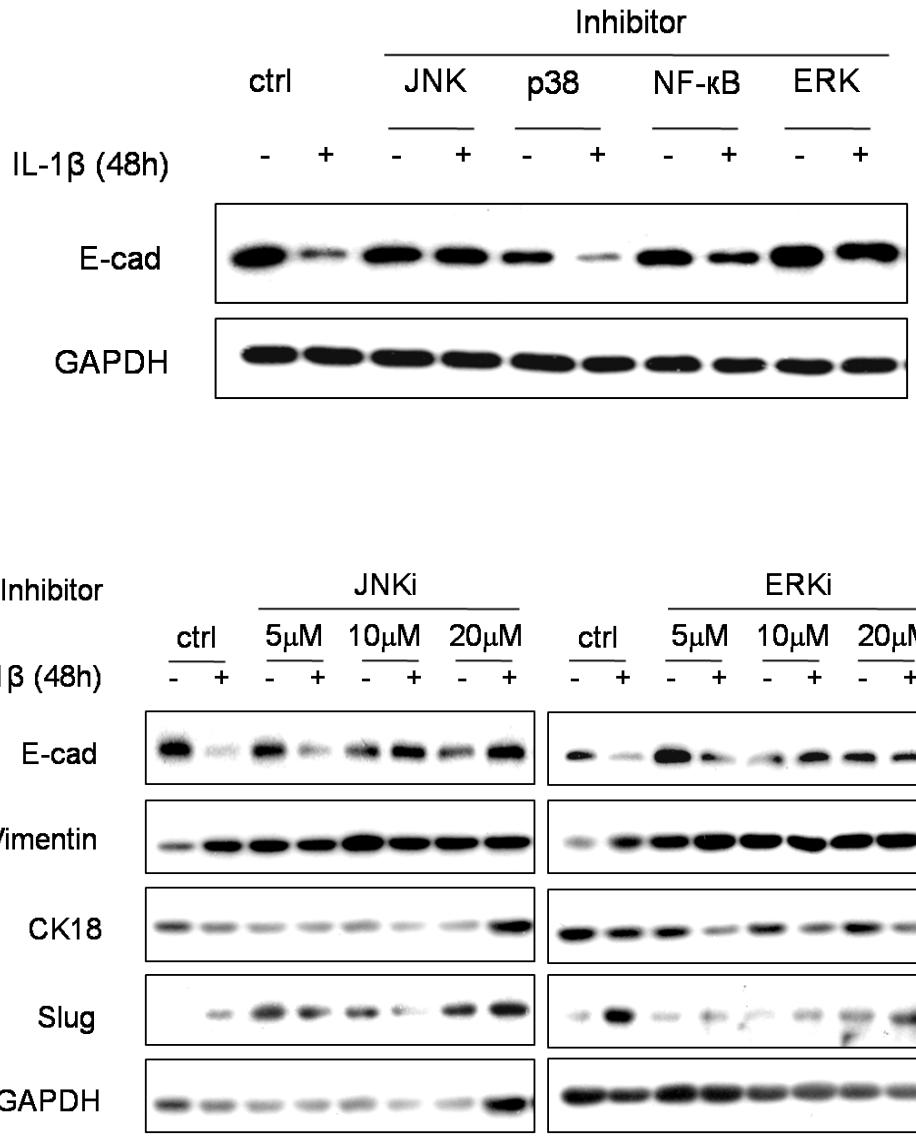

Figure 3.9: Phosphorylation of Fra-1 and c-Jun after 30 minutes of IL-1β treatment (top). The relative expression of Fra-1 and c-Jun after 48 hours of IL-1β treatment, as determined by RT-PCR (bottom).

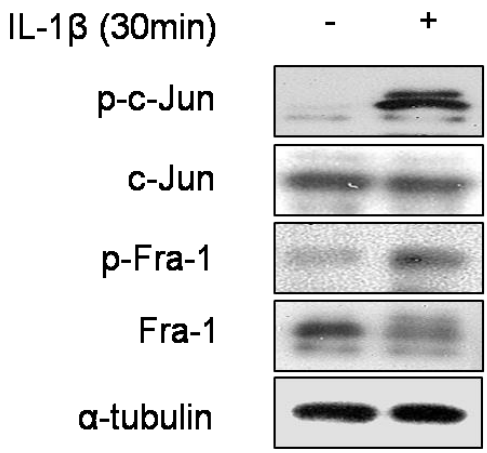

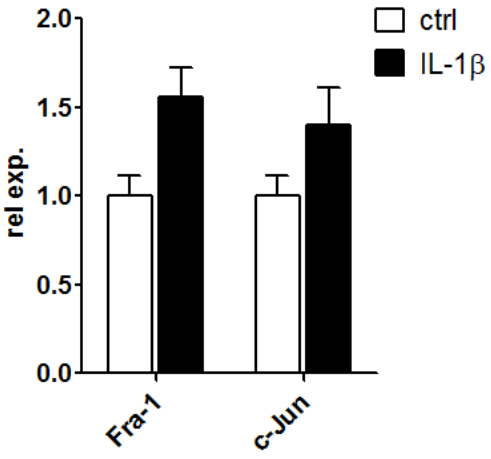

Figure 3.10: The relative expression of Snail, Slug, Zeb1, Zeb2 and Twist1 after 48 hours of IL-1β treatment, as determined by RT-PCR.

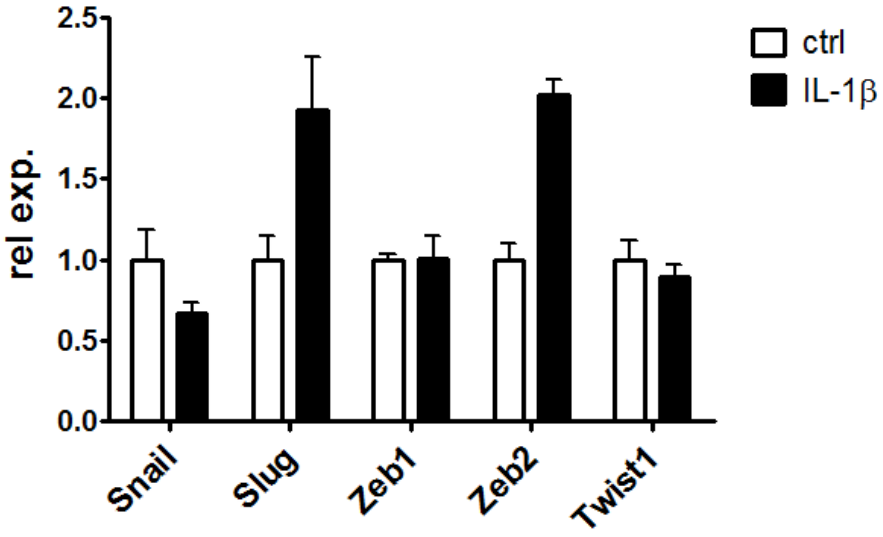

Figure 3.11: Knockdown of Slug, Zeb2 (top) or Fra-1 (bottom) by siRNA 24 hours before the acute IL-1β treatment. Expression levels of the EMT markers, Fra-1 and Slug were determined by immunoblotting.

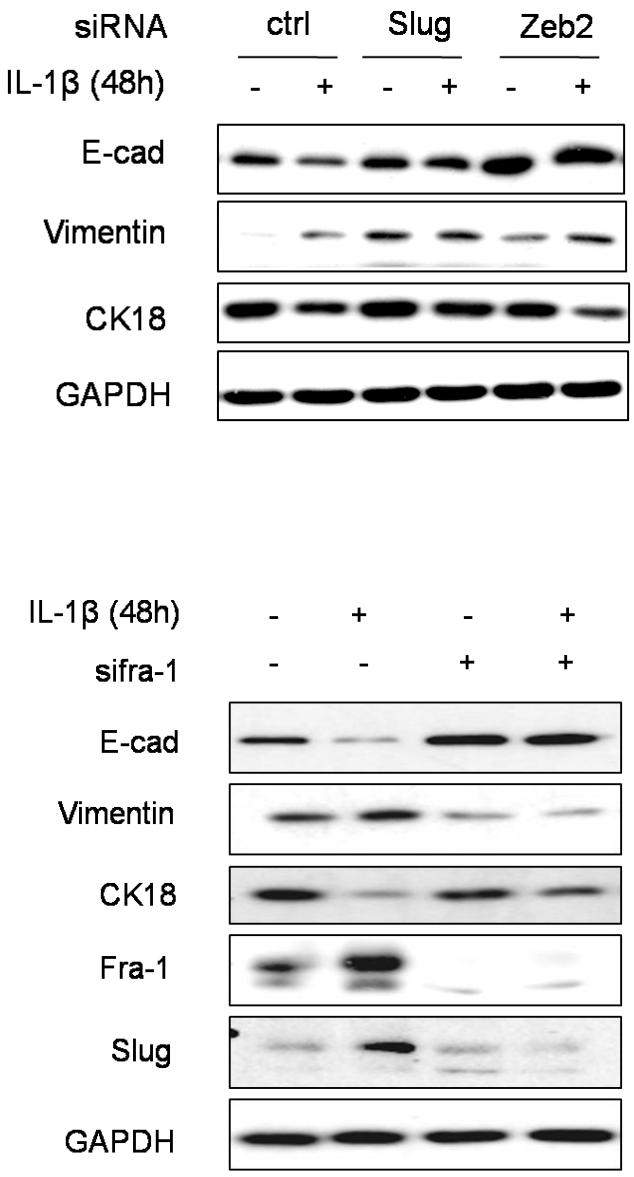

Figure 3.12: The relative expression levels of other AP-1 components after 48 hours of IL-1β treatment. N.D., not detectable.

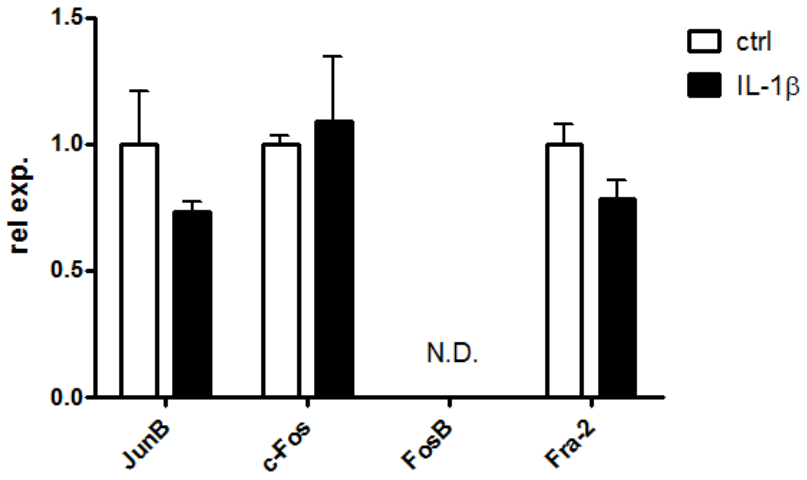

Figure 3.13: Schematic mechanism of EMT induced by the acute IL-1β treatment. IL-1β activates the ERK and JNK pathways that further increase the expression as well as phosphorylation of Fra-1 and c-Jun. Subsequently, Slug and Zeb2 is upregulated and repression E-cadherin. P indicates phosphorylation.

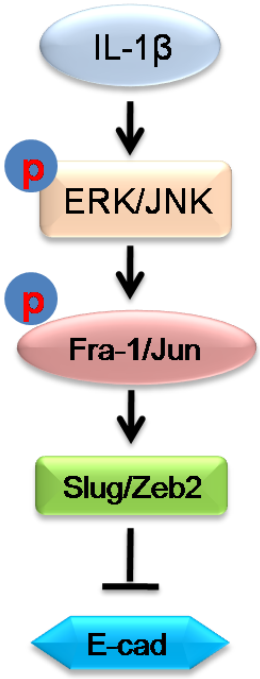

Figure 3.14: Schematic model of the experimental design (top). Changes in cell morphology and growth pattern upon chronic IL-1β treatment and IL-1β withdrawal under bright light microscope (4x) (bottom). "-" indicates IL-1β withdrawal. -6d, 6 days after IL-1β withdrawal.

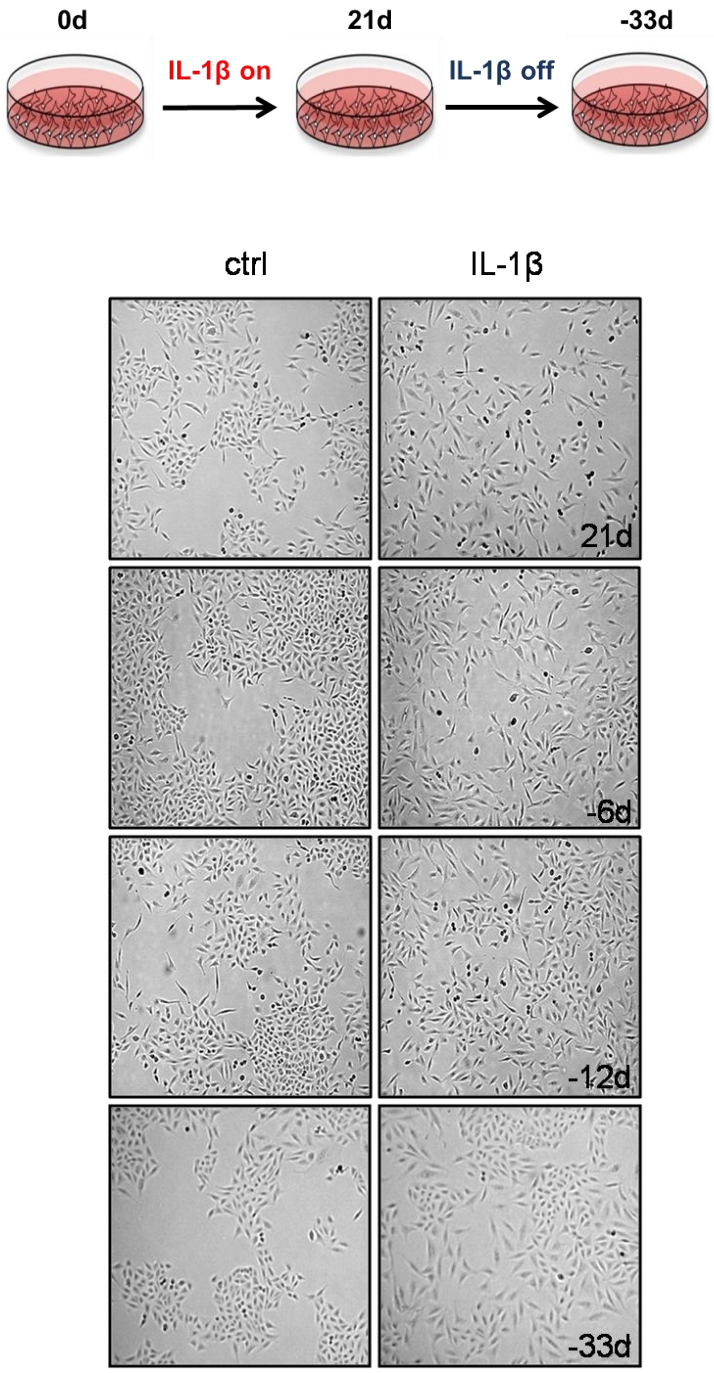

Figure 3.15: Expression levels of EMT markers determined by immunoblotting at the indicated time points during the experiment. IL-1β was withdrawn at day 21.

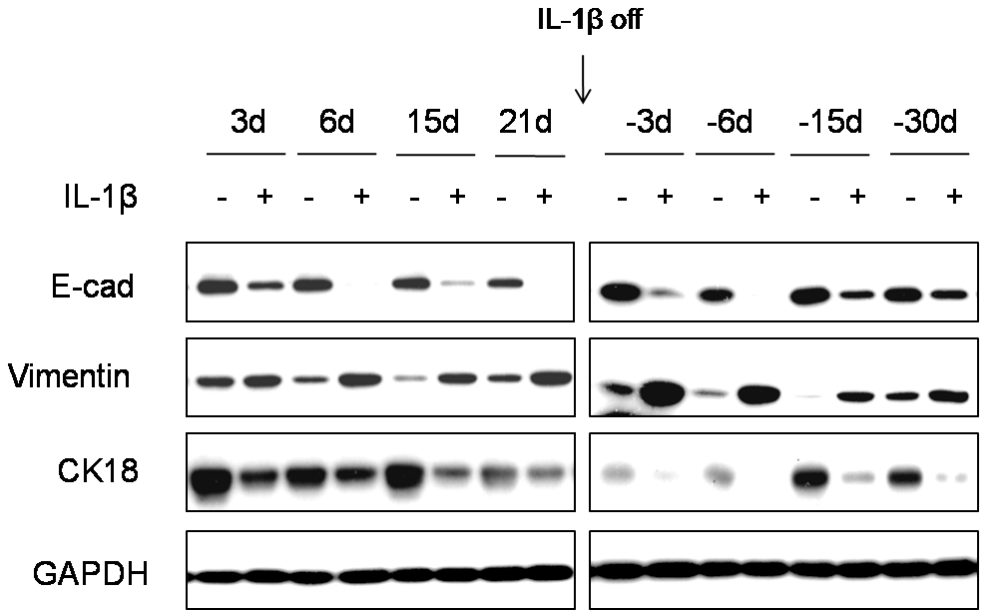

Figure 3.16: Cells were treated with IL-1β for the indicated number of days (3 days, 6 days and 14 days) and cultured without IL-1β for additional days. Expression levels of EMT markers were determined by immunoblotting.

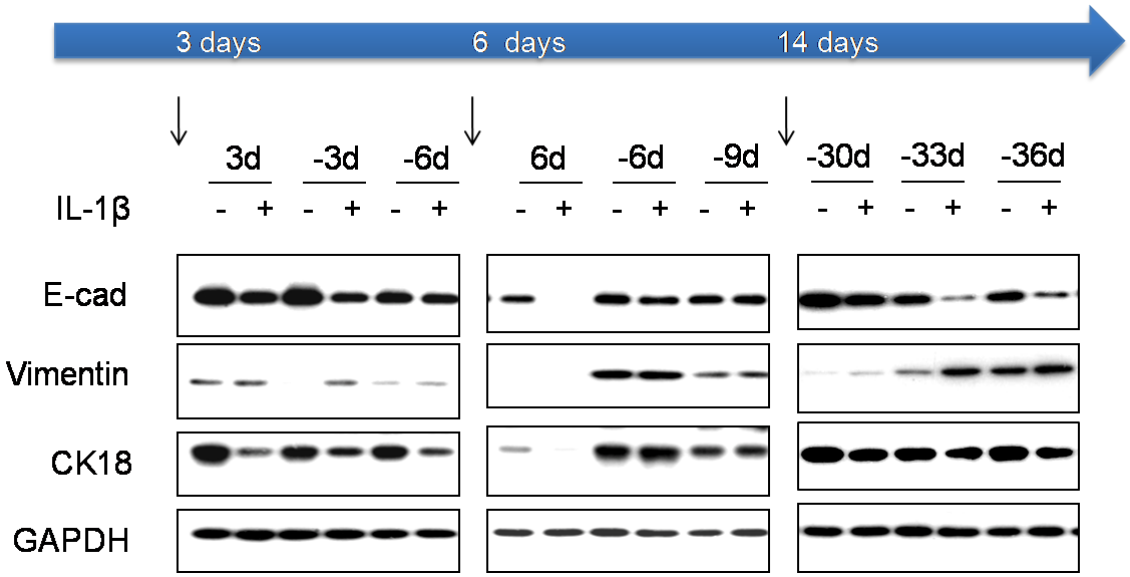

Figure 3.17: Cells were treated with both a low dose (L, 1ng/ml) and a high dose (H, 10ng/ml) of IL-1β for 9 days and cultured without IL-1β for an additional12 days. Expression levels of EMT markers were determined by immunoblotting.

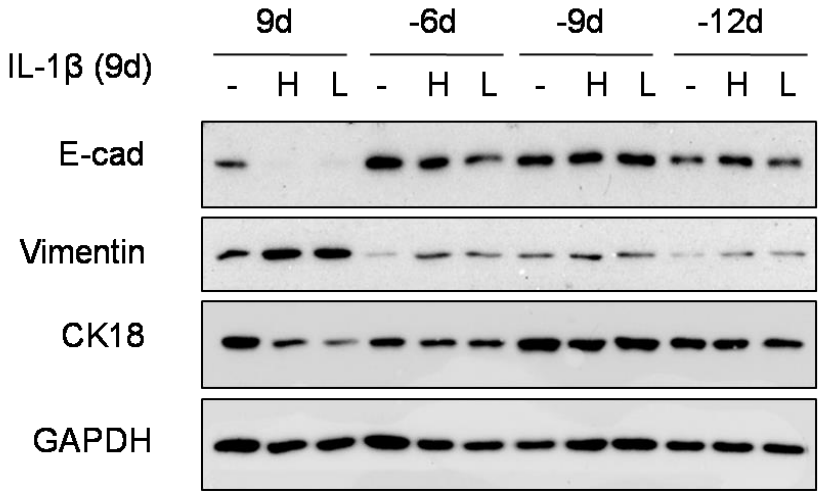

Figure 3.18: NSCLC cell lines A427 and H460 were chronically exposed to IL-1β for 21 days and cultured without IL-1β for additional days as indicated. Expression levels of EMT markers were determined by immunoblotting. The expression of E-cadherin was not detectable in these two cell lines.

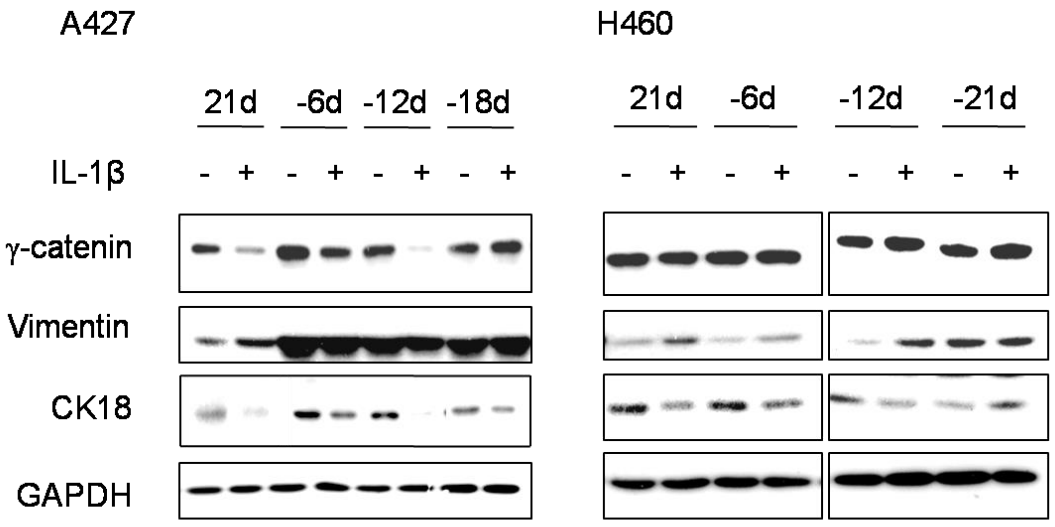

Figure 3.19: A549 cells were treated with TNF-α (10ng/ml) and TGF-β (5ng/ml) for 21 days and cultured without the cytokines for an additional 28 days. Expression levels of EMT markers were determined by immunoblotting. 0, ctrl; 1, TNF-α; 2, TGF-β.

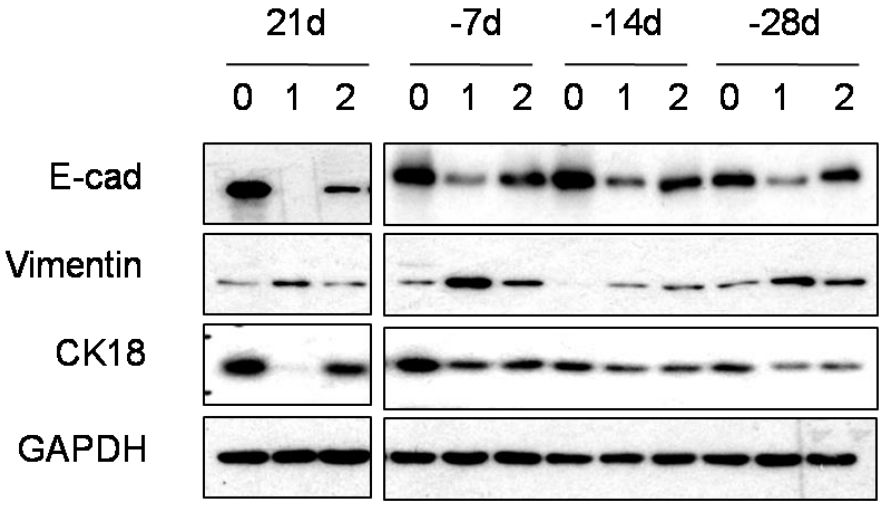

Figure 3.20: The relative expression levels of Fra-1/c-Jun (top) and Slug/Zeb2 (bottom) over the course of the experiment, as determined by RT-PCR. IL-1β was withdrawn on day 21 as the arrow indicated.

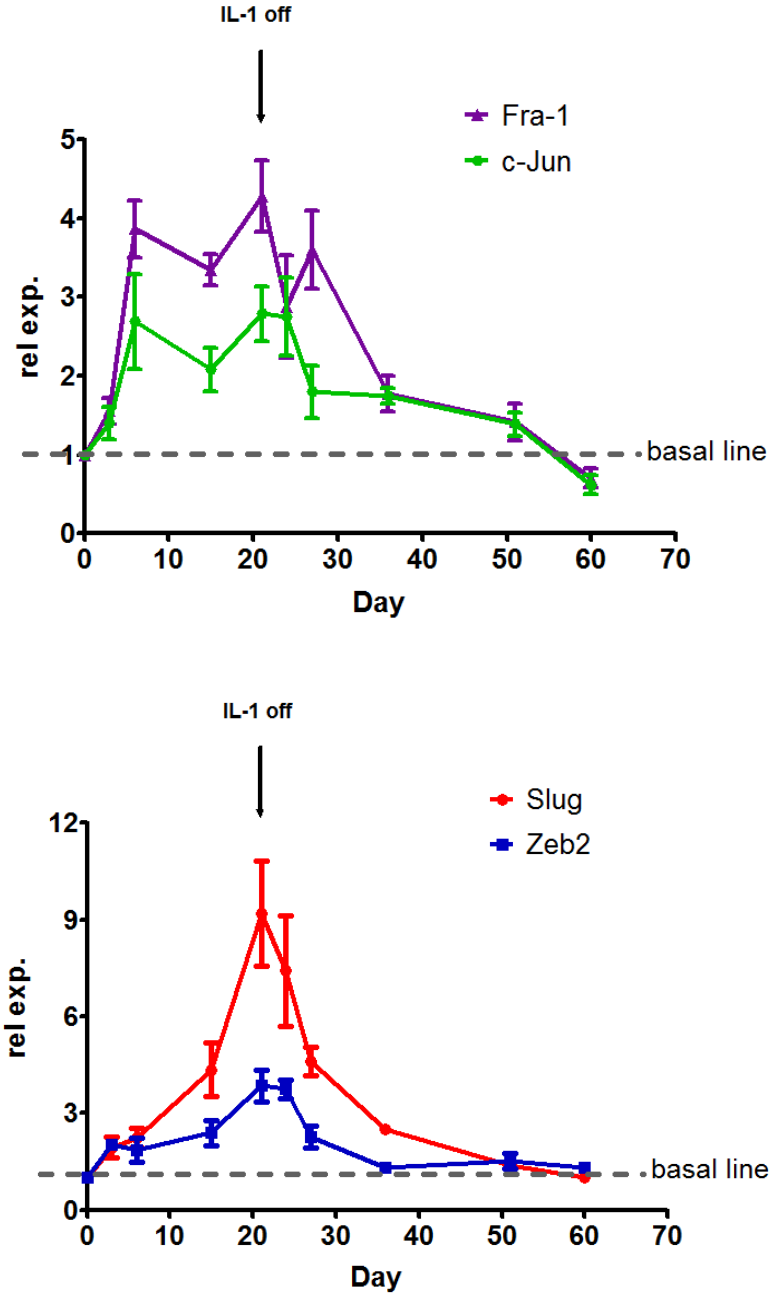

Figure 3.21: Immunoblot analysis shows the activation of signaling pathways at the indicated experimental time points. Phosphorylation of p38, JNK and p65 was not detected after IL-1β withdrawal.

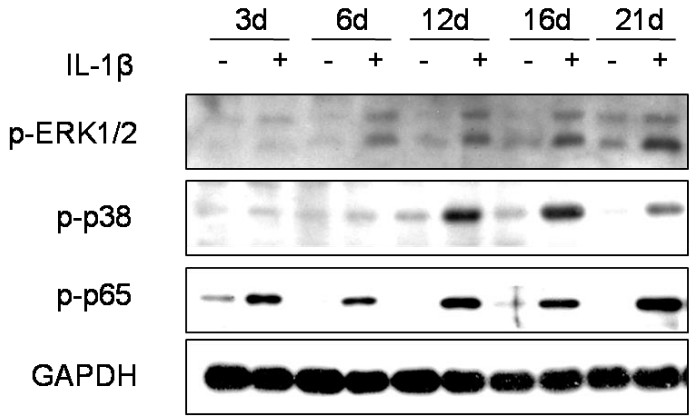

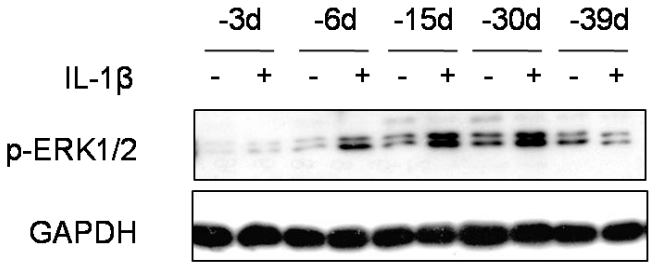

Figure 3.22: Immunoblot analysis of EMT markers after either siRNA knockdown of Fra-1 or inhibition of the ERK/JNK pathways for 72 hours (top) and after prolonged silencing of Fra-1 for 12 days during EMT memory (bottom). Ei+Ji, combined inhibition of the ERK and JNK pathways.

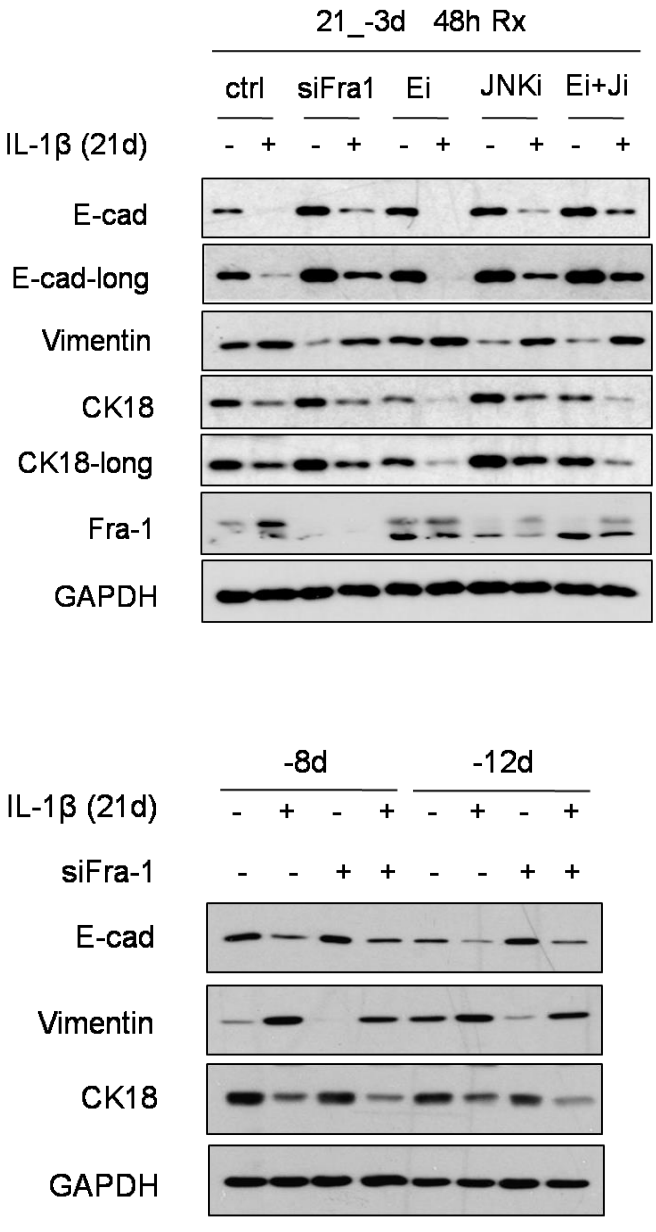

Figure 3.23: Schematic model of the experimental design (top). Immunoblotting of EMT markers following the repetitive siRNA knockdown of Fra-1 starting 9 days after the initial IL-1β treatment (bottom).

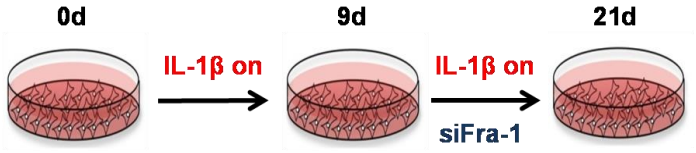

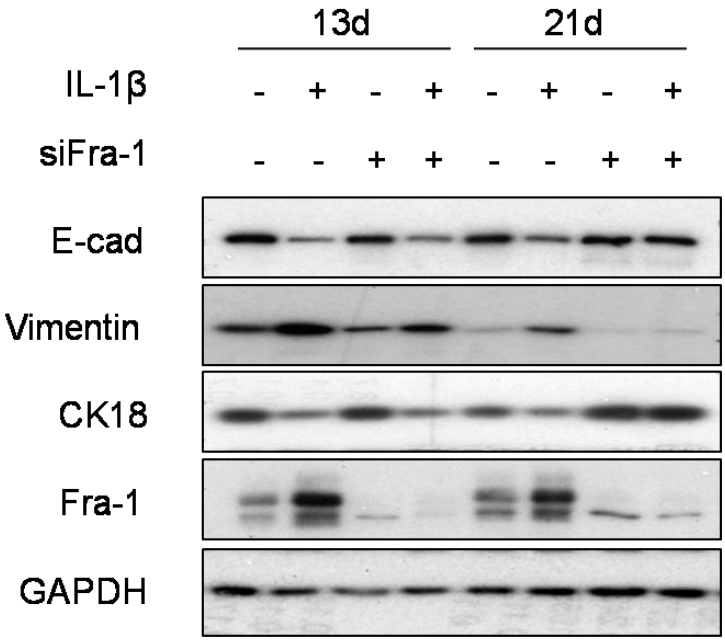

Figure 3.24: Schematic model of the experimental design. At every stage, cells were incubated with epigenetic inhibitors for 72 hours. EpiI: epigenetic inhibitors. EMT induction: treatment with EpiI before 48-hour IL-1β exposure. Acute EMT: treatment with EpiI 4 days after IL-1β exposure. Chronic EMT: treatment with EpiI after 21-day IL-1β exposure. EMT memory: treatment with EpiI 4 days after withdrawing IL-1β from 21-day IL-1β exposure.

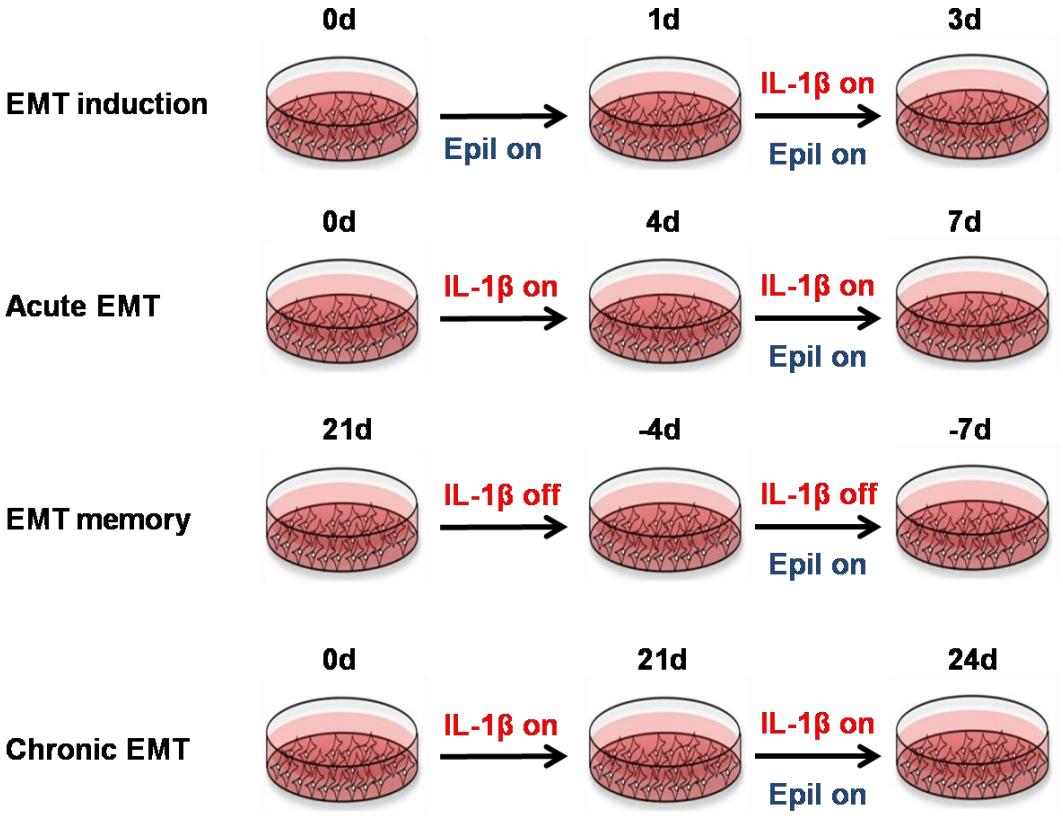

Figure 3.25: Schematic model of the experimental design (top). Immunoblotting shows the effect of epigenetic inhibitors on EMT induction (bottom). TSA: Trichostatin A (50nM). Aza: 5'-Aza-2'-deoxycytidine (5µM). EPZ: EPZ-6438 (20µM). BIX: BIX01294 (1µM). OG-L: OG-L002 (50µM).

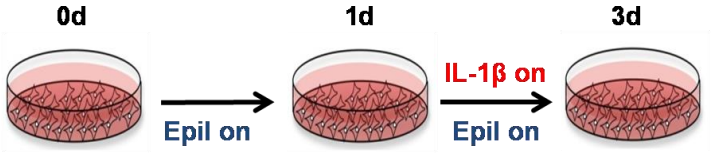

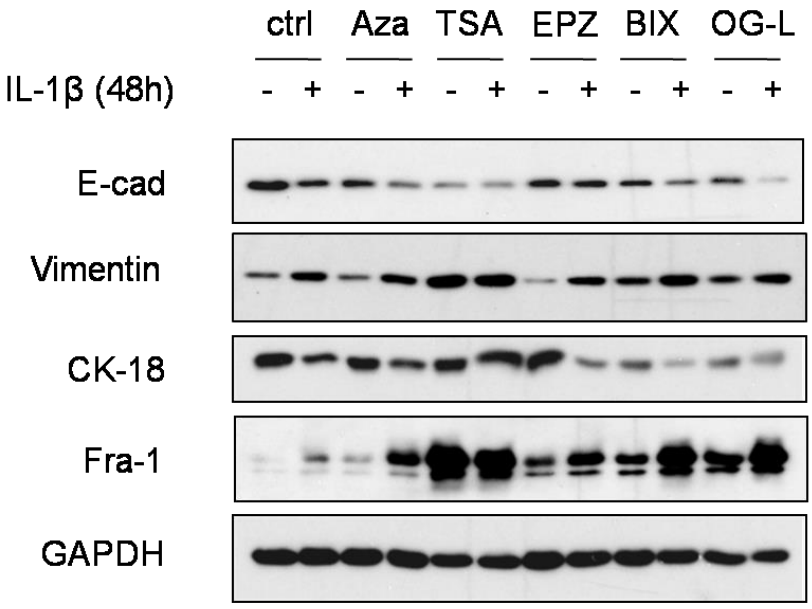

Figure 3.26: Schematic model of the experimental design (top). Immunoblotting shows the effect of epigenetic inhibitors in acute EMT (bottom). TSA: Trichostatin A (50nM). Aza: 5'-Aza-2'-deoxycytidine (5µM). EPZ: EPZ-6438 (20µM). BIX: BIX01294 (1µM). OG-L: OG-L002 (50µM).

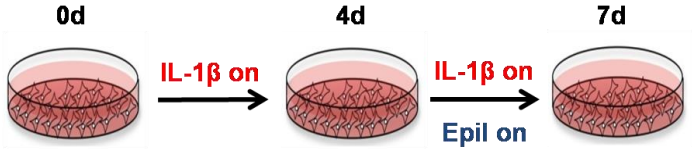

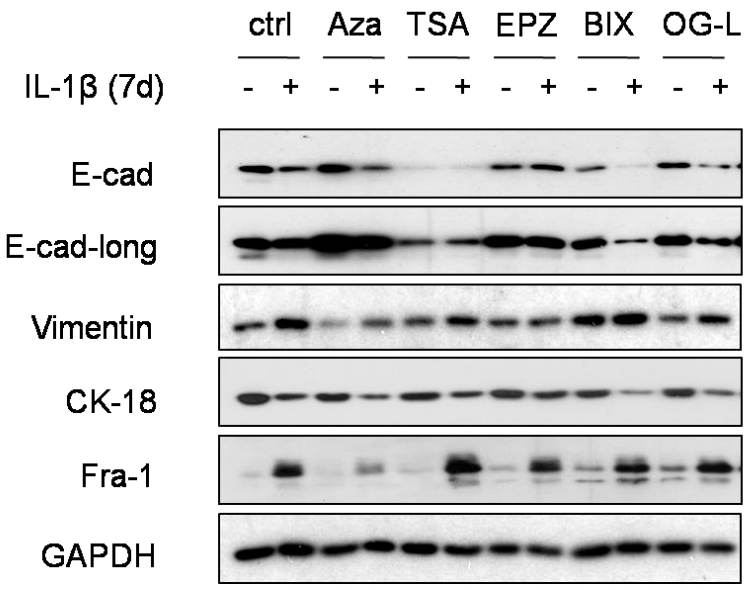

Figure 3.27: Schematic model of the experimental design (top). Immunoblotting shows the effect of epigenetic inhibitors on EMT memory (bottom). TSA: Trichostatin A (50nM). Aza: 5'-Aza-2'-deoxycytidine (5µM). EPZ: EPZ-6438 (20µM). BIX: BIX01294 (1µM). OG-L: OG-L002 (50µM).

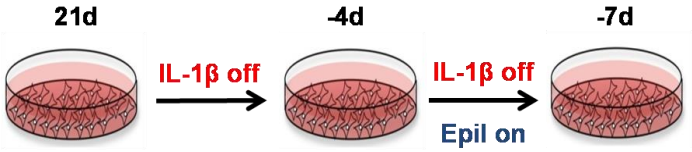

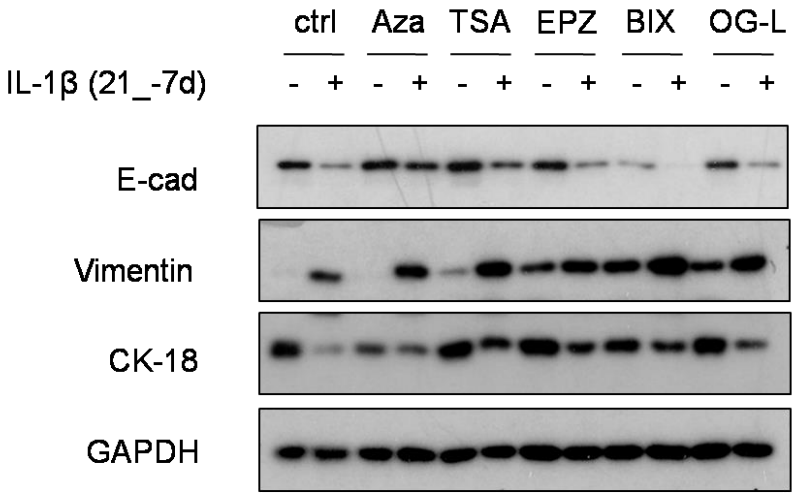

Figure 3.28: Schematic model of the experimental design (top). Immunoblotting shows the effect of epigenetic inhibitors in chronic EMT (bottom). TSA: Trichostatin A (50nM). Aza: 5'-Aza-2'-deoxycytidine (5μM). EPZ: EPZ-6438 (20μM). BIX: BIX01294 (1μM). OG-L: OG-L002 (50μM).

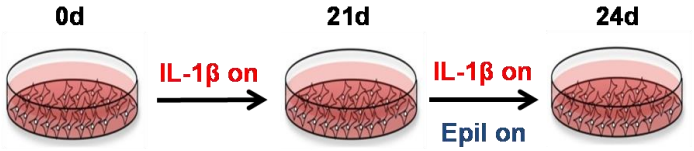

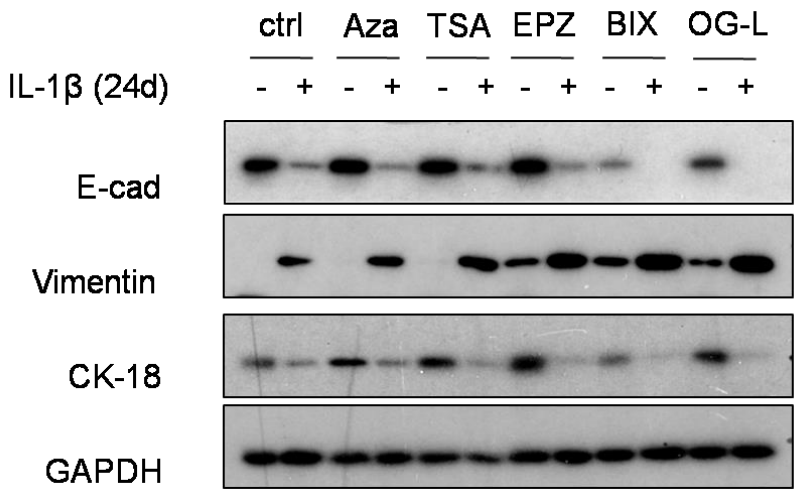

Figure 3.29: Immunoblotting of EMT markers following EZH2 knockdown in EMT induction and acute EMT.

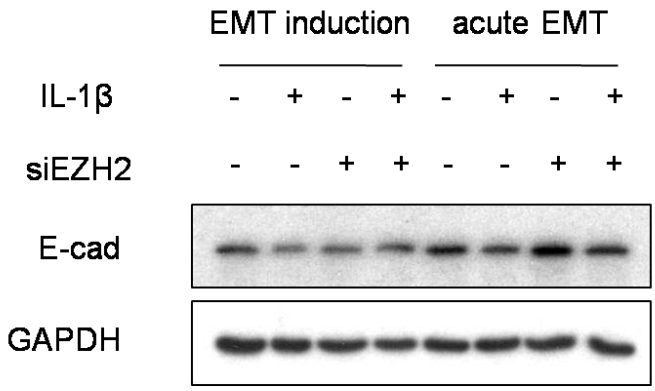

Figure 3.30: The relative enrichment of H3K9ac, H3K4me3, H3K27me3, H3K9me2 and H3K9me3 in E-cadherin promoter, as determined by ChIP-PCR over the indicated time course. Actin promoter serves as an internal control. IL-1β was withdrawn on day 21 as indicated by the arrow.

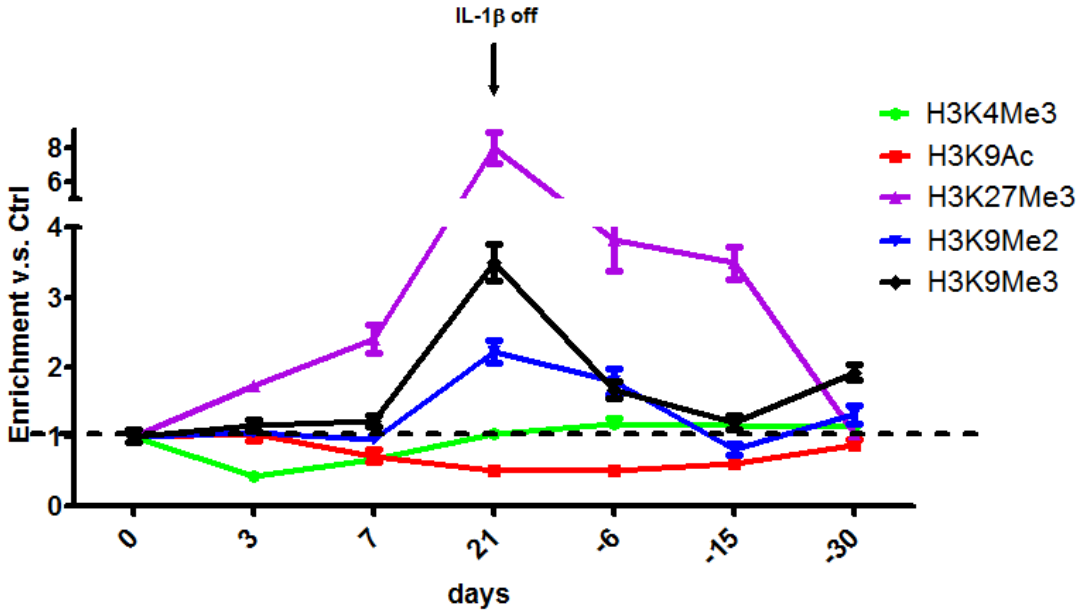

Figure 3.31: MSP analysis of the E-cadherin promoter. Top: cells were treated with IL-1β for 21 days and cultured for an additional 30 days after IL-1β withdrawal. Bottom: cells were treated with the indicated cytokines for 21 days and cultured for an additional 7 days after cytokine withdrawal. U, unmethylated band; M, methylated band.

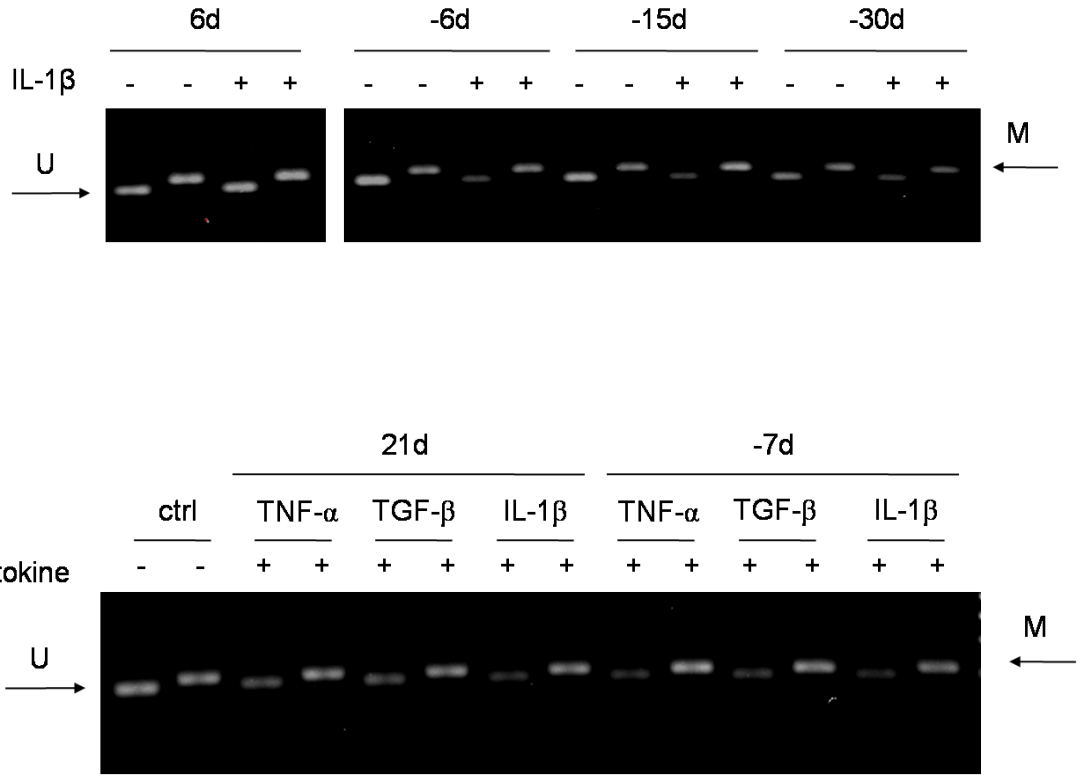

Figure 3.32: Regulation of EMT markers by a gradual increased concentration of doxycycline (indicated by the blue triangle) shown by immunoblot analysis (left to right: 0, 0.1ng/ml, 0.5ng/ml, 1ng/ml and 1µg/ml). P, parental A549 cells as a control.

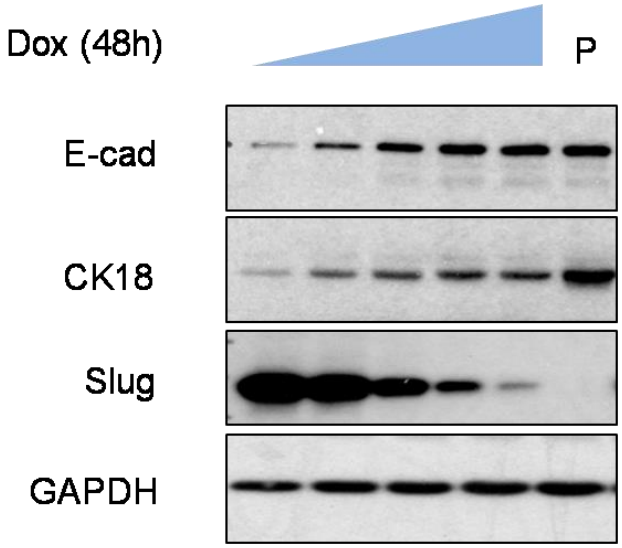

Figure 3.33: Regulation of EMT markers by a gradual increased concentration of doxycycline shown by immunoblot analysis (left to right 0, 0.5ng/ml, 1ng/ml and 1µg/ml) (left). MSP analysis of E-cadherin promoter with low or high level of doxycycline (left to right, 0 and1µg/ml) (right). The very left lane is the DNA marker.

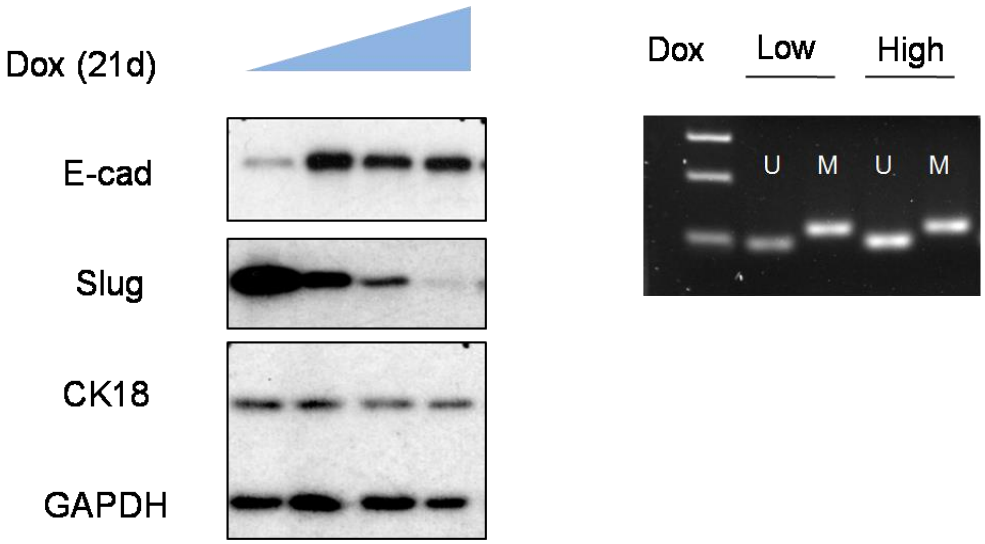

Figure 3.34: Proliferation of A549 cells on indicated conditions (top). Cell colonies from the representative well of the AIG assay (bottom) and quantification of colonies from replicated wells (top right). IL-1β on: cells were plated for experiment after chronic IL-1β treatment (21 days). IL-1β off: cells were plated for experiment 21 days after IL-1β withdrawal from chronic IL-1 β treatment.

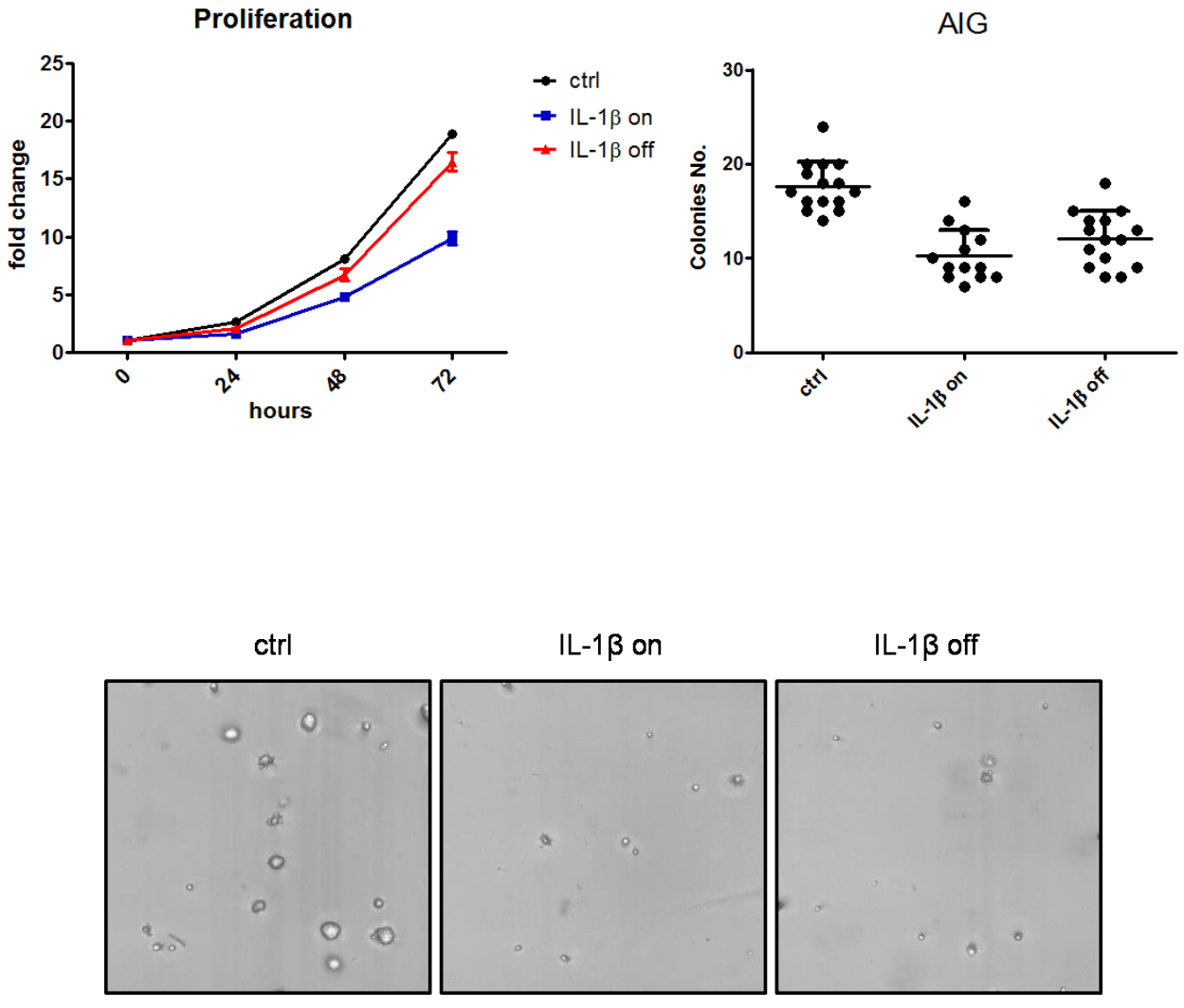

Figure 3.35: Relative expression of the indicated epigenetic enzymes after chronic IL-1β treatment.

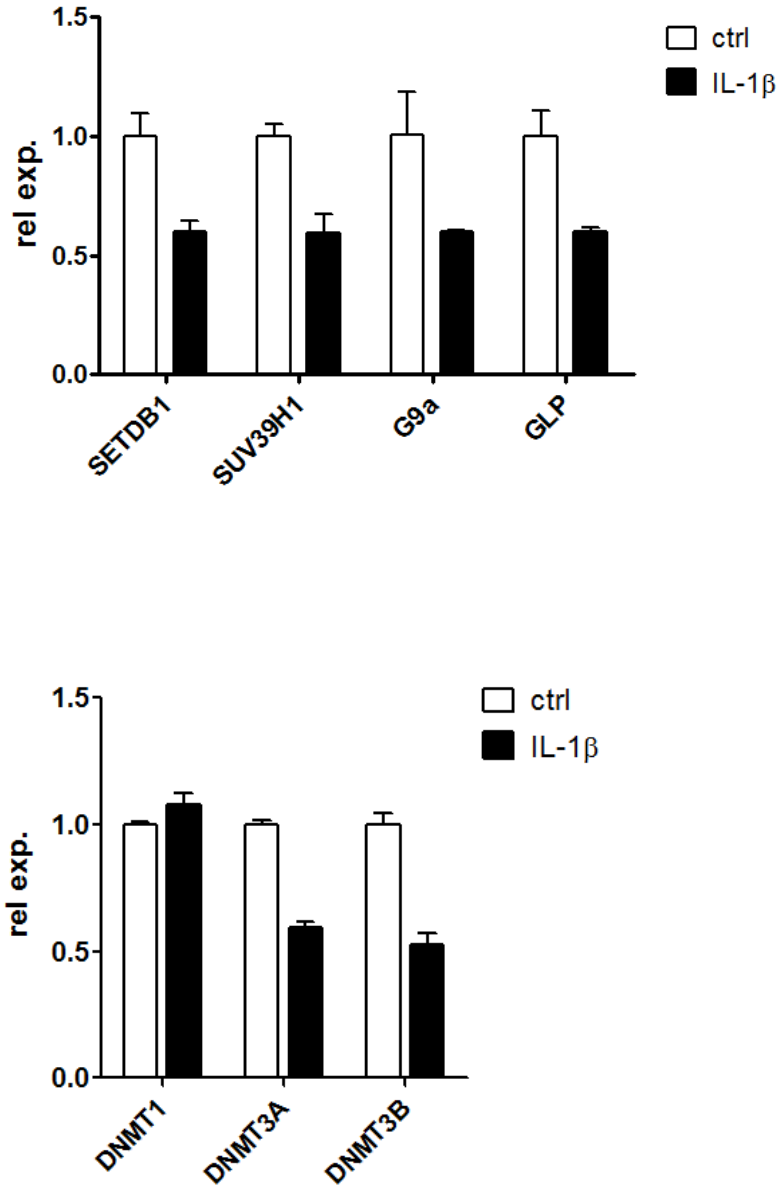

References

1. Siegel RL, Miller KD, & Jemal A (2016) Cancer statistics, 2016. *CA: a cancer journal for clinicians* 66(1):7-30.

2. Torre LA, Siegel RL, & Jemal A (2016) Lung Cancer Statistics. *Advances in experimental medicine and biology* 893:1-19.

3. Doll R & Hill AB (1950) Smoking and carcinoma of the lung; preliminary report. *British medical journal* 2(4682):739-748.

4. Thun MJ*, et al.* (2013) 50-year trends in smoking-related mortality in the United States. *The New England journal of medicine* 368(4):351-364.

5. Zuo L, Otenbaker NP, Rose BA, & Salisbury KS (2013) Molecular mechanisms of reactive oxygen species-related pulmonary inflammation and asthma. *Molecular immunology* 56(1-2):57-63.

6. Durham AL & Adcock IM (2015) The relationship between COPD and lung cancer. *Lung cancer* 90(2):121-127.

7. Warnock ML & Isenberg W (1986) Asbestos burden and the pathology of lung cancer. *Chest* 89(1):20-26.

8. Enewold L*, et al.* (2009) Serum concentrations of cytokines and lung cancer survival in African Americans and Caucasians. *Cancer epidemiology, biomarkers & prevention : a*

publication of the American Association for Cancer Research, cosponsored by the American Society of Preventive Oncology 18(1):215-222.

9. He X*, et al.* (2015) Advanced Lung Cancer Inflammation Index, a New Prognostic Score, Predicts Outcome in Patients With Small-Cell Lung Cancer. *Clinical lung cancer* 16(6):e165-171.

10. Kasymjanova G*, et al.* (2010) The predictive value of pre-treatment inflammatory markers in advanced non-small-cell lung cancer. *Current oncology* 17(4):52-58.

11. Pinato DJ*, et al.* (2014) Prognostic performance of inflammation-based prognostic indices in primary operable non-small cell lung cancer. *British journal of cancer* 110(8):1930-1935.

12. Dubinett SM (2015) *Inflammation and Lung Cancer* (Springer-Verlag New York).

13. Kalluri R & Weinberg RA (2009) The basics of epithelial-mesenchymal transition. *The Journal of clinical investigation* 119(6):1420-1428.

14. Thiery JP, Acloque H, Huang RY, & Nieto MA (2009) Epithelial-mesenchymal transitions in development and disease. *Cell* 139(5):871-890.

15. Garber K (2008) Epithelial-to-mesenchymal transition is important to metastasis, but questions remain. *Journal of the National Cancer Institute* 100(4):232-233, 239.

16. Ledford H (2011) Cancer theory faces doubts. *Nature* 472(7343):273.

17. Tarin D, Thompson EW, & Newgreen DF (2005) The fallacy of epithelial mesenchymal transition in neoplasia. *Cancer research* 65(14):5996-6000; discussion 6000-5991.

18. Thompson EW, Newgreen DF, & Tarin D (2005) Carcinoma invasion and metastasis: a role for epithelial-mesenchymal transition? *Cancer research* 65(14):5991-5995; discussion 5995.

19. Tam WL & Weinberg RA (2013) The epigenetics of epithelial-mesenchymal plasticity in cancer. *Nature medicine* 19(11):1438-1449.

20. Tsai JH & Yang J (2013) Epithelial-mesenchymal plasticity in carcinoma metastasis. *Genes & development* 27(20):2192-2206.

21. Ocana OH*, et al.* (2012) Metastatic colonization requires the repression of the epithelial-mesenchymal transition inducer Prrx1. *Cancer cell* 22(6):709-724.

22. Tsai JH, Donaher JL, Murphy DA, Chau S, & Yang J (2012) Spatiotemporal regulation of epithelial-mesenchymal transition is essential for squamous cell carcinoma metastasis. *Cancer cell* 22(6):725-736.

23. Lamouille S, Xu J, & Derynck R (2014) Molecular mechanisms of epithelial-mesenchymal transition. *Nature reviews. Molecular cell biology* 15(3):178-196.

24. Lin T, Ponn A, Hu X, Law BK, & Lu J (2010) Requirement of the histone demethylase LSD1 in Snai1-mediated transcriptional repression during epithelial-mesenchymal transition. *Oncogene* 29(35):4896-4904.

25. Peinado H, Ballestar E, Esteller M, & Cano A (2004) Snail mediates E-cadherin repression by the recruitment of the Sin3A/histone deacetylase 1 (HDAC1)/HDAC2 complex. *Molecular and cellular biology* 24(1):306-319.

26. Dong C*, et al.* (2013) Interaction with Suv39H1 is critical for Snail-mediated E-cadherin repression in breast cancer. *Oncogene* 32(11):1351-1362.

27. Dong C*, et al.* (2012) G9a interacts with Snail and is critical for Snail-mediated E-cadherin repression in human breast cancer. *The Journal of clinical investigation* 122(4):1469-1486.

28. Herranz N*, et al.* (2008) Polycomb complex 2 is required for E-cadherin repression by the Snail1 transcription factor. *Molecular and cellular biology* 28(15):4772-4781.

29. Tong ZT*, et al.* (2012) EZH2 supports nasopharyngeal carcinoma cell aggressiveness by forming a co-repressor complex with HDAC1/HDAC2 and Snail to inhibit E-cadherin. *Oncogene* 31(5):583-594.

30. Barbieri SS & Weksler BB (2007) Tobacco smoke cooperates with interleukin-1beta to alter beta-catenin trafficking in vascular endothelium resulting in increased permeability and induction of cyclooxygenase-2 expression in vitro and in vivo. *FASEB journal : official*

publication of the Federation of American Societies for Experimental Biology 21(8):1831-1843.

31. Elaraj DM*, et al.* (2006) The role of interleukin 1 in growth and metastasis of human cancer xenografts. *Clinical cancer research : an official journal of the American Association for Cancer Research* 12(4):1088-1096.

32. Lewis AM, Varghese S, Xu H, & Alexander HR (2006) Interleukin-1 and cancer progression: the emerging role of interleukin-1 receptor antagonist as a novel therapeutic agent in cancer treatment. *Journal of translational medicine* 4:48.

33. Rusznak C*, et al.* (2000) Effect of cigarette smoke on the permeability and IL-1beta and sICAM-1 release from cultured human bronchial epithelial cells of never-smokers, smokers, and patients with chronic obstructive pulmonary disease. *American journal of respiratory cell and molecular biology* 23(4):530-536.

34. Saijo Y*, et al.* (2002) Proinflammatory cytokine IL-1 beta promotes tumor growth of Lewis lung carcinoma by induction of angiogenic factors: in vivo analysis of tumor-stromal interaction. *Journal of immunology* 169(1):469-475.

35. Bakiri L*, et al.* (2015) Fra-1/AP-1 induces EMT in mammary epithelial cells by modulating Zeb1/2 and TGFbeta expression. *Cell death and differentiation* 22(2):336-350.

36. Nguyen PT*, et al.* (2013) The FGFR1 inhibitor PD173074 induces mesenchymal-epithelial transition through the transcription factor AP-1. *British journal of cancer* 109(8):2248-2258.

37. Bartchewsky W, Jr.*, et al.* (2009) Effect of Helicobacter pylori infection on IL-8, IL-1beta and COX-2 expression in patients with chronic gastritis and gastric cancer. *Scandinavian journal of gastroenterology* 44(2):153-161.

38. Dina R. Hammad AGE, Tarek S. Essawy, Sohair A. Abd El Sameie (2015) Evaluation of serum interleukin-1 beta as an inflammatory marker in COPD patients. *Egyptian Journal of Chest Diseases and Tuberculosis* 64(2):347-352.

39. Javaid S*, et al.* (2013) Dynamic chromatin modification sustains epithelial-mesenchymal transition following inducible expression of Snail-1. *Cell reports* 5(6):1679-1689.

CHAPTER FOUR: Future directions

Regulation of CXCR2 ligands by LKB1 in the development of NSCLC

Utilizing clinical biospecimens, it has been shown that high levels of CXCR2 ligands are correlated with tumor burden, patient survival and prognosis in multiple malignancies including NSCLC. Sanmamed *et al.* have found that the CXCL8 serum concentration is significantly higher in stage IV NSCLC patients than patients with earlier stages (1). Two other studies have identified CXCL5 and CXCL8 as prognostic markers of overall survival in patients with lung adenocarcinoma (2, 3). However, the status of these ligands in the early stages of lung cancer development is largely unknown. Therefore, we will seek to examine CXCR2 ligands in early stages of lung tumor development, including atypical adenomatous hyperplasia (AAH), adenocarcinoma in situ (AIS) and minimal invasive adenocarcinoma (MIA) in clinical samples as well as in genetically engineered murine models (4).

Based on our preliminary data, we are able to identify these early lesions from 2 to 4 weeks following tumor induction in mice with *Kras* and *Lkb1* mutation. We plan to collect the broncho-alveolar lavage (BAL) to measure the secreted ligands and whole lung tissue to identify the histopathologic subtypes. We will use mice with *Kras* and *Tp53* mutation background (KP) as the control. As we have already learned from our earlier studies, LKB1-dependent regulation of CXCR2 ligands is a cell-intrinsic regulation, we anticipate the ligands will also be abundantly produced in the premalignant and early cancerous lesions in *KL* tumors compared to *KP* tumors and normal lungs. It is important to understand the dynamic relationships of these ligands because it will allow us to better understand their biological significance in the early stages of lung cancer development and provide rationales for therapeutic and/or preventive applications.

Blockade of CXCR2 via the antagonist SB332235 *in vivo* will determine the contribution of CXCR2 ligands to the *KL* tumor development. Therefore, to assess the therapeutic merits of SB332235 in both the early and late stages of tumor development, we will treat the early

premalignant and cancerous lesions in *KL* mice as well as the invasive *Lkb1*-deficient tumors in syngeneic mice respectively. These experiments are promising because previous publications have already demonstrated reduced tumor incidence as well as tumor burden with CXCR2 blockade in multiple cancers. For example, using two inflammation-driven tumor models, Jamieson *et al.* were able to show that CXCR2 inhibition reduced the incidence of TPA-induced skin papilloma and AOM/DSS-induced GI adenoma, eventually suppressing tumorigenesis (5). Another study has demonstrated decreased tumor burden with CXCR2 inhibitor treatment after bacteria-induced inflammation in a murine *Kras* NSCLC model (6). There are also more data suggesting CXCR2 inhibition or CXCL5/CXCL8 blockade can reduce burden of full-blown tumors in xenograft, syngeneic and genetically engineered murine models (7-11).

As CXCR2 is expressed by neutrophils, macrophages, endothelial cells and epithelial cells, the mechanisms underlying the cancer-promoting effect of CXCR2 ligands are most likely involving these cells. Although some studies have shown a reverse correlation of CXCR2 expression in tumor cells with patient survival (3), our *in vitro* studies do not reveal any alterations in cell proliferation, invasion or major oncogenic signaling pathways with CXCR2 blockade in HBECs (data not shown), suggesting paracrine effects of CXCR2 ligands. Indeed, endothelial cells cultured with the supernatants from LKB1-deficent HBECs formed more and longer blood vessel-like tubes *in vitro* (data not shown), consistent with our previous data and other studies showing the reduction of blood vessel density with CXCR2 inhibition (6, 12-14).

The roles of tumor-associated neutrophils (TAN) are particularly interesting because there is increasing evidence showing their intensive involvement but controversial functions in tumor progression (15-17). Depending on different contexts, TAN can be further divided into an anti-tumor phenotype (N1) and a tumor-promoting phenotype (N2). N1 neutrophils dominantly secrete immune-activating cytokines or chemokines such as IL12 that assists T cell-dependent killing of cancer cells while N2 neutrophils function in the opposite way, characterized by high

level of arginase, VEGF and MMP9. The presence of N2 neutrophils facilitates tumor proliferation, metastasis, anti-tumor immunosuppression as well as resistance to chemotherapy (16). Importantly, tumors often preserve the ability to re-educate the N1 neutrophils and switch them to the N2 phenotype neutrophils. Therefore, a plethora of studies have demonstrated that depletion of neutrophils is able to decrease primary as well as metastatic tumor burden and restores active immune response against tumor cells (18-20). Intriguingly, the neutrophil-lymphocyte ratio has been intensively studied as a predictor of patient survival, responsiveness to chemotherapy as well as tumor recurrence in different cancers (21-24).

One paradoxical finding of TANs is their distinct roles in different stages of cancer. A recent study has isolated TANs from patients with early stage of lung cancer and compared their gene expression pattern with blood neutrophils (25). They found these TANs displayed activated phenotypes and produced large amounts of pro-inflammatory cytokines, which were able to stimulate T proliferation and INF-gamma release, suggesting a good anti-tumor response. Conversely, in a setting of inflammation-induced cancer, depletion of neutrophils significantly reduced pre-cancerous lesions and tumor incidence in a variety of cancers (5, 6, 26-28).

Myeloid-derived suppressor cells (MDSCs) can also be recruited by CXCR2 ligands. MDSCs are comprised of the monocytic cells (M-MDSCs) and the granulocytic cells (G-MDSCs), both of which are functionally immature and capable of inducing profound immune suppression in the tumor microenvironment. These MDSCs are able to suppress the cytotoxic effects of T cells by releasing high levels of ROS, arginase and myeloperoxidase (29, 30). In addition, a recent study has also shown that depletion of MDSCs enhances the efficacy of PD1/PD-L1 blockade in melanoma and rhabdomyosarcoma (31, 32).

It has been shown that LKB1-deficient lung tumors are characterized with a pro-inflammatory yet immunosuppressive tumor microenvironment along with a large infiltration of neutrophils (33).

Importantly, blockade of the inflammatory cytokine IL-6 reduced tumor burden. Therefore, based on all these previous studies, we hypothesize that CXCR2 ligands in *KL* tumors recruit neutrophils and/or MDSCs which not only facilitate tumor growth and metastasis by promoting tumor-favored inflammation, but also suppress T cell-mediated anti-tumor responses. In addition to our CXCR2 inhibition experiments, specific depletion of neutrophils and/or MDSCs via neutralizing antibodies will delineate the anti-tumor effects of CXCR2 blockade in LKB1-deficient tumors if there is any. Also, to understand the roles of neutrophil in premalignant lesions and early stage tumors, it will also be very informative to perform these experiments in the early stages of tumor development.

Study of the dynamics in cytokine-induced EMT in NSCLC

In the above studies, we have shown that EMT memory cells prolong the mesenchymal phenotype and gradually revert back to the epithelial state. However, the mechanism of MET, as part of the EMT plasticity, has not been fully explored. It is unclear whether absence of the EMT stimulus is sufficient for MET or if it requires additional signals. In a skin tumor model, MET occurs in distant organ when Twist induction is artificially switched off (34). However, it does not exclude the possibility that these cancer cells receive a MET stimulus in the metastatic microenvironment. Indeed, Chao *et al.* have shown that the breast cancer cell lines co-cultured with hepatocytes reverted back to an epithelial morphology and re-expressed E-cadherin (35). Gao *et al.* have also showed that Versican expression by myeloid cells in the pre-metastatic lung promoted lung metastasis by inducing MET (36). These studies suggest that signals from the metastatic niche facilitate metastasis via MET induction in distant sites. However, in our isolated *in vitro* model, DNA methylation is the primary mechanism of maintaining EMT in the setting of chronic cytokine exposure and that MET occurs due to the absence of EMT-inducing inflammatory cytokines.

DNA demethylation takes place either by passive dilution or active demethylation mediated by enzymes such as ten-eleven translocation (TET) family enzymes (37). Active DNA demethylation is generally a rapid process that has been shown in mammalian embryogenesis along with dynamic tissue differentiation and also reported as a rapid response to environmental stimulus at specific loci (37-40). In our studies, we have found that 1) DNA demethylation occurs slowly and 2) RNA sequencing of these cells does not reveal any changes of TET expression, supporting the hypothesis that DNA demethylation during MET is likely a consequence of passive dilution rather than active demethylation. In this case, daughter cells with the epithelial phenotype will gradually dominate the population following each cycle of cell division. If this is true, it is important to note that the original methylated DNA allele is not removed in the process. Theoretically, there are twice as many daughter cells as the original EMT memory cells carrying one allele of the methylated DNA in the whole tumor population. Importantly, these daughter cells may still display partial EMT. Further experiments such as examination of DNA methylation following inhibition of cell proliferation or cell sorting for low E-cadherin expression will help to support the hypothesis.

In addition, drug resistance and stem cell properties are also emerging events associated with EMT. Using NSCLC cell lines, Thomson *et al.* have shown that EMT is a determinant of sensitivity against EGFR inhibitor (41). In another study, inhibition of the EMT signaling ERK1/2 increased the sensitivity to EGFR inhibition (42). Recently, two *in vivo* studies have shown that EMT induction is responsible for chemoresistance in breast and pancreatic cancer (43, 44). In addition, tumor specimens from NSCLC patients after chemotherapy or recurrent tumors both display mesenchymal markers (45).

It is still unclear how the EMT program directly impacts on drug resistance but several mechanisms have been proposed (46). It has been shown that initially, EMT slows cell proliferation and increases resistance to chemotherapy, which generally targets fast-growing

cells. Then the EMT transcription factors including Snail, Slug and Twist are known to confer resistance via various mechanisms. For example, Snail and Slug can desensitize cells to the p53-dependent apoptotic cell death following DNA damage or ROS stress (47). Also, numerous studies have also linked EMT with cancer stem cells (CSCs), characterized with not only drug resistance but also tumor initiation and tumor relapse (46, 48). In contrast, reversion of EMT via epigenetic reprogramming impairs tumor initiation and increases susceptibility to conventional chemotherapies (48).

Indeed, similar events occur in our cells following chronic IL-1ß treatment in our model. Analysis of the dysregulated pathways using RNA sequencing data, we have shown that gene groups including Gefinitib resistance, xenobiotics metabolism as well as Notch signaling are significantly altered in our model, suggesting induction of drug resistance and stem cell features (data not shown). It is possible that chronic inflammation can facilitate tumor recurrence by prolonging the time window of resistance to chemo and/or target therapy and promoting the generation of CSCs. More importantly, if DNA methylation is also involved in EMT-associated drug resistance and CSC properties, these traits will not be removed with MET as previously discussed. Therefore, cells with partial EMT may still display partial drug resistance and partial stemness even when metastatic tumors grow out. Subsequently, the cells with the original DNA methylated alleles will possibly serve as a reservoir for tumor relapse. Therefore, interventions targeting EMT will be necessary in addition to therapies against fast-growing epithelial cells in metastatic tumors.

References

1. Sanmamed MF*, et al.* (2014) Serum interleukin-8 reflects tumor burden and treatment response across malignancies of multiple tissue origins. *Clinical cancer research : an official journal of the American Association for Cancer Research* 20(22):5697-5707.
2. Sunaga N*, et al.* (2014) Clinicopathological and prognostic significance of interleukin-8 expression and its relationship to KRAS mutation in lung adenocarcinoma. *British journal of cancer* 110(8):2047-2053.
3. Saintigny P*, et al.* (2013) CXCR2 expression in tumor cells is a poor prognostic factor and promotes invasion and metastasis in lung adenocarcinoma. *Cancer research* 73(2):571-582.
4. Westra WH (2000) Early glandular neoplasia of the lung. *Respiratory research* 1(3):163-169.
5. Jamieson T*, et al.* (2012) Inhibition of CXCR2 profoundly suppresses inflammation-driven and spontaneous tumorigenesis. *The Journal of clinical investigation* 122(9):3127-3144.
6. Gong L*, et al.* (2013) Promoting effect of neutrophils on lung tumorigenesis is mediated by CXCR2 and neutrophil elastase. *Molecular cancer* 12(1):154.
7. Grepin R*, et al.* (2014) The CXCL7/CXCR1/2 axis is a key driver in the growth of clear cell renal cell carcinoma. *Cancer research* 74(3):873-883.
8. Ijichi H*, et al.* (2011) Inhibiting Cxcr2 disrupts tumor-stromal interactions and improves survival in a mouse model of pancreatic ductal adenocarcinoma. *The Journal of clinical investigation* 121(10):4106-4117.
9. Ning Y*, et al.* (2012) The CXCR2 antagonist, SCH-527123, shows antitumor activity and sensitizes cells to oxaliplatin in preclinical colon cancer models. *Molecular cancer therapeutics* 11(6):1353-1364.

10. Singh S*, et al.* (2009) Small-molecule antagonists for CXCR2 and CXCR1 inhibit human melanoma growth by decreasing tumor cell proliferation, survival, and angiogenesis. *Clinical cancer research : an official journal of the American Association for Cancer Research* 15(7):2380-2386.

11. Stadtmann A & Zarbock A (2012) CXCR2: From Bench to Bedside. *Frontiers in immunology* 3:263.

12. Keane MP, Belperio JA, Xue YY, Burdick MD, & Strieter RM (2004) Depletion of CXCR2 inhibits tumor growth and angiogenesis in a murine model of lung cancer. *Journal of immunology* 172(5):2853-2860.

13. Khan MN*, et al.* (2015) CXCR1/2 antagonism with CXCL8/Interleukin-8 analogue CXCL8(3-72)K11R/G31P restricts lung cancer growth by inhibiting tumor cell proliferation and suppressing angiogenesis. *Oncotarget* 6(25):21315-21327.

14. Yanagawa J*, et al.* (2009) Snail promotes CXCR2 ligand-dependent tumor progression in non-small cell lung carcinoma. *Clinical cancer research : an official journal of the American Association for Cancer Research* 15(22):6820-6829.

15. Mishalian I, Granot Z, & Fridlender ZG (2016) The diversity of circulating neutrophils in cancer. *Immunobiology*.

16. Powell DR & Huttenlocher A (2016) Neutrophils in the Tumor Microenvironment. *Trends in immunology* 37(1):41-52.

17. Uribe-Querol E & Rosales C (2015) Neutrophils in Cancer: Two Sides of the Same Coin. *Journal of immunology research* 2015:983698.

18. Ginestier C*, et al.* (2010) CXCR1 blockade selectively targets human breast cancer stem cells in vitro and in xenografts. *The Journal of clinical investigation* 120(2):485-497.

19. Houghton AM*, et al.* (2010) Neutrophil elastase-mediated degradation of IRS-1 accelerates lung tumor growth. *Nature medicine* 16(2):219-223.

20. Rotondo R, *et al.* (2009) IL-8 induces exocytosis of arginase 1 by neutrophil polymorphonuclears in nonsmall cell lung cancer. *International journal of cancer* 125(4):887-893.

21. Morizawa Y, *et al.* (2016) Neutrophil-to-lymphocyte ratio as a detection marker of tumor recurrence in patients with muscle-invasive bladder cancer after radical cystectomy. *Urologic oncology*.

22. Passardi A, *et al.* (2016) Inflammatory indexes as predictors of prognosis and bevacizumab efficacy in patients with metastatic colorectal cancer. *Oncotarget*.

23. Suzuki R, *et al.* (2016) Derived neutrophil/lymphocyte ratio predicts gemcitabine therapy outcome in unresectable pancreatic cancer. *Oncology letters* 11(5):3441-3445.

24. Tang L, *et al.* (2016) Prognostic Value of Neutrophil-to-Lymphocyte Ratio in Localized and Advanced Prostate Cancer: A Systematic Review and Meta-Analysis. *PloS one* 11(4):e0153981.

25. Eruslanov EB, *et al.* (2014) Tumor-associated neutrophils stimulate T cell responses in early-stage human lung cancer. *The Journal of clinical investigation* 124(12):5466-5480.

26. Garcia-Mendoza MG, *et al.* (2016) Neutrophils drive accelerated tumor progression in the collagen-dense mammary tumor microenvironment. *Breast cancer research : BCR* 18(1):49.

27. Guglietta S, *et al.* (2016) Coagulation induced by C3aR-dependent NETosis drives protumorigenic neutrophils during small intestinal tumorigenesis. *Nature communications* 7:11037.

28. Antonio N, *et al.* (2015) The wound inflammatory response exacerbates growth of pre-neoplastic cells and progression to cancer. *The EMBO journal* 34(17):2219-2236.

29. Gabrilovich DI & Nagaraj S (2009) Myeloid-derived suppressor cells as regulators of the immune system. *Nature reviews. Immunology* 9(3):162-174.

30. Talmadge JE & Gabrilovich DI (2013) History of myeloid-derived suppressor cells. *Nature reviews. Cancer* 13(10):739-752.

31. Highfill SL*, et al.* (2014) Disruption of CXCR2-mediated MDSC tumor trafficking enhances anti-PD1 efficacy. *Science translational medicine* 6(237):237ra267.

32. Stiff A*, et al.* (2016) Myeloid-derived suppressor cells express Bruton's tyrosine kinase and can be depleted in tumor bearing hosts by ibrutinib treatment. *Cancer research*.

33. Koyama S*, et al.* (2016) STK11/LKB1 Deficiency Promotes Neutrophil Recruitment and Proinflammatory Cytokine Production to Suppress T-cell Activity in the Lung Tumor Microenvironment. *Cancer research* 76(5):999-1008.

34. Tsai JH, Donaher JL, Murphy DA, Chau S, & Yang J (2012) Spatiotemporal regulation of epithelial-mesenchymal transition is essential for squamous cell carcinoma metastasis. *Cancer cell* 22(6):725-736.

35. Chao YL, Shepard CR, & Wells A (2010) Breast carcinoma cells re-express E-cadherin during mesenchymal to epithelial reverting transition. *Molecular cancer* 9:179.

36. Gao D*, et al.* (2012) Myeloid progenitor cells in the premetastatic lung promote metastases by inducing mesenchymal to epithelial transition. *Cancer research* 72(6):1384-1394.

37. Kohli RM & Zhang Y (2013) TET enzymes, TDG and the dynamics of DNA demethylation. *Nature* 502(7472):472-479.

38. Wu SC & Zhang Y (2010) Active DNA demethylation: many roads lead to Rome. *Nature reviews. Molecular cell biology* 11(9):607-620.

39. Kangaspeska S*, et al.* (2008) Transient cyclical methylation of promoter DNA. *Nature* 452(7183):112-115.

40. Thillainadesan G*, et al.* (2012) TGF-beta-dependent active demethylation and expression of the p15ink4b tumor suppressor are impaired by the ZNF217/CoREST complex. *Molecular cell* 46(5):636-649.

41. Thomson S*, et al.* (2005) Epithelial to mesenchymal transition is a determinant of sensitivity of non-small-cell lung carcinoma cell lines and xenografts to epidermal growth factor receptor inhibition. *Cancer research* 65(20):9455-9462.

42. Buonato JM & Lazzara MJ (2014) ERK1/2 blockade prevents epithelial-mesenchymal transition in lung cancer cells and promotes their sensitivity to EGFR inhibition. *Cancer research* 74(1):309-319.

43. Fischer KR*, et al.* (2015) Epithelial-to-mesenchymal transition is not required for lung metastasis but contributes to chemoresistance. *Nature* 527(7579):472-476.

44. Zheng X*, et al.* (2015) Epithelial-to-mesenchymal transition is dispensable for metastasis but induces chemoresistance in pancreatic cancer. *Nature* 527(7579):525-530.

45. Shintani Y*, et al.* (2011) Epithelial to mesenchymal transition is a determinant of sensitivity to chemoradiotherapy in non-small cell lung cancer. *The Annals of thoracic surgery* 92(5):1794-1804; discussion 1804.

46. Tsai JH & Yang J (2013) Epithelial-mesenchymal plasticity in carcinoma metastasis. *Genes & development* 27(20):2192-2206.

47. Kurrey NK*, et al.* (2009) Snail and slug mediate radioresistance and chemoresistance by antagonizing p53-mediated apoptosis and acquiring a stem-like phenotype in ovarian cancer cells. *Stem cells* 27(9):2059-2068.

48. Pattabiraman DR*, et al.* (2016) Activation of PKA leads to mesenchymal-to-epithelial transition and loss of tumor-initiating ability. *Science* 351(6277):aad3680.